

Electrochemical Synthesis and Spectroelectrochemical Characterization of Novel Conducting Poly(*o*- phenylenediamine-co-*o*-/*m*-toluidine)

von der Fakultät für Naturwissenschaften der Technischen Universität Chemnitz
genehmigte Dissertation zur Erlangung des akademischen Grades

doctor rerum naturalium
(Dr. rer. nat.)

vorgelegt von
M.Sc. Salma Bilal
geboren am 07.09.1979 in Nowshera, Pakistan

eingereicht am 21 Mai 2007

Gutachter: Prof. Dr. Rudolf Holze
Prof. Dr. Werner A. Goedel
Prof. Dr. Klaus Jüttner

Tag der Verteidigung: 23 Oktober 2007

Bibliographische Beschreibung und Referat

S. Bilal

Electrochemical Synthesis and Spectroelectrochemical Characterization of Novel Conducting Poly(*o*-phenylenediamine-co-*o*/*m*-toluidine)

In den vergangenen Jahren löste die Nachfrage nach hochwertigen organischen Werkstoffen die Suche nach neuen Materialien mit maßgeschneiderten Eigenschaften für mögliche technische Anwendungen aus. In der vorliegenden Arbeit wurde ein Ansatz entwickelt, neue organische Materialien zu synthetisieren, wobei die Untersuchung der Copolymerisation von *o*-Phenylendiamin (OPD) mit *o*-Toluidin (OT) und *m*-Toluidin (MT) in wässriger Schwefelsäure im Vordergrund stand. Dabei fand die zyklische Voltammetrie sowohl bei der elektrochemischen Synthese als auch für die Charakterisierung der Homo- und Copolymere auf einer Goldelektrode Anwendung. Die Copolymere wurden aus gemischten Monomerlösungen synthetisiert, die unterschiedliche OPD-Konzentrationen sowie eine konstante OT- oder MT-Konzentration aufwiesen. Die Voltammogramme zeigten ein unterschiedliches Verhalten für die verschiedenen OPD-Konzentrationen bei der Zugabe. Die Mischung der Monomerlösungen mit geeigneten Konzentrationen ergab ein Copolymer mit einem großen potenziell nutzbaren Bereich der Redoxaktivität relativ zu den korrespondierenden Homocopolymeren. Die Homopolymere Poly-*o*-toluidin (POT) und Poly-*m*-toluidin (PMT) zeigten ähnliche elektrochemische Eigenschaften. Es wurden jedoch Unterschiede in den Eigenschaften zwischen den OT- und MT-Copolymeren mit OPD beobachtet, die möglicherweise auf eine Abweichung in den Monomereinheiten und der Ausrichtung entlang der Copolymerkette zurückzuführen sind. Die Copolymerisation der OPD wird offenbar gefördert, wenn OT statt MT als einer der Comonomere verwendet wird. Weiterhin wurde der Einfluss der Vorschubgeschwindigkeit (dE/dt) und des pH-Wertes auf die elektrochemische Aktivität untersucht. Die Copolymere waren oberflächengebunden, elektrisch aktiv und zeigten sogar bei einem pH-Wert = 8,0 bei Poly(OPT-co-MT) bzw. 9,0 bei Poly(OPT-co-OT) eine gute elektrochemische Aktivität. Die Messungen der *in situ* Leitfähigkeit unterstützte die Herausbildung eines neuen Stoffes (Copolymer), da die Copolymere Elektrodenpotenzialbereiche für eine maximale Leitfähigkeit besitzen, die sich völlig von jenen der Homopolymere unterscheiden. Die Leitfähigkeitswerte der Copolymere lagen zwischen den Werten der Homopolymere.

Die *in situ* UV-Vis spektroelektrochemischen Untersuchungen der Copolymerisation von OPD mit OT und MT bei konstanter potenzieller Polymerisation auf mit Indiumzinnoxid (ITO) beschichteten Glaselektroden zeigten, dass ein Kopf-Schwanz-verknüpfter *p*-Aminodiphenylamin (PPD)-Typ eines gemischten Dimers/Oligomers, der wahrscheinlich aus der Dimerisation der Kationenradikale von OPD und OT oder MT resultiert, vorwiegend zu Beginn der Elektropolymerisation der Mischlösungen entsteht. Ein Absorptionsspektrum bei $\lambda = 497$ nm in den UV-Vis-Spektren wurde diesen Zwischenprodukten zugeordnet. Es erfolgte eine Identifizierung der charakteristischen UV-Vis- und Raman- ($\lambda = 647,1$ nm) Eigenschaften der Copolymere, synthetisiert mit verschiedenen Zugabekonzentrationen auf ITO-beschichtetem Glas bzw. auf Goldelektroden, sowie eine Diskussion ihrer Abhängigkeit vom Elektrodenpotenzial. Die spektroelektrochemischen Ergebnisse zeigten, dass die Hauptkette des Copolymers wahrscheinlich aus einer Mischung aus Copolymerketten mit unterschiedlichen Monomergehalten und einer signifikanten Anzahl an Blocksegmenten besteht. Die Eigenschaften der Copolymere erwiesen sich als sehr sensibel gegenüber der OPD Zugabekonzentration, so dass eindeutige Änderungen in den elektrochemischen und spektroelektrochemischen Eigenschaften der Stoffe aus Mischlösungen durch bloße Variierung der OPD-Konzentration bei der Zugabe beobachtet werden konnten.

Die FT-IR-Spektralanalyse der Copolymere deutet auf die Anwesenheit von sowohl OPD- als auch OT- oder MT-Einheiten und daher auf die Copolymerbildung während der Elektrolyse der Mischlösungen aus OPD und OT oder MT hin. Die zyklischen Strukturen des Phenazintyps erhöhen sich im Copolymer mit steigender OPD-Konzentration bei der Zugabe.

Stichworte: Poly(*o*/*m*-toluidine); Poly (*o*-phenylenediamine); Copolymerisation; zyklische Voltammetrie; UV-Vis und Raman Spektroelektrochemie; FT-IR.

Abstract

S. Bilal

Electrochemical Synthesis and Spectroelectrochemical Characterization of Novel Conducting Poly(*o*-phenylenediamine-co-*o*/*m*-toluidine)

In recent years the demand for advanced organic materials has sparked the search for new materials with tailored properties for possible technological applications. In the present study an attempt has been made to synthesize new organic conducting materials by exploring the possibility of the copolymerisation of *o*-phenylenediamine (OPD) with *o*-toluidine (OT) and *m*-toluidine (MT) in aqueous sulfuric acid. Cyclic voltammetry was used both for the electrochemical synthesis and characterization of the homopolymers and copolymers on a gold electrode. The copolymers were synthesized from mixed solutions of the monomers having different concentrations of OPD and a constant concentration of OT or MT. The voltammograms exhibited different behavior for different concentrations of OPD in the feed. Mixing of the monomer solutions with appropriate concentrations resulted in a copolymer that shows an extended useful potential range of the redox activity relative to the corresponding homopolymers. The homopolymers poly(*o*-toluidine) (POT) and poly(*m*-toluidine) (PMT) show similar electrochemical properties. However, differences were observed in the properties between the copolymers of OT and MT with OPD that could be due to the variation in the monomer units and orientation along the copolymer chains. The copolymerization of OPD seems to be more facilitated if instead of MT, OT is present as one of the comonomers. The effect of scan rate and pH on the electrochemical activity was studied. The copolymers were surface confined, electroactive and showed good electrochemical activity even at pH 8.0 and pH 9.0 in case of poly(OPD-co-MT) and poly(OPD-co-OT), respectively. *In situ* conductivity measurements further suggest the formation of new material (copolymer) because the copolymers have electrode potential regions for maximum conductivity completely different from those of the homopolymers. The conductivity values of the copolymers were between the conductivities of the homopolymers.

In situ UV-Vis spectroelectrochemical studies of the copolymerization of OPD with OT and MT at constant potential polymerization on indium tin oxide (ITO) coated glass electrodes reveal that head to tail coupled *p*-aminodiphenylamine (PPD) type of mixed dimers/oligomers, presumably resulting from the dimerization of OPD and OT or MT cation radicals, are predominantly formed during the initial stages of the electropolymeriz-

ation of the mixed solutions. An absorption peak at $\lambda = 497$ nm in the UV-Vis spectra was assigned to these intermediates. Characteristic UV-Vis and Raman ($\lambda_{\text{ex}} = 647.1$ nm) features of the copolymers synthesized with different feed concentrations on ITO coated glass and gold electrodes, respectively, have been identified and their dependencies on the electrode potential are discussed. Spectroelectrochemical results reveal that the copolymer backbone probably consist of a mixture of copolymer chains with different monomer contents and has significant number of block segments. The properties of the copolymers were found to be very sensitive to the OPD feed concentration and clear variations in the electrochemical and spectroelectrochemical properties of the materials from mixed solutions can be observed just by varying the concentration of OPD in the feed.

FT-IR spectral analysis of the copolymers suggests the presence of both OPD and OT or MT units and thus formation of copolymer during the electrolysis of mixed solutions of OPD and OT or MT. The phenazine type cyclic structures increase in the copolymer with increasing OPD concentration in the feed.

Keywords: Poly(*o*/*m*-toluidine); Poly(*o*-phenylenediamine); Copolymers; Cyclic voltammetry; UV-Vis and Raman spectroelectrochemistry; FT-IR

Die vorliegende Arbeit wurde in der Zeit von Dez. 2004 bis Jan. 2007 unter Leitung von Prof. Dr. Rudolf Holze am Lehrstuhl für Physikalische Chemie/Elektrochemie der Technischen Universität Chemnitz durchgeführt.

Acknowledgements

I would like to thank to several people without whom this research would have been extremely difficult. Generally I wish to give my grateful acknowledgements to all the members of the Institute of Chemistry, Chemnitz University of Technology, who provide a pleasant atmosphere where I spent two years of my happy time.

I would like to express my gratitude to my supervisor **Prof. Dr. Rudolf Holze**, whose expertise, valuable suggestions, comments, guidance and patience added considerably to my knowledge. I deeply appreciate his vast knowledge in the field of Electrochemistry.

Special thanks also go to Prof. Dr. Werner. A. Goedel and Prof. Dr. Klaus Jüttner for acting as the reviewers of this thesis.

I owe a special debt to my parents for their endless love and tremendous sacrifices to ensure that I had a great success in life. Huge thanks to my husband Dr. Anwar-ul-Haq for being incredibly loving, understanding, supportive and patient. My sincere thanks with extreme love go to my cute and beloved son Misbah-ul-Haq, who was a great source of motivation to finish this work in a short time. I am highly obliged to my brother Yousaf shah for his timely support and help. I am greatly indebted to the parents, brothers and sisters of my husband for their love, affection and prayers.

I wish to express my appreciation to the love and good wishes extended by Rabia Gul, Arsalan Gee, Honey Gul, Sheema, Sadaf, Mashaal, my relatives and friends.

I also wish to thank the present and former members of Electrochemistry group for their encouragement, support and respect. I deeply appreciate the Chemnitz University of Technology that embraced me as one of its students.

Last but not the least, I gratefully acknowledge Higher Education Commission (HEC), Pakistan, for one year Scholarship under partial support programme.

Dedicated to

My Nice Husband and Cute Son

Table of Contents

Bibliographische Beschreibung und Referat	2
Abstract	3
Zeitraum, Ort der Durchführung	5
Acknowledgments	6
Dedication	7
Table of Contents	8
List of Abbreviations and Symbols	12
Chapter 1	14
1 Introduction	14
1.1 Conducting Polymers	14
1.2 Synthesis of Conducting Polymers	15
1.2.1 Chemical Synthesis	15
1.2.2 Electrochemical Synthesis	16
1.3 Cyclic Voltammetry	17
1.4 Conductivity Measurements	18
1.5 Spectroelectrochemical Techniques	19
1.5.1 UV-Visible Spectroelectrochemistry	19
1.5.2 Raman Spectroelectrochemistry	20
1.6 Concept of Doping in Conducting Polymers	21
1.7 Types of Conducting Polymers	23
1.8 Conduction Mechanism in Conjugated Polymers	23

1.9	The Most Commonly Studied Conjugated Polymers	26
1.10	Polyaniline	27
1.11	Substituted Anilines	30
1.11.1	Toluidines	30
1.11.2	Phenylenediamines	32
1.12	Electroactive Copolymers	34
1.13	Aims and Tasks of the Study	35
Chapter 2		36
2	Experimental	36
2.1	Chemicals and Solutions	36
2.2	Electrochemical Measurements	36
2.3	<i>In situ</i> Conductivity Measurements	37
2.4	UV-Visible Spectroelectrochemical Measurements	37
2.5	Raman Spectroelectrochemical Measurements	38
2.6	Fourier Transform Infrared Spectroscopical Measurements	38
Chapter 3		39
3	Electrochemical Measurements	39
3.1	Electrochemical Homopolymerization of <i>o</i> -/ <i>m</i> -Toluidine	39
3.2	Electrochemical Homopolymerization of <i>o</i> -Phenylenediamine	41
3.3	Electrochemical Copolymerization of <i>o</i> -Phenylenediamine and <i>o</i> -Toluidine	43
3.3.1	Electrochemical Behavior of Poly(<i>o</i> -phenylenediamine-co- <i>o</i> -toluidine)	48
3.3.2	Stability of Poly(<i>o</i> -phenylenediamine-co- <i>o</i> -toluidine)	50
3.3.3	Effect of pH on the Electrochemical Activity of Poly(<i>o</i> -phenylenediamine-co- <i>o</i> -toluidine)	51

3.4	Electrochemical Copolymerization of <i>o</i> -Phenylenediamine and <i>m</i> -Toluidine	53
3.4.1	Electrochemical Behavior of Poly(<i>o</i> -phenylenediamine-co- <i>m</i> -toluidine)	56
3.4.2	Stability of Poly(<i>o</i> -phenylenediamine-co- <i>m</i> -toluidine)	59
3.4.3	Effect of pH on the Electrochemical Activity of Poly(<i>o</i> -phenylenediamine-co- <i>m</i> -toluidine)	60
Chapter 4		62
4	<i>In Situ</i> Conductivity Measurements	62
4.1	<i>In Situ</i> Conductivity Measurements of Poly(<i>o</i> -/ <i>m</i> -toluidine)	62
4.2	<i>In Situ</i> Conductivity Measurements of Poly(<i>o</i> -phenylenediamine)	63
4.3	<i>In Situ</i> Conductivity Measurements of Poly(<i>o</i> -phenylenediamine-co- <i>o</i> -toluidine)	64
4.4	<i>In Situ</i> Conductivity Measurements of Poly(<i>o</i> -phenylenediamine-co- <i>m</i> -toluidine)	67
Chapter 5		69
5	UV-Visible Spectroelectrochemical Measurements	69
5.1	Spectroelectrochemical Studies of the Homopolymerization of <i>o</i> -/ <i>m</i> -Toluidine	69
5.2	Spectroelectrochemical Studies of the Homopolymerization of <i>o</i> -Phenylenediamine	70
5.3	Spectroelectrochemical Studies of the Comopolymerization of <i>o</i> -Phenylenediamine and <i>o</i> -Toluidine	73
5.4	Spectroelectrochemical Studies of the Comopolymerization of <i>o</i> -Phenylenediamine and <i>m</i> -Toluidine	77
5.5	Spectroelectrochemistry of Poly(<i>o</i> -/ <i>m</i> -toluidine)	78
5.6	Spectroelectrochemistry of Poly(<i>o</i> -phenylenediamine)	81
5.7	Spectroelectrochemistry of Poly(<i>o</i> -phenylenediamine-co- <i>o</i> -toluidine)	82
5.8	Spectroelectrochemistry of Poly(<i>o</i> -phenylenediamine-co- <i>m</i> -toluidine)	86
Chapter 6		89

6	FT-IR Measurements	89
6.1	FT-IR Measurements of Poly(<i>o</i> -/ <i>m</i> -toluidine)	90
6.2	FT-IR Measurements of Poly(<i>o</i> -phenylenediamine)	91
6.3	FT-IR Measurements of Poly(<i>o</i> -phenylenediamine-co- <i>o</i> -toluidine)	92
6.4	FT-IR Measurements of Poly(<i>o</i> -phenylenediamine-co- <i>m</i> -toluidine)	94
	Chapter 7	97
7	Raman Spectroelectrochemical Measurements	97
7.1	Raman Spectroelectrochemistry of Poly(<i>o</i> -/ <i>m</i> -toluidine)	97
7.2	Raman Spectroelectrochemistry of Poly(<i>o</i> -phenylenediamine)	102
7.3	Raman Spectroelectrochemistry of Poly(<i>o</i> -phenylenediamine-co- <i>o</i> -toluidine)	105
7.4	Raman Spectroelectrochemistry of Poly(<i>o</i> -phenylenediamine-co- <i>m</i> -toluidine)	111
	Summary	117
	Future work	120
	References	121
	Selbständigkeitserklärung	132
	Curriculum Vitae	133

List of Abbreviations and Symbols

Aniline	ANI
B	Benzoid
CV	Cyclic voltammogram
Def	Deformation mode
DMF	Dimethylformamide
DMSO	Dimethylsulfoxide
EB	Emeraldine base
ES	Emeraldine salt
Fig.	Figure
FT-IR	Fourier transform-infrared
IR	Infrared
ITO	Indium doped tin oxide
LE	Leucoemeraldine
MT	<i>m</i> -Toluidine
OPD	<i>o</i> -Phenylenediamine
OT	<i>o</i> -Toluidine
PA	Polyacetylene
PANI	Polyaniline
PMT	Poly(<i>m</i> -toluidine)
PN	Pernigraniline
POPD	Poly(<i>o</i> -phenylenediamine)
POT	Poly(<i>o</i> -toluidine)
PPD	<i>p</i> -Aminodiphenylamine
Q	Quinoid
SCE	Saturated calomel electrode
SQR	Semiquinone radical
UV-Vis	Ultraviolet-Visible
V	Volt
WE	Working electrode
A	Absorbance

Au	Gold
E_{SCE}	Potential vs. saturated calomel electrode
β	Bending mode
γ	Out-of-plane deformation mode
δ	In-plane deformation mode
λ	Wavelength
λ_{ex}	Laser excitation wavelength
ν	Stretching mode

1 Introduction

1.1 Conducting Polymers

Nowadays, polymer science is attractive due to the unique properties of polymers (they are also called plastic materials) such as, material structure, mechanical properties, low production cost and many other advantages.

Conducting polymers are novel plastics that conduct electricity. The evolution of conducting polymers did not draw significant scientific attention before the mid 1970s, although they have been known for many years. In 1973, Waltaka et al [1] discovered that conjugated poly(sulfur nitride) (PSN) could conduct electricity. Two years later Greene, Street and Suter discovered super conductivity nature of PSN at low temperature [2].

The polymer that had attracted most attention in the early development of conducting polymers is poly(acetylene) (PA), which is a conjugated polymer with alternating-single-double bond. It was first synthesized in the late 1950s, but for 20 years researchers were interested only in spectroscopic and theoretical studies of PA as the ultimate member of the polyene family. In 1977, MacDiarmid, Heeger, Shirakawa and coworkers have revolutionized the development of electrically conducting polymers by synthesizing PA as the simplest conjugated conducting polymer [3, 4]. They discovered that when the insulating PA films are exposed to Iodine vapours at room temperature, a dramatic increase in the conductivity occurred. With the discovery of conducting polymers a period of intensive theoretical and experimental research began and the efforts of MacDiarmid, Heeger and Shirakawa were recognized by the award of Nobel prize in chemistry in the year 2000 [5, 6, 7].

In the field of polymer technology, one of the most valued characteristics of synthetic polymers is the ability to act as excellent electrical insulators. Research has shown that most of the conducting polymers undergo transition from insulator to electric conductor upon doping with weak oxidizing or reducing agents. Thus the synthesis of conjugated polymers provides a possibility to combine, in one material, the electrical properties of a semiconductor and metal with the ease and low cost of preparation and fabrication. Flexibility, density and chemical inertness, non-linear optical behavior and exceptional mechanical properties [8, 9, 10] such as tensile strength and resistance to harsh environments are other important advantages of the conducting polymers.

1.2 Synthesis of Conducting Polymers

Conducting polymers are generally prepared by direct oxidation of the monomer using appropriate chemical oxidant or by electrochemical oxidation on different electrode materials. The characteristics of the polymer depend on the mode of synthesis. The syntheses of conducting polymers fall broadly into two categories [11], chemical and electrochemical synthesis.

1.2.1 Chemical Synthesis

Chemical synthesis can be carried out in a solution containing the monomer and an oxidant. Various chemical oxidizing agents have been used such as potassium dichromate, persulfates or peroxodisulfate, hydrogen peroxide, ceric nitrate and ceric sulfate, chromyl chloride, trimethylsilyl chlorochromate or perchlorates and hydrogen peroxide [12, 13, 14, 15]. The reaction is mainly carried out in acidic media, in particular sulfuric acid at a pH between 0 and 2 [13]. Sometimes alkaline or ammonium salts are also added to the solution which act as a buffer, increasing the conductivity and yield. Neutral and basic media in acetonitrile [16] and in aqueous solutions at pH values in the range of 9 to 10 have also been used. The concentration of the monomer varies greatly and generally lies between 0.01 and 0.1 M.

Chemical polymerization is the versatile technique for preparing large amounts of conducting polymers. Oxidative chemical polymerizations result in the formation of the polymers in their doped and conducting state. Isolation of the neutral polymer is achieved by exposing the material to a strong reducing agent such as ammonia or hydrazine. One of the criteria, governing the quality of the material, is its molecular mass. It is believed that the properties of the material are more interesting, in particular the stability, when the molecular mass is large. Different approaches are used to deposit chemically synthesized conducting polymer films on a certain substrate. These include spin-coating, dip-coating, drop-coating, thermal evaporation [17, 18], Langmuir-Blodgett [17, 19, 20] and self-assembly techniques [21, 22]. In general chemical methods of preparation lack the control of reaction conditions.

1.2.2 Electrochemical Synthesis

Generally, in electrochemical synthesis, the monomer dissolved in an appropriate solvent containing the desired anionic doping salt, is oxidized at the surface of an electrode by application of an anodic potential (oxidation). The radical coupling polymerization mechanism is encountered most often in literature to describe electrochemical polymerization [23, 24, 25]. The electropolymerization is achieved, in an electrochemical cell, by various electrochemical techniques including potentiostatic (constant-potential), galvanostatic (constant current) and potentiodynamic (cyclic voltammetry) methods.

An electrochemical cell normally comprises of three electrodes and one medium that consists of solvent containing a supporting electrolyte. The electrode that responds to target analyte(s) is termed as indicating electrode also known as the test or working electrode (WE). This is the electrode at which the electrochemical phenomenon being investigated takes place. A range of materials has found applications as working electrodes for electroanalysis. The most popular are those involving mercury, carbon or noble metals, particularly platinum, gold and silver followed occasionally by palladium, rhodium and iridium [26, 27, 28, 29, 30]. Various polycrystalline forms including sheets, rods and wires are commercially available in high purity and the materials are readily machined into useful shapes. The second functional electrode is the reference electrode (RE). This is the electrode whose potential is constant enough that it can be taken as the reference standard against which the potentials of the other electrodes present in the cell can be measured. Such “buffering” against potential changes is achieved by a constant composition of both forms of its redox couple, e.g. Ag/AgCl or Hg/Hg₂Cl₂, commonly known as silver-silver chloride and the saturated calomel reference electrode (SCE), respectively. The final functional electrode is the counter or auxiliary electrode (CE or AE) that serves as a source or sink for electrons so that current can be passed from the external circuit through the cell. In general, neither its true potential nor current is ever measured or known.

An electrolyte solution provides the medium through which charge transfer can take place by the movement of ions. While water has been used as a solvent more than any other medium, non-aqueous solvents, e.g. acetonitrile, propylene carbonate, dimethylformamide (DMF), dimethylsulfoxide (DMSO) or methanol, have also been used frequently. Mixed solvents may also be considered for certain applications. Double-distilled water is adequate for most work in aqueous media. Organic solvents often require drying or purification procedures. The inert supporting electrolyte may be an inorganic salt, a mineral acid

or a buffer. While potassium chloride or nitrate, ammonium chloride, sodium hydroxide, sulfuric acid, perchloric acid or hydrochloric acid are widely used when using water as a solvent, tetraalkylammonium salts are often employed in organic media. Buffer systems such as acetate, phosphate or citrate are used when pH control is essential.

The electrochemical polymerization has some advantages over the chemical route allowing a better control of the deposition parameters (growth rate, thickness and composition) and the advantage of synthesis and film deposition in a single step. The polymerization can proceed only when the monomer is oxidized at the electrode. The behavior of the electropolymerized films can be controlled by the polymerization conditions including the electrolyte, solvent, applied potential or current and duration. In addition changes in the polymer properties can be induced by attaching various functionalities to the monomer prior to polymerization. However, this method is of limited applicability in saturated polymers that are electrically non-conducting, as an insulating barrier quickly builds up on the electrode where the radical ions are generated and the polymerization is terminated.

1.3 Cyclic Voltammetry

Cyclic voltammetry is a powerful and most widely used electrochemical technique used both to polymerize the monomers and to characterize the resultant polymers electrochemically. Electrochemical monitoring of the electropolymerization process is primarily performed using cyclic voltammetry. A cyclic potential sweep is imposed on an electrode and the current response is observed. A potentiostat system sets the control parameters of the experiment. Its purpose is to impose on the WE a cyclic potential sweep and to output the resulting current-potential curve known as cyclic voltammogram (CV). This sweep is described in general by its initial, switching and the final potential (E_i , E_s , and E_f , respectively) and the scan rate in V/s.

In the first potential cycle, during anodic electropolymerization by potential cycling, the oxidation peak corresponds to formation of radical cations of the monomers. On the reverse scan, the reduction peak corresponding to this oxidation is not always observed. This indicates that in the time scale of the experiment, the intermediate reactive monomeric radical cations dimerize in the subsequent chemical reaction. Starting with the second potential scan a current peak at lower potential than the monomer oxidation peak is observed. This corresponds to oxidation of the formed oligomer chains. On the reverse scan, a peak current due to reduction of the oxidized oligomer species is observed. During subsequent

potential scans oxidation and reduction of the growing polymer film can be followed. The redox peak current increases until the polymer stops growing on the electrode. On the other hand, the current peak corresponding to the monomer oxidation progressively diminishes indicating that less and less monomer is converted to radical cations in the vicinity of the electrode.

Cyclic voltammetry is also one of the first methods to be applied to an electrode coated with a conducting polymer film because besides the instrumental simplicity of the cyclic voltammetry, a considerable amount of information about a conducting polymer can be obtained on the basis of recording a single CV. Important parameters characterizing the conducting materials, such as rate constants for oxidation reduction processes and the doping/dedoping within the polymer film can be calculated from the analysis of the current response.

1.4 Conductivity Measurements

Conducting polymers have been studied extensively in the past few years for possible technological applications. Electrical conductivity of these materials is a crucial factor in addition to their electroactivity in potential applications. The conductivity depends to a great extent on the method of preparation and manipulation of the polymers. Conductivity is an important aspect of conducting polymers and its measurement is regarded as an important step in the characterization of these materials.

Conductivity of the polymers can be measured both with *ex situ* (two or four-probe method) and *in situ* techniques. However, *in situ* conductivity measurements, using a bandgap electrode with a special setup are greatly simplified for polymer film deposited on this electrode [31, 32]. The two strips of the bandgap electrode can be easily bridged through the deposition of conducting polymers, as the separation between them is only few micrometers. The important aspect of this setup is that one can judge the dependence of the resistance on different applied potentials for a particular conductive polymer film. In addition to this one can also compare the ranges of resistance variation, with varying applied potential, of different conductive polymer films.

One of the problems associated with this technique is the deposition of comparable amounts of different polymer films of identical thickness across the insulating gap. However, this problem can be overcome up to certain extent by adjusting experimental conditions e.g. number of cycles or time of electrolysis and recording of cyclic voltammograms

(CVs) of the deposited polymer films before each series of conductivity measurements in the monomer free electrolyte solution.

1.5 Spectroelectrochemical Techniques

The coupling of optical and electrochemical methods (spectroelectrochemistry) has been widely employed for the qualitative as well as the quantitative analysis of samples. Such a combination of electrochemical perturbations with the molecular specificity of optical monitoring successfully addresses the limited structural information available from these measurements. A variety of informative optical methods has been coupled with electrochemical techniques [33, 34, 35, 36]. The following sections will focus primarily on the spectroelectrochemical techniques used in this dissertation for analyzing and characterizing the polymers under investigations.

1.5.1 UV-Visible Spectroelectrochemistry

UV-Visible (UV-Vis) spectroscopy provides information about structure and stability of the materials in solution. Absorption spectra are produced when ions or molecules absorb electromagnetic radiation in the ultraviolet or visible regions. Various kinds of electronic excitation may occur in organic molecules by absorbing the energies available in the UV-Vis region. As a rule, energetically favored electron promotion will be from the highest occupied molecular orbital (HOMO) to the lowest unoccupied molecular orbital (LUMO). An optical spectrometer records the wavelengths at which absorption occurs, together with the degree of absorption at each wavelength. The resulting spectrum is presented as a graph of absorbance versus wavelength [37]. The intensity of the absorption is proportional to the number, type and location of color absorbing structures (chromophores) in the molecule. When coupled with electrochemistry, UV-Vis spectroscopy appears to be a very helpful tool in analyzing and characterizing a conducting polymer.

The primary advantage of spectroelectrochemistry is the cross-correlation of the information from simultaneous electrochemical and optical measurements. In a typical experiment one measures the absorption changes resulting from species produced (or consumed) in the redox process. The change in the absorbance is related to concentration and optical path length. Careful evaluation of the temporal absorbance response (Absorbance vs time curve) during the electrochemical generation (or consumption) of an optically ac-

tive species can yield useful insights on reaction mechanism and kinetics. Such experiments are particularly useful when the reactants and products have sufficiently different spectra. Optically transparent electrodes (OTEs), which enable light to pass through their surface and the adjacent solution, are the keys for performing the spectroelectrochemical experiment. Various kinds of OTEs are available. Usually a semiconductor (e.g. indium doped tin oxide, ITO), deposited on a transparent material such as quartz or glass substrate, is employed in the UV-Vis spectroelectrochemical studies of the conducting polymers.

Electronic absorption spectra recorded for a conducting polymer film deposited on an ITO coated electrode at certain applied potential or a conducting polymer dissolved in a suitable solvent gives qualitative information about the level of doping, extent of conjugation and the presence of radical cations in the polymer. Fortunately, conjugation in conducting polymers moves the absorption maxima to higher or lower wavelengths [38, 39, 40], so conjugation becomes the major structural feature identified by this technique. Furthermore, UV-Vis spectroelectrochemistry (*in situ*) is very helpful in understanding the interconversion of different oxidation states of a conducting polymer [41]. In recent years UV-Vis spectroelectrochemistry has also been used extensively for the detection of the intermediate species involved in the electropolymerization process of a conducting polymer [42, 43, 44, 45, 46, 47, 48, 49, 50, 51, 52].

1.5.2 Raman Spectroelectrochemistry

Generally Raman spectroscopy is a spectroscopic technique that relies on inelastic or Raman scattering of monochromatic light, usually from a laser in the visible, near infrared or near ultra violet range [53, 54]. The Raman effect occurs when light impinges upon a molecule and interacts with the electron cloud of the bonds of that molecule. Typically, a sample is illuminated with a laser beam. Light from the illuminated spot is collected with a lens and sent through a monochromator. Wavelengths close to the laser line (due to elastic Rayleigh scattering) are filtered out and those in a certain spectral window away from the laser line are dispersed onto a detector. The Raman scattering depends upon the polarizability (the amount of deformation of electron cloud) of the molecules. The amount of the polarizability of the bond will determine the intensity and frequency of the Raman shift. The photon excites one of the electrons into the virtual state. When the photon is released the molecule relaxes back into vibrational energy state. The molecule will typically relax into the first vibrational energy state and this generates Stokes Raman scattering. If the

molecule is excited from an elevated vibrational energy state, it will relax into the vibrational ground energy state and the Raman scattering is then called anti-Stokes Raman scattering. Since most molecules are in their vibrational ground energy state at ambient temperature the intensity of Stokes lines are higher than the anti-Stokes lines. This is the reason why only the Stokes lines are recorded as the Raman spectrum.

Raman spectroscopy is commonly used in electrochemistry, since vibrational information is very specific for the chemical bonds in molecules. The advantage of Raman spectroscopy arises from the resonance enhancement of the Raman signals. If the laser excitation wavelength matches with one of the band maxima in the UV-Vis spectra of the conducting polymer, the intensity of the scattered light is strongly increased. This is called ‘resonance enhancement’ [55]. When recorded at different applied potentials, the Raman spectra of the conducting polymer film provide useful information about the changes occurring in the polymer structure upon oxidation or reduction [18].

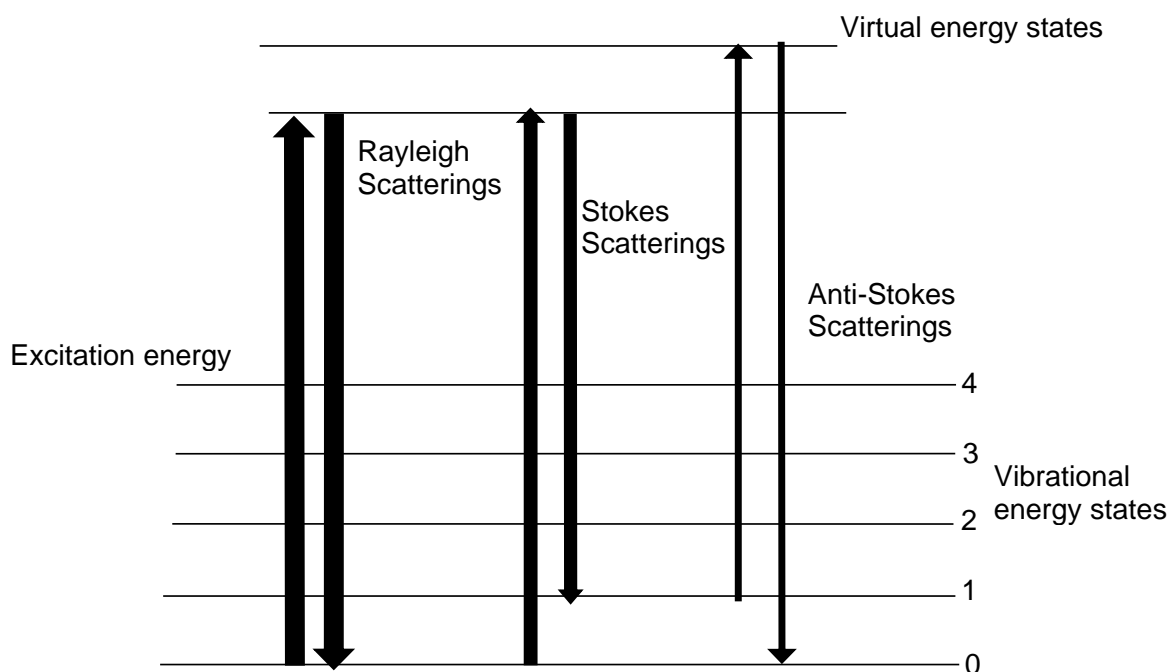


Fig. 1.1 Schematic diagram of Raman scatterings.

1.6 Concept of Doping in Conducting Polymers

The term “doping” in connection with conducting polymers is generally understood as a process that involves oxidation or reduction of the polymer backbone and the concomitant changes in the electronic structure [56]. The concept of doping is the unique, central, underlying and unifying theme, which distinguishes conducting polymers from all other types

of polymers. During the process an organic polymer, either an insulator or semiconductor having a small conductivity typically in the range from 10^{-10} to 10^{-5} S/cm, is converted to a polymer that is in the 'metallic' conducting regime ($1\sim 10^4$ S/cm). The controlled addition of usually small ($\leq 10\%$ w/w) nonstoichiometric quantities of chemical species causes dramatic changes in the electronic, electrical, magnetic, optical and structural properties of the polymer. Doping is reversible with little or no degradation of the polymer backbone. Both doping and undoping processes, involving dopant counterions which stabilize the doped state, may be carried out chemically or electrochemically.

Chemical or electrochemical doping can be divided in *p*-doping, *n*-doping and doping without dopant ions (Photo-doping, Charge-injection doping and Non-redox doping). *p*-Doping is partial oxidation of the π -backbone of an organic polymer, the dopant being an anion. It was first discovered by treating trans-PA with an oxidizing agent such as iodine. During *p*-doping (oxidation) of a conjugated polymer an electron is removed from the polymer film and structural relaxation causes a local distortion of charge in the polymer chain. The twisted benzoid like structure of the affected segments transforms into a quinoid like structure. This form is energetically favorable and functions to stabilize the charge. The quinoid structure possesses a slightly higher energy than the benzoid structure and the conjugated polymer is said to have a non-degenerate ground state. *n*-Doping is partial reduction of the backbone of the π -system of an organic polymer and the dopant being a cation. It was also discovered using trans-PA by treating it with a reducing agent such as liquid sodium amalgam or preferably sodium naphthalide.

In all chemical and electrochemical *p*- and *n*-doping processes discovered for conducting polymers, counter 'dopant' ions are introduced to stabilize the charge on the polymer backbone. Oxidation caused by a chemical species generates a positively charged conjugated polymer and an associated anion. Reduction similarly generates a negatively charged conjugated polymer and an associated cation. Redox reactions in conjugated polymers introduce charges into the polymer material and in order to maintain electroneutrality counter ions are incorporated. Both ionic species and solvent molecules are transported into and out of the film during redox reactions.

1.7 Types of Conducting Polymers

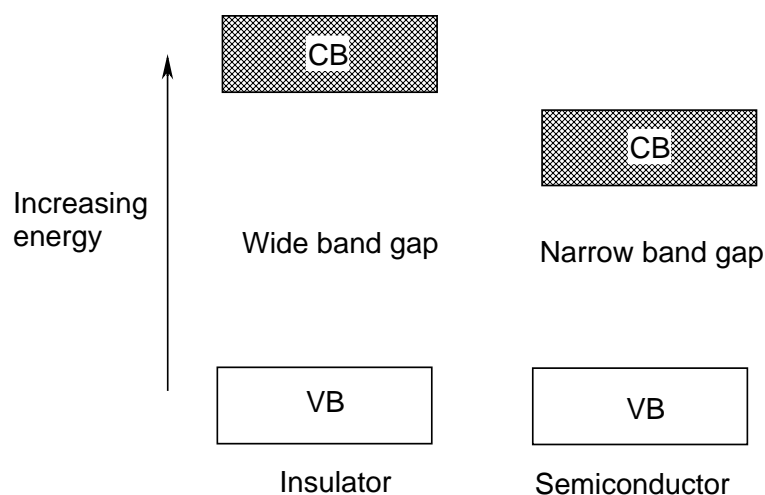
There are generally considered to be four main types of conducting polymers on the basis of their conduction mechanism [57]. The first and commercially important are “composites”. In composites the filling of polymer matrix, which is originally nonconducting, with a powdered conductive medium such as metal or carbon gives rise to conductivity. These composite polymers are used as antistatic coatings, substitutes for solder and many other applications. The second group of polymers is called “ionically conducting polymers”. They are organic polymers in which electric charge is carried by ions. These systems involve dissolution and solvation of salts in a polymer matrix. The polymer solvates the ion and facilitates ion separation. The ions are sufficiently mobile to move along the polymer when an electric field is applied. Polyethylene oxides, in which lithium ion is mobile, are example. These polymers are gaining importance in the battery industry.

The third and fourth groups are “redox” and “electron conducting polymers”, respectively, and will be discussed extensively in this work. The redox polymers contain immobilized electroactive centers (or redox centers), which, although not in direct contact with one another, can exchange electrons by a “hopping” mechanism. The density of redox centers needs only to be great enough that the probability of electrons tunneling through the insulating barrier is sufficiently high. While the electron conducting polymers consist of alternating single and double bonds, creating an extended π -network. Electron movement within this π -framework is the source of conductivity rather than the hopping observed in redox polymers. Due to the fact that the conductivity arises from the inherent properties of the polymer, these polymers are also known as intrinsically conducting polymers (ICPs). The difference between redox polymers and electron conducting polymers is not always clear-cut. However, in electron conducting polymers, conduction within one polymer chain is based on the conjugated nature of the polymer molecules and the resulting mobility of π -electrons, not on immobilized redox centers.

1.8 Conduction Mechanism in Conjugated Polymers

A major obstacle to the rapid development of conjugated polymers is the lack of understanding of how electrical current passes through them. Conjugated polymers have one thing in common, they contain extended π -conjugated systems. A basic research goal in

this field is to understand the relationship between the chemical structure of the repeat units of the polymer and its electrical properties. Such an understanding would enable the electronic and mechanical properties of these materials to be tailored at the molecular level. The electrical properties of a material are determined by its electronic structure. In the solid state, the atomic orbitals of each atom overlap with the same orbitals of their neighboring atoms in all directions to produce molecular orbitals similar to those in small molecules. The large number of orbitals involved in the solid state are spaced together in a given range of energies, which give rise to continuous energy bands. The highest occupied molecular orbital forms the valance band and lowest unoccupied molecular orbital forms the conduction band (Fig. 1.2). The energy spacing between the valance and conduction band is called band gap. If the band gap is narrow, at room temperature thermal excitation of electrons from the valance band to the conduction band gives rise to conductivity. This is what happens in classical semiconductors. In insulators the band gap is too wide and thermal excitation at room temperature is insufficient to excite electrons across the gap [58]. In metals the empty orbitals are very close in energy to the highest occupied molecular orbital (Fermi level) of the occupied levels, so it requires hardly any energy to excite the uppermost electrons. Some of the electrons are therefore very mobile and account for the high electrical conduction of metals.



VB = Valance band, CB = Conduction band

Fig. 1.2 Schematic diagram of valance and conduction bands of solid materials.

Conjugated polymers are peculiar in that they conduct current without having a partially empty or partially filled band. Their electrical conductivity cannot be explained well

by simple band theory. For example, simple band theory cannot explain why the charge carriers, usually electrons or holes, in conjugated polymers are spinless. To explain some of the electronic phenomena in these organic polymers, concepts from physics that are new for chemists, including solitons, polarons and bipolarons, have been applied to conducting polymers.

When an electron is removed from the top of the valance band of a conjugated polymer a vacancy (hole or radical cation) is created that does not delocalize completely, as would be expected from classical band theory. Only partial delocalization occurs, extending over several repeat units and causing them to structurally deform. This radical cation has a higher energy than the energies in the valance band. In other words, its energy is in the band gap. In solid state physics, a radical cation that is partially delocalized over some polymer segment is called polaron (Fig. 1.3).

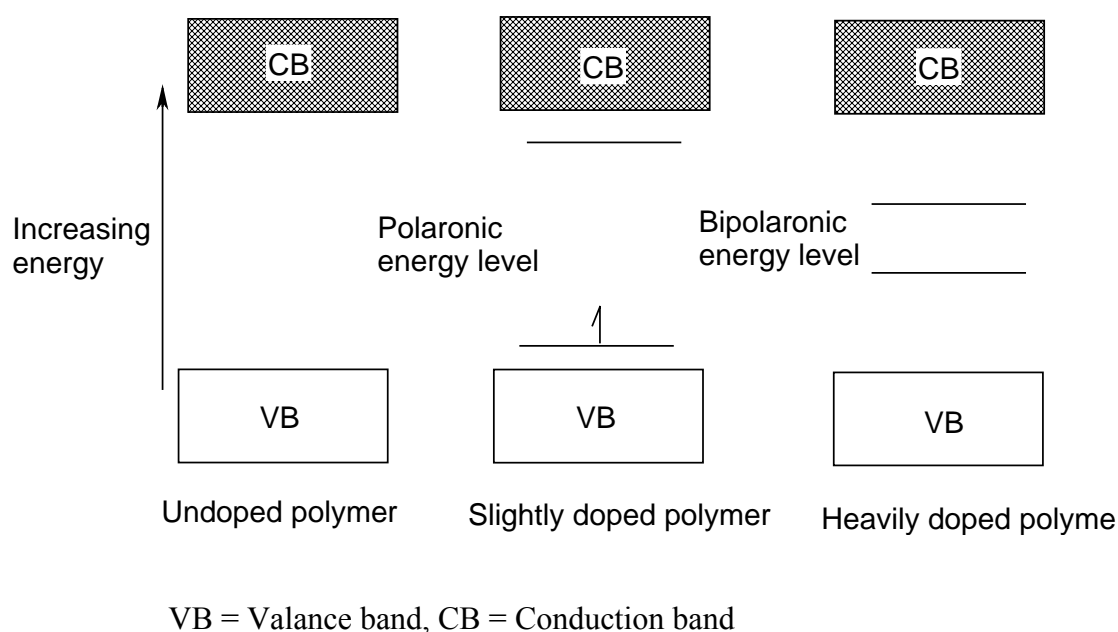
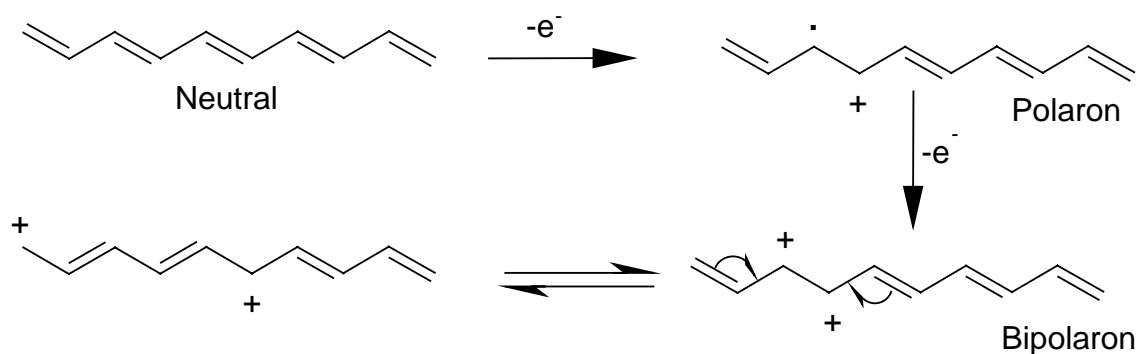


Fig. 1.3 Schematic diagram of polaronic and bipolaronic states of conducting polymers.

When a second electron is removed from the system, it may come from either a different segment of the polymer chain creating another polaron, or from the first polaron to generate a dication that is known as bipolaron. A bipolaron is also associated with struc-

tural deformation and the two charges are not independent but act as a pair. Application of an external electric field makes both polaron and bipolaron mobile via the rearrangement of conjugation. Scheme 1.1 exemplifies the neutral, polaronic and bipolaronic states of PA.



Scheme 1.1 Polaronic and bipolaronic states of polyacetylene.

1.9 The Most Commonly Studied Conjugated Polymers

For the last three decades a large effort on the development of conducting polymers has continued to accelerate at a rapid rate. A variety of new polymers such as polythiophene (PT), polypyrrol (PPY), polyphenylene (PP), polyphenylenevinylene (PPV), polysulfone (PS), polyaniline (PANI) etc, and their derivatives have been discovered. These polymers have been applied in a really impressive application range in different fields such as in batteries [59, 60, 61], electromagnetic shielding [62], energy storage systems [63], corrosion protection [64], electrochemical chromatography [65], electrochromic devices [66], optical and electronic devices [67, 68], sensors [69, 70, 71] and so on [72, 73, 74, 75, 76]. Structural formula of some commonly encountered conjugated polymers is shown in Fig. 1.4. Among these polymers PANI is presumably the most widely studied conjugated polymer.

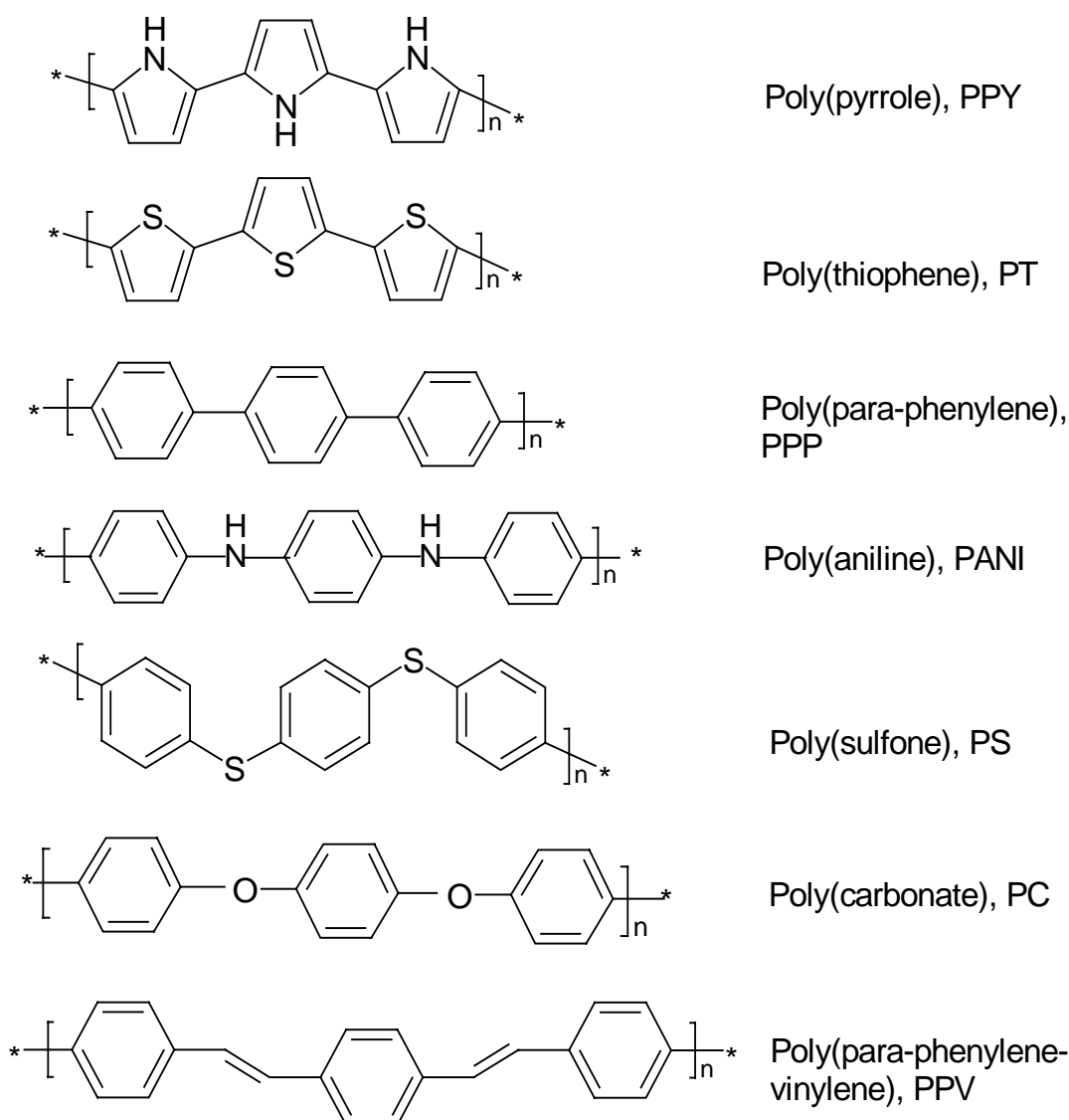
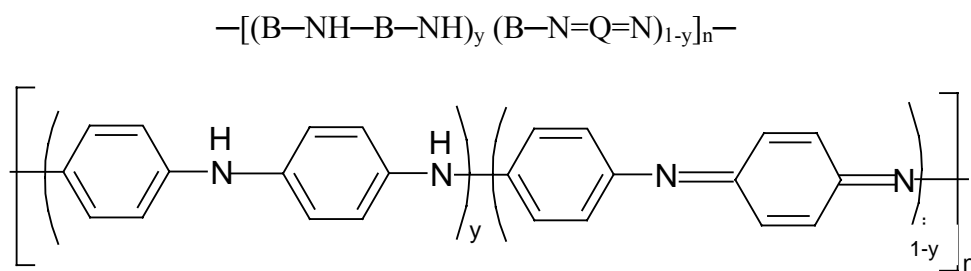


Fig. 1.4 Chemical structures of some common conjugated polymers.

1.10 Polyaniline

Polyaniline occupies the most important place in the very promising class of ICPs. It is unique and has been in the forefront of the global search because of its low cost, ease of preparation, chemical stability, variable electrical conductivity, well behaved electrochemistry, electrochromic effects as well as excellent environmental stability [66, 77, 78, 79, 80]. In addition to chemical and electrochemical syntheses, PANI can also be polymerized by inverse emulsion polymerization [18, 81, 82], plasma polymerization [27, 83] and autocatalytic polymerization [84]. PANI is represented by the general following formula and structure, where B denotes a benzoid reduced unit and Q is a quinoid oxidized unit.



PANI exists in various oxidation states characterized by the ratio of amine to imine nitrogen atoms [85, 86, 87]. When $y = 1$, the polymer is in the fully reduced leucoemeraldine (LE) state and is found to be insulating and yellow. The half oxidized polymer ($y = 0.5$) is called emeraldine base (EB) and is insulating and blue. The only conducting state of PANI is the green colored emeraldine salt (ES), which is the protonated form of EB [88]. The ES may be viewed as a polaronic lattice that confers metallic properties to the polymer [86, 89]. Finally, pernigraniline base (PN) is the fully oxidized form of PANI ($y = 0$) and is insulating and purple. It is obtained from the oxidation and deprotonation of polaronic lattice. All these oxidation states of PANI are shown in Fig. 1.5.

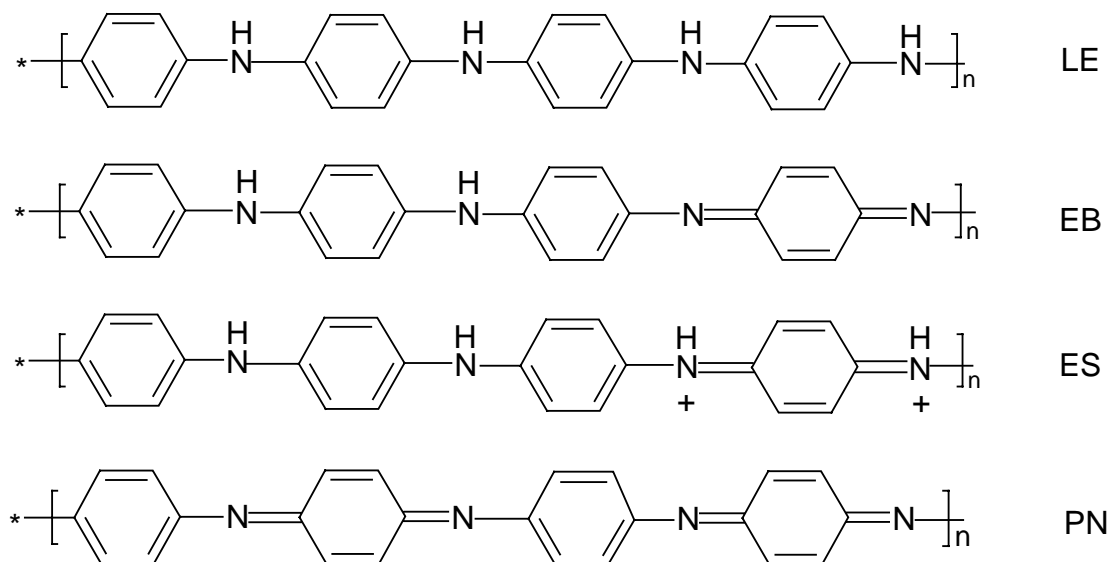
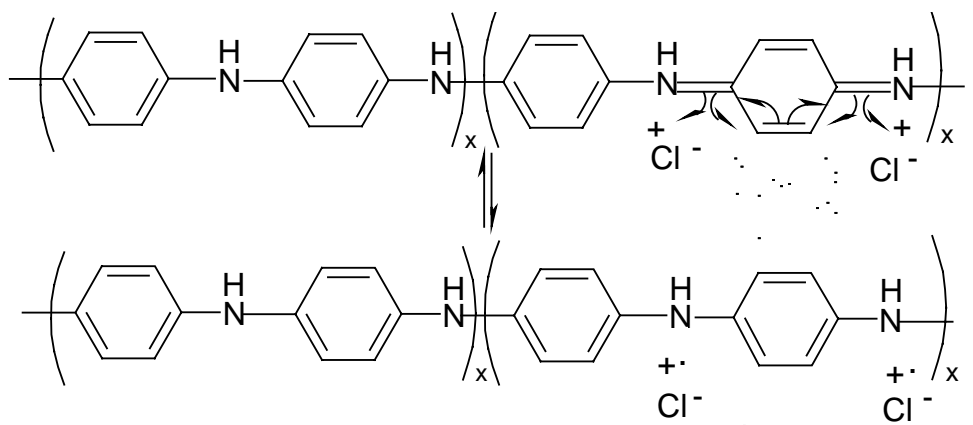


Fig. 1.5 Different oxidation states of PANI, leucoemeraldine (LE), emeraldine base (EB), emeraldine salt (ES) and pernigraniline (PN).

Another distinguishing property of PANI is its unique doping behavior. In addition to normal oxidative doping of conducting polymers, PANI can also be doped protonically. The oxidative doping of PANI involves the removal of electrons from the polymer chain (analogous to p-type doping, see Section 1.6). The totally reduced leucoemeraldine state of PANI can be oxidatively doped to the conductive emeraldine state either by chemical or electrochemical means. The progressive oxidative doping of leucoemeraldine base to emeraldine salt and finally to pernigraniline by electrochemical means can be clearly observed using cyclic voltammetry.

The protonic doping involves the doping of a conjugated polymer to its conducting regime without any change in the number of electrons associated with the polymer. PANI was the first well-established example of such kind of doping. This was accomplished by treating the emeraldine base with aqueous protonic acids. For example, emeraldine base can be doped by HCl to yield the conducting emeraldine hydrochloride as shown in the scheme below. The dication can form a resonance structure, consisting of two separated polarons.



Scheme 1.2 Protonic doping in PANI.

The ability of PANI to exist in various forms via acid/base treatment and oxidation/reduction, either chemically or electrochemically, has made PANI the most tunable member of the conducting polymer. PANI finds wide variety of applications in different fields [62, 63, 65, 68, 69, 71]. However, PANI has a rigid backbone originating from an extended conjugated double bond [90]. The rigid structure of PANI restricts its common usage and results in the insolubility, infusibility and incompatibility of this material with common polymers. This necessitates the modification of the structure of PANI. Therefore, during the past decade researchers have directed their attention to modify PANI structure and to

overcome the difficulties associated with the use of PANI by using different approaches. For example the utilization of a soluble precursor method, in which a processable precursor polymer is first prepared in an appropriate form and then chemically converted into the final conducting polymer [91, 92, 93]. Another approach is the formation of conductive blends/composites [94, 95, 96, 97] or the formation of PANI filled interpenetrating polymer networks [98, 99, 100]. Efforts have been made to improve the properties of PANI through the post treatment of PANI such as sulfonation or incorporation of N-alkylsulfonic acid pendant group [101, 102], the use of functional dopants [103] and the design of self-doping polymer [101, 104]. Extensive studies on the polymerization of aniline (ANI) derivatives and/or the polymerization of ANI in the presence of another monomer (copolymerization) have also been carried out frequently in order to improve the properties of PANI.

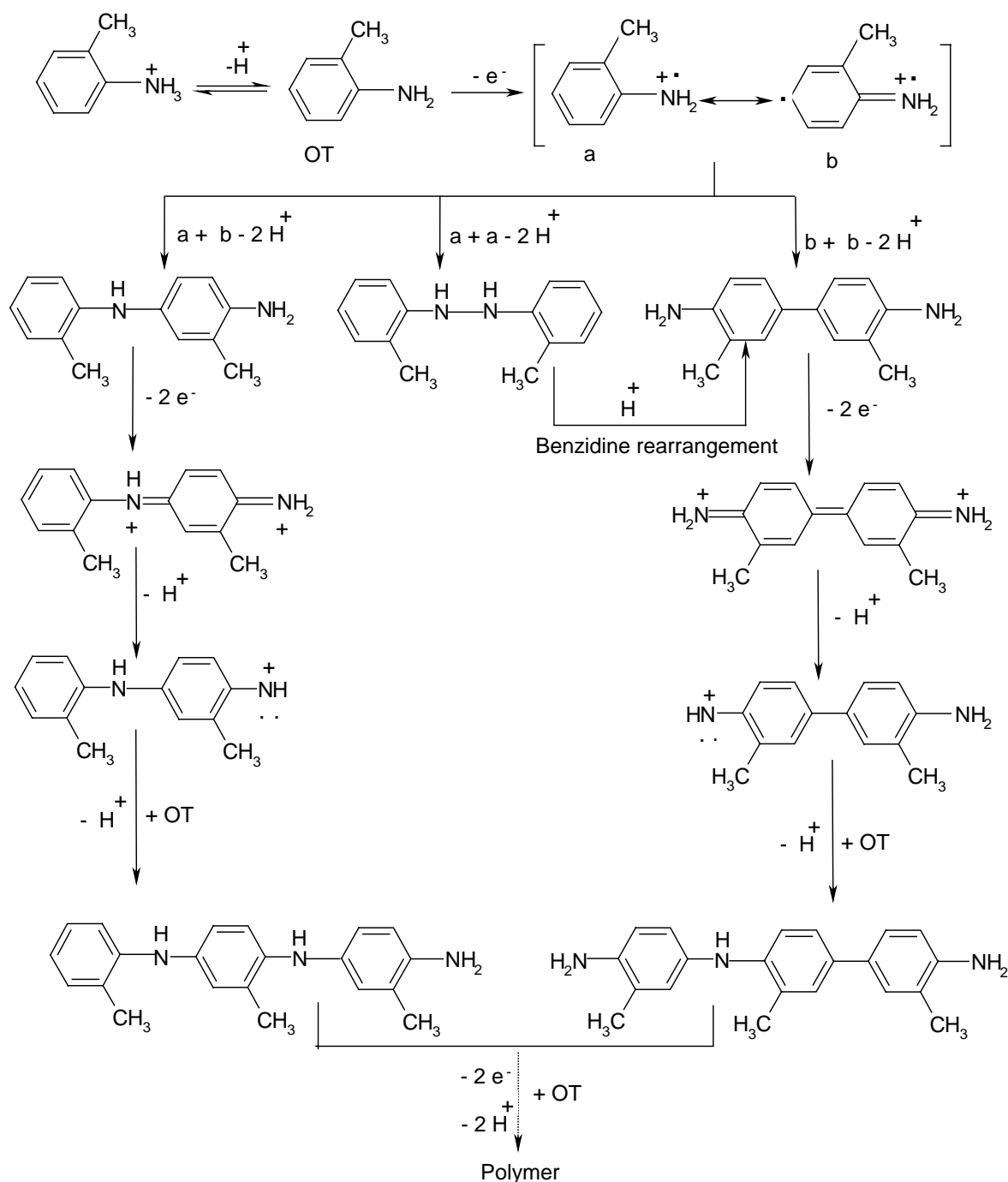
1.11 Substituted Anilines

The success of PANI has attracted many investigators to study the synthesis and properties of the polymers from aniline (ANI) derivatives. One of the ways to make derivatives of PANI is to polymerize substituted anilines. Electrochemical or chemical polymerization of ring- or *N*-substituted ANI has been effectively used for the preparation of substituted PANIs. It has been shown that toluidines [105, 106, 107, 108, 109], phenylenediamines [110, 111], alkoxyaniline [112,113], halogenated anilines [114], aminophenols [115, 116, 117, 118, 119], aminobenzenesulfonic acid [101, 102, 120], aminopyrene [121], diphenylamines [122, 123], 1-amino-2-pyridine [124], *N*-alkylaniline [20, 125], *N,N*-dimethylaniline [126, 127] and *N*-phenylaniline [128] can be used to form interesting semi-conducting polymers.

1.11.1 Toluidines

Toluidines are derivatives of ANI where a $-\text{CH}_3$ group is substituted in the aromatic ring at *o*-, *m*- or *p*-position. A number of reports are available on the studies of polytoluidines [78, 107, 108, 129, 130, 131]. The polymers derived from *o*-toluidine (OT) and *m*-toluidine (MT) are important because the redox and electrochromic behavior of these polymers is closely similar to that of PANI. However, poly(*o*-toluidine) (POT) and poly(*m*-toluidine), (PMT) are anticipated to be more soluble in comparison with PANI [78, 107, 132, 133].

The first chemical synthesis of POT was achieved by Green and Woodhead in 1910 as an analogue of PANI [134]. Following the analogy with the polymerization of ANI, the polymerization of toluidine is a bimolecular reaction involving a radical cation intermediate (Scheme 1.3). The radical coupling of various resonance forms of the radical cation results in head to head (*N,N*-diphenylhydrazine) and tail to tail (benzidine) as minor by-products [135] in addition to the normal head to tail (*p*-aminodiphenylamine, PPD) coupling.



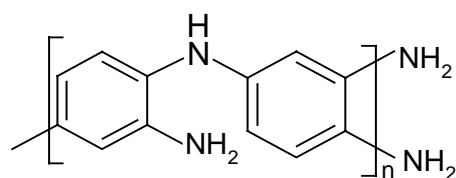
Scheme 1.3 Electropolymerization mechanism of toluidine.

Since *N,N*-diphenylhydrazine type dimer undergoes benzidine rearrangement reaction in the acidic media, the benzidine and *p*-aminodiphenylamine type dimers will mainly contribute to the growth of the polymer chain. Soon after formation, the two dimers will be oxidized to their diimine forms, which could be deprotonated to afford nitrenium ions. An electrophilic attack of toluidine monomer by the diimines or nitrenium ions would accomplish a growth step and lead eventually to the final polymer.

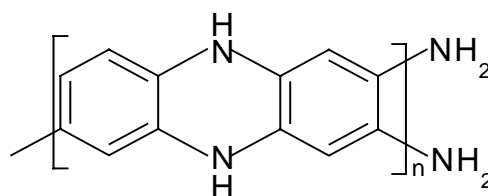
The conductivities and rate of polymerization of POT and PMT has been reported to be lower than that of PANI, which are considered to be due to the effect of methyl group on the phenyl ring in polytoluidines [107]. The substituent on the phenyl ring increases the torsional angle between adjacent rings to relieve the steric strain, which may contribute to the lower conductivities in polytoluidines as compared to unsubstituted PANI [136].

1.11.2 Phenylenediamines

It is believed that the investigation of polymers synthesized from aromatic diamine are more attractive since they exhibit more novel multifunctionality than PANI. Phenylenediamines are a class of ANI derivatives having an extra -NH_2 group in the *o*-, *m*- or *p*-position. Although reports are available on polymerization of *m*- and *p*- isomers [137], *o*-phenylenediamine (OPD) is the most frequently studied member. Poly(*o*-phenyldiamine) (POPD) has apparently shown different characteristics of molecular structure and properties when compared with PANI [138]. It has been reported to be a highly aromatic polymer containing 2,3-diaminophenazine or quinoxaline repeat unit and exhibits unusually high thermostability [137, 139, 140] although a PANI like structure has also been proposed [141].



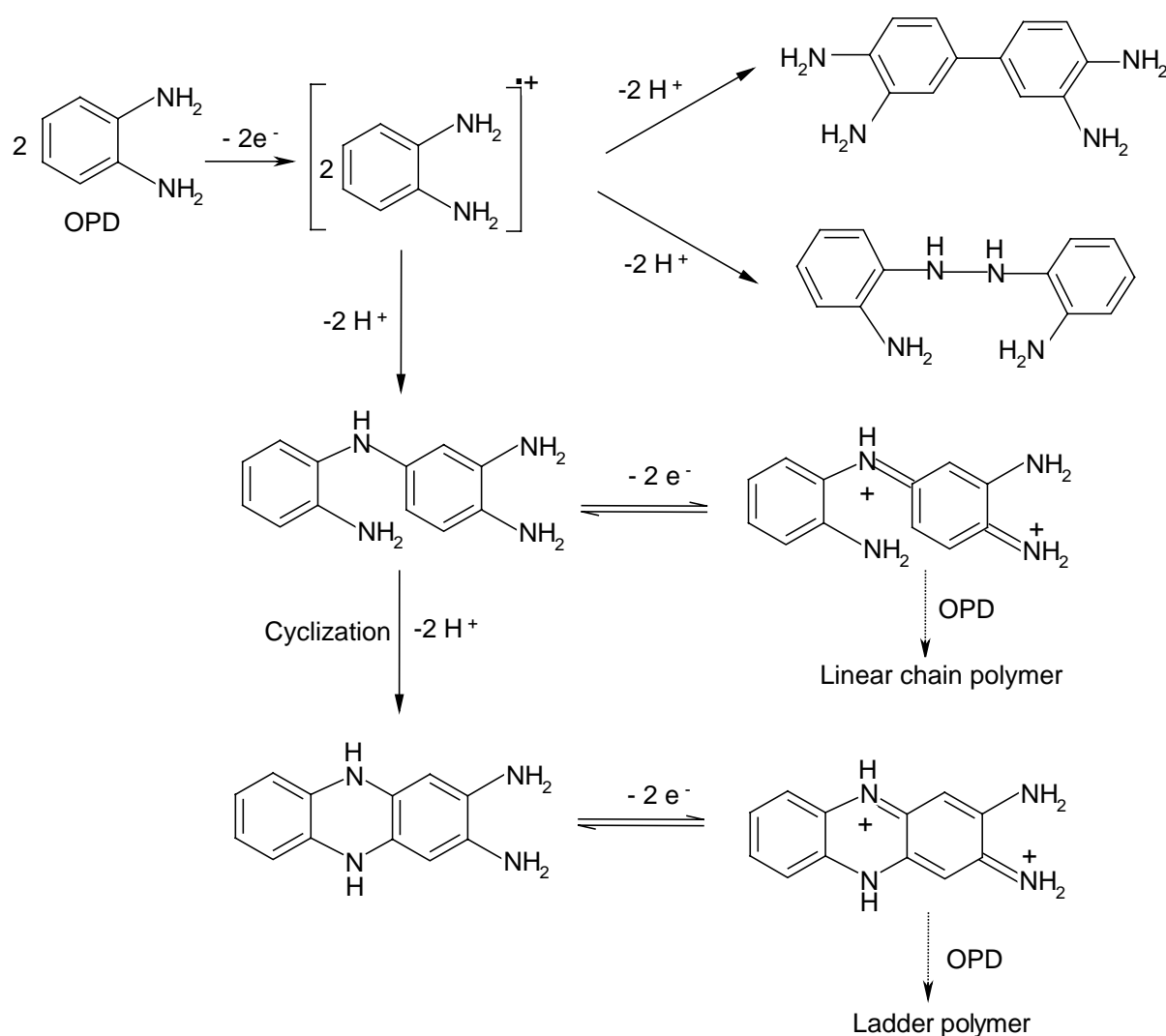
PANI like structure



Phenazine like structure

It has been suggested that the first stage of the electropolymerization mechanism of OPD is the monomer oxidation to the corresponding radical cation, followed by radical coupling (head-to-head, head-to-tail and tail-to-tail) yielding conceivably three different

dimers that can be further oxidized [142] (Scheme 1.4). The dimers arising from tail to tail and head to head coupling play a very minor role [143]. The head to tail dimer of OPD may be involved in two competitive processes: (a) further radical coupling leading to chain propagation as in formation of PANI and (b) internal coupling (cyclization) leading to phenazine type structures.



Scheme 1.4 Electropolymerization mechanism of *o*-phenylenediamine.

However, it has been demonstrated that the formation of a ladder type polymer from *p*-phenylenediamine goes through the formation of a linear structure, which then becomes a ladder type configuration and this is the only product obtained [137]. Works based on infrared, Raman and UV-Vis spectroscopies, quartz crystal microbalance, radiometry and electrochemical techniques have also led to the hypothesis of phenazine type structure of

POPD [144, 145, 146, 147, 148, 149, 150]. POPD has a variety of applications in the field of electrochromism [141], sensors [151, 152, 153], rechargeable batteries [154] and corrosion protection [155].

1.12 Electroactive Copolymers

Next to PANI and polysubstituted ANIs, a great deal of attention has been paid to copolymers based on aniline or substituted aniline. In recent years electrochemical copolymerization has been developed as one of the most essential and attractive strategies for modifying physical and chemical properties of conducting polymers. It greatly increases the ability of polymer scientists to tailor a material with specific properties. For example copolymerization of ANI with some of its derivatives, which bear various functional groups, leads to modified copolymers. These copolymers show electrochemical characteristics reasonably different from those of the homopolymers [38, 104, 146, 156, 157, 158, 159, 160, 161, 162, 163, 164, 165]. Consequently copolymerization is also considered to be an important method to improve the properties of homopolymers.

With respect to ANI based copolymers pioneering work was carried out by Wei et al. [78]. They reported that ANI could be polymerized with *o*-toluidine yielding a copolymer film with a conductivity, which could be controlled over a broad range of electrode potentials. Pekmez-Ozcicek et al. [166] reported that incorporation of ANI units within polythiophene chains led to copolymers having an increased range of electrochemical stability. Similarly, small quantities of 2-fluoroaniline and 2-chloroaniline have been demonstrated to have a dramatic effect on the conductivities of poly(aniline-co-2-fluoroaniline) and poly(aniline-co-2-chloroaniline) [160].

Monomers bearing sulfonate, alkylsulfonate and carboxylate groups were copolymerized with ANI, yielding self-doped copolymers [167, 168, 169, 170]. These do not need anions from a solution for doping during their redox reaction. Savitha and Sathyanarayana chemically synthesized copolymers of ANI with *o*-/*m*-toluidine and reported that copolymers have better stabilities and comparatively higher conductivities than the homopolymers [171]. They have also synthesized copolymers of *o*-nitroaniline (which does not homopolymerize under conditions employed for the polymerization of aniline and its derivatives) with *o*-/*m*-toluidine and reported better solubilities of the copolymers in DMSO, DMF, *N*-dimethylpyrrolidone (NMP) and tetrahydrofuran (THF) and higher conductivities, than the homopolymers [172]. Malinauskas et al. [146] electrochemically synthesized co-

polymers and bilayer structures of polyaniline and poly(*o*-phenylenediamine). Electrochemical copolymerization of aniline with *p*-phenylenediamine was reported to enhance drastically the copolymerization rate [163], whereas its isomer *m*-phenylenediamine caused an opposite effect [161]. Thus copolymerization could provide a convenient synthetic method and process for preparing new conducting materials with improved properties.

1.13 Aims and Tasks of the Work

A call for novel material, new ideas, applications and techniques is still and will be challenging all the time. The increased development of science and modern technology allows one to use a high-throughput search for novel materials that could give positive feedback in different areas of life. The wide scope of tuning different properties of PANI triggered us to explore possibilities of copolymerization of toluidine with phenylenediamine, both being substituted anilines. A close analysis of the literature shows a large number of reports on the chemical and electrochemical synthesis of polytoluidine, polyphenylenediamine and their copolymers with aniline and other substituted anilines [78, 107, 108, 146, 171, 172]. These homo- and copolymers have also been tested for various applications in sensors [151, 173], in corrosion inhibition [155] and in rechargeable batteries [154]. So far there is no report on the chemical or electrochemical copolymerization of phenylenediamine with toluidine.

The present study describes the electrochemical copolymerization of *o*-/*m*-toluidine with *o*-phenylenediamine. Cyclic voltammetry was used for the synthesis of homo-/copolymers. The electrochemical growth characteristics of the copolymers were compared with those of the corresponding homopolymers in order to obtain evidence for copolymer deposition when a mixture of monomers was used. *In situ* conductivities were measured in order to identify the variations in the conductivities of homopolymers and copolymers and supporting the assumption of true copolymers instead of merely mixed homopolymers being electropolymerized. In addition to this, *in situ* spectroelectrochemical studies were carried out to get information about any changes in the spectroelectrochemical response of the copolymers in comparison with the homopolymers. Additional evidence needed for suggesting a molecular structure of the electrosynthesized copolymers was obtained with FT-IR spectroscopy (*ex situ*).

2 Experimental

2.1 Chemicals and Solutions

Reagent grade *o*-/*m*-toluidine (Merck) was distilled under vacuum, the resulting colorless liquid was stored under nitrogen. *o*-Phenylenediamine (Merck) was used as received. Ultrapure water (Seralpur pro 90 C) was used for the preparation of solutions. H₂SO₄, Na₂SO₄ and NaOH were from Merck.

A 1.5 M H₂SO₄ solution was used for the preparation of monomer solutions. Electrolysis of OT was carried out from a 0.1 M solution while the electrolysis of MT was performed from solution of two different concentrations, i.e. 0.1 and 0.2 M. Electropolymerization of OPD was carried out from five different solutions of varying OPD concentration ranging from 0.01 to 0.05 M. Copolymerization was done using various solution systems having different concentrations of OPD and a constant concentration of OT or MT in the feed. These solutions were labeled as system OTA (0.01 M OPD + 0.1 M OT), system OTB (0.02 M OPD + 0.1 M OT), system OTC (0.03 M OPD + 0.1 M OT), system OTD (0.04 M OPD + 0.1 M OT) and system OTE (0.05 M OPD + 0.1 M OT), respectively, when OT was used as a comonomer. In the case of MT as a comonomer the solution systems were labeled as system MTA (0.01 M OPD + 0.2 M MT), system MTB (0.02 M OPD + 0.2 M MT), system MTC (0.03 M OPD + 0.2 M MT), system MTD (0.04 M OPD + 0.2 M MT) and system MTE (0.05 M OPD + 0.1 M MT), respectively.

2.2 Electrochemical Measurements

Electrochemical polymerization and copolymerization were carried out potentiodynamically by cycling the potential in the range of $-0.2 < E_{\text{SCE}} < 0.85$ V for OT and MT and $-0.3 < E_{\text{SCE}} < 0.85$ V for OPD and copolymers at a scan rate of 50 mV/s. A three-electrode cell was used with a saturated calomel reference electrode. Gold sheets served as working and counter electrodes. The surface area of the working electrode was 2.0 cm². Electrochemical synthesis and characterization were carried out under nitrogen atmosphere. Cyclic voltammetry studies were performed with a custom-build potentiostat with general-purpose electrochemical system software. Cyclic voltammograms of the growing films were recorded continuously during synthesis. The deposited films of homo-/copolymers were washed with deionized water and subsequently placed in the monomer free background electrolyte solution wherein CVs of the film-coated electrode were recorded. The

CVs of the homo-/copolymer films were recorded in their respective potential ranges at various scan rates. The dependence of electrochemical activity of polymers on pH was studied in 0.2 M Na₂SO₄ adjusted with H₂SO₄ and NaOH to different pH values. The pH of the electrolyte solution was controlled by using a MV81 Präcitronic pH meter calibrated with standard buffer solutions.

2.3 *In situ* Conductivity Measurements

For *in situ* conductivity measurements the polymers were deposited on a double-band gold electrode [31] in a three-electrode cell under nitrogen atmosphere. The resistivities were measured with a specially designed electronic circuit described elsewhere [32]. During measurements a dc voltage of 10 mV was applied to the double-band electrode. The current flowing across the band was measured with a I/V converter with an amplification factor F_{ac} ranging from 10^2 to 10^6 . The film resistance R_x is related to the measured voltage U_x and the amplification factor F_{ac} according to

$$R_x = (0.01 \times F_{ac}) / U_x$$

Electrode potential was increased stepwise by 50 mV and after approximately 5 minutes the electrochemical cell was cut off from the potentiostat and stable value of U_x was recorded.

2.4 UV-Visible Spectroelectrochemical Measurements

In situ UV-Vis spectroelectrochemical studies were performed using a spectroelectrochemical cell containing an optically transparent ITO coated glass as working electrode, a platinum wire and saturated calomel electrode as counter and reference electrode, respectively. The electropolymerization process was carried out in a quartz cuvette of 1 cm path length assembled as an electrochemical cell by keeping the working electrode (ITO coated glass electrode with a specific surface resistance of 10-20 $\Omega \text{ cm}^{-2}$) perpendicular to the light path. The reference electrode was connected to the cuvette with a salt bridge. In the reference channel of the spectrometer a quartz cuvette containing an ITO coated glass electrode without polymer coating was inserted. Before each experiment, the ITO coated glass sheets were degreased with acetone and rinsed with plenty of ultrapure water. Before each

spectroscopic measurement base line correction was made. A constant potential of $E_{\text{SCE}} = 1.0 \text{ V}$ was applied by using the custom-build potentiostat. UV-Vis spectra were collected continuously at different polymerization times for the pure and mixed solutions of the monomers and at different applied potentials for the respective polymer films, with a PC-driven Shimadzu UV-2101 PC scanning spectrometer (resolution 0.1 nm).

2.5 Raman Spectroelectrochemical Measurements

In situ Raman spectroelectrochemical studies were performed in a three-compartment cell containing an aqueous electrolyte solution of 1.5 M H_2SO_4 , purged with nitrogen for a few minutes prior to the measurements, and a gold disc as the working electrode. Before each experiment, the working electrode was polished with fine grade alumina and ultrasonicated for a few minutes in ultrapure water. A gold sheet and a saturated calomel electrode were used as counter and reference electrodes, respectively. The Raman spectra obtained were slightly smoothed and baseline-corrected. Raman spectra were recorded by using an ISA 64000 spectrometer equipped with a liquid nitrogen cooled CCD camera detector at a resolution of approximately 2 cm^{-1} . Samples were illuminated with 647.1 nm laser light from a Kr^+ -ion laser Coherent Innova 70. The laser power delivered at the sample was held at 50 mW.

2.6 Fourier Transform Infrared Spectroscopical Measurements

For FT-IR experiments the polymers were deposited potentiostatically in a three-electrode setup. The polymer films were peeled off in their completely oxidized state from the electrode surface, washed with plenty of deionized water and then dried at 100°C . FT-IR spectra were recorded with a Perkin Elmer FT-IR-1000 spectrophotometer and KBr pellets at 2 cm^{-1} resolution (8 scans each).

3 Electrochemical Measurements

3.1 Electrochemical Homopolymerization of *o*-/*m*-Toluidine

Fig. 3.1 a shows CVs recorded for the homopolymerization of OT. In the first cycle an irreversible oxidation peak appeared at $E_{\text{SCE}} = 0.84$ V, which corresponds to the oxidation of the monomer. On the second and subsequent scans a reversible process at about $E_{\text{SCE}} = 0.45/0.41$ V is either due to soluble products that may be identified as the dimers [43] or loosely surface bound hydrolysis products such as quinone/hydroquinone [174, 175, 176]. In further potential scans additional reversible systems progressively develop at $E_{\text{SCE}} = 0.28/0.15$ and $0.65/0.62$ V, respectively, and the electrode is covered with a green deposit.

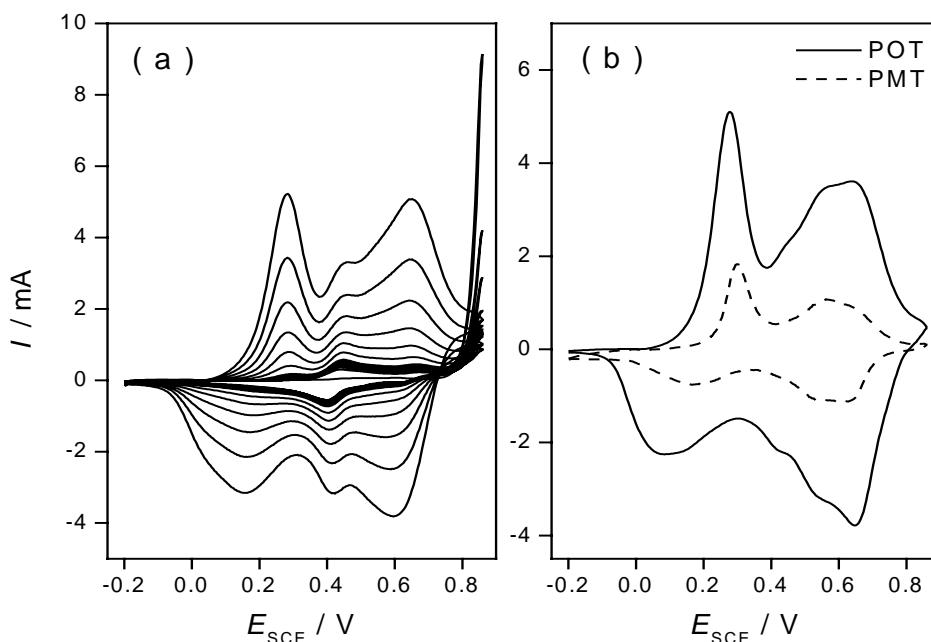
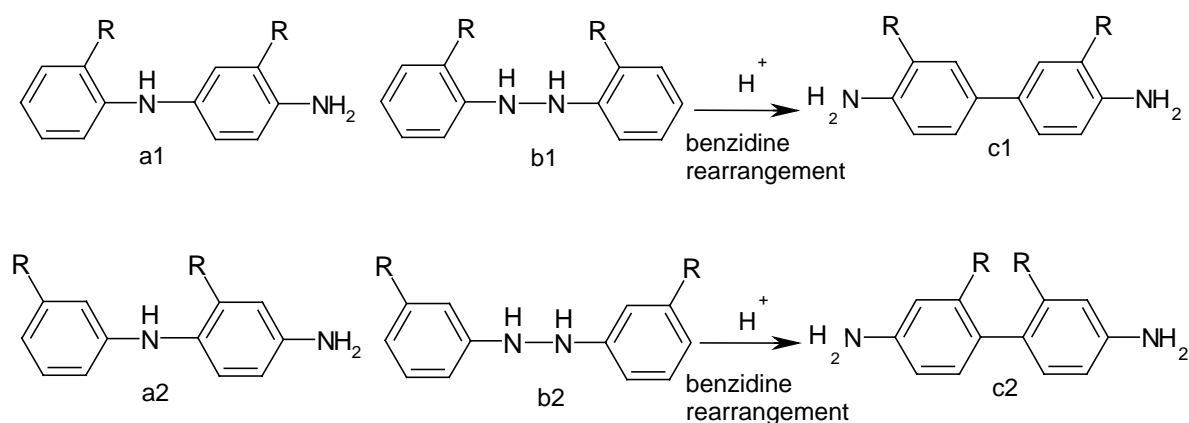


Fig. 3.1 (a) CVs recorded during the growth of POT film (40 cycles) and (b) CVs of POT and PMT films, as indicated, in 1.5 M H_2SO_4 at a scan rate of 50 mV/s.

The peak currents for these peaks increase very quickly with increase in the number of potential cycles especially after 10th cycle. This is probably due to the autocatalytic polymerization that causes quick POT film growth as the electrolysis proceeds [41, 176]. Initially, up to 10th cycle the peak current is nearly constant but once the electrode is covered with POT film it accelerates further growth of the polymer. Comparatively limited potential scans were recorded for POT in order to facilitate the comparison of peak potentials of POT with those of the copolymers and POPD.

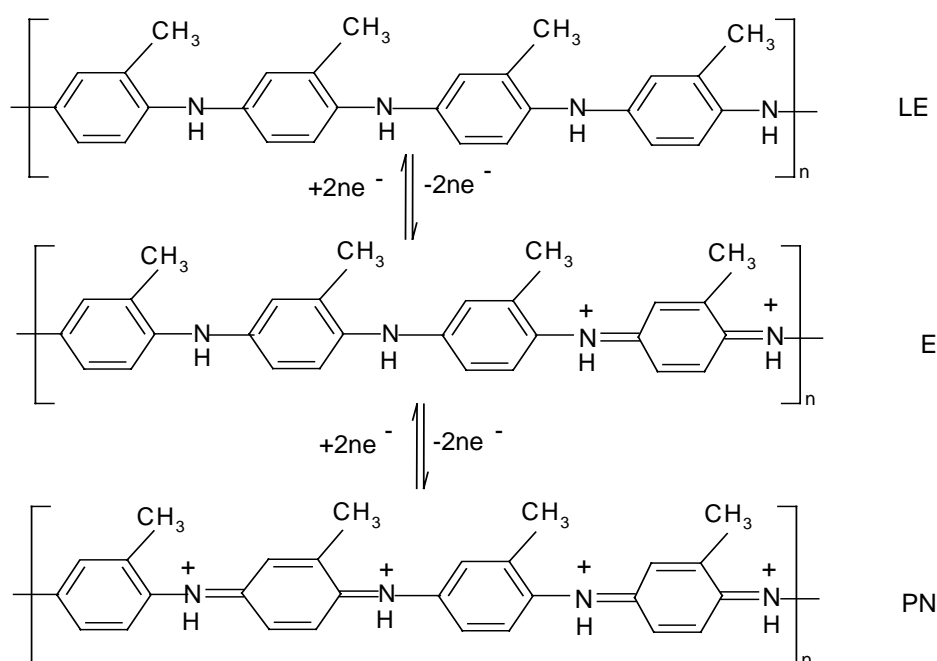
The electrochemical growth behavior of PMT, under identical conditions, is similar to that of POT with little shifting in the redox peak positions. The three redox processes of PMT appear at $E_{\text{SCE}} = 0.29/0.16$, $0.47/0.45$ and $0.56/0.53$ V, respectively, during its growth (Fig. not shown). However, the initial growth rate of the PMT formation was lower than that of POT. The peak current of the redox processes is nearly constant up to 20 cycles and after that the polymer seems to grow quickly. This difference in the initial rate of polymerization between OT and MT monomer could be explained by examining the steric effect of the methyl substituent during the formation of the dimeric species (Scheme 3.1).



Scheme 3.1 Benzidine rearrangement of the dimeric species of OT and MT (R = CH₃).

As already discussed in Section 1.11.1 that *N,N*-diphenylhydrazine type dimers, resulting from head to head coupling of the monomers during electropolymerization of OT and MT (structures b1 and b2, respectively), undergo benzidine rearrangement reaction in acidic media. Therefore, benzidine (structure c1 and c2) and *p*-aminodiphenylamine type dimers (structure a1 and a2) mainly contribute to the initial growth of the polymer. It should be noted that there are two possible growing centers in the benzidine type of dimers but only one in the *p*-aminodiphenylamine type of dimers. Thus the rate of formation of benzidine type of dimers could have a great effect on the initial rate of polymerization of OT or MT. Apparently formation of structure c2 from structure b2 is less favorable than that of structure c1 from structure b1 because of the steric hindrance of the methyl substituent group. This would result in fewer benzidine type molecules (structure c2) generated from benzidine rearrangement of the structure b2. Therefore, the initial rate of polymerization MT is expected to be slower than that of OT [78].

Fig. 3.1 b represents the CVs of POT and PMT-coated electrode in monomer free electrolyte solution. The first anodic peak on the anodic sweep in the respective CV is assigned to the conversion of leucoemeraldine to emeraldine, while the second anodic peak is assigned to the further oxidation of emeraldine to pernigraniline. In the reverse sweep the two cathodic peaks indicate the reduction processes corresponding to respective anodic peaks [175, 177, 178]. The striking similarities between POT and PMT are quite evident from Fig 3.1 b indicating that electropolymerization of OT and MT leads to the same polymer [133]. Scheme 3.2 represents, as an example, the conversion of fully reduced leucoemeraldine form of POT to its fully oxidized pernigraniline form [178].



Scheme 3.2 Reaction scheme for the electrochemical process of POT film in strong acidic electrolyte solution. The reduced leucoemeraldine, emeraldine and pernigraniline forms are indicated as LE, E and PN.

3.2 Electrochemical Homopolymerization of *o*-Phenylenediamine

Fig. 3.2 a shows the CVs of the electropolymerization of OPD from an aqueous solution of 0.02 M OPD in 1.5 M H₂SO₄. In the first anodic sweep a peak corresponding to oxidation of OPD occurs at $E_{\text{SCE}} = 0.68$ V. In subsequent cycling, two redox processes were noticed at round about $E_{\text{SCE}} = 0.00/-0.03$ and 0.40/0.30 V, respectively. The first redox process

showed an increase in peak current with increase in the number of cycles while the second one diminished with continuous potential cycling. At the end of the experiment a bronze-brown film was observed on the working electrode. The growth process or behavior of POPD during electropolymerization for all concentrations of OPD studied (0.01 to 0.05 M) is closely similar with the only difference in the peak current values of the main redox process. Therefore, CVs recorded during electropolymerization of OPD solution are shown only for one concentration (0.02 M).

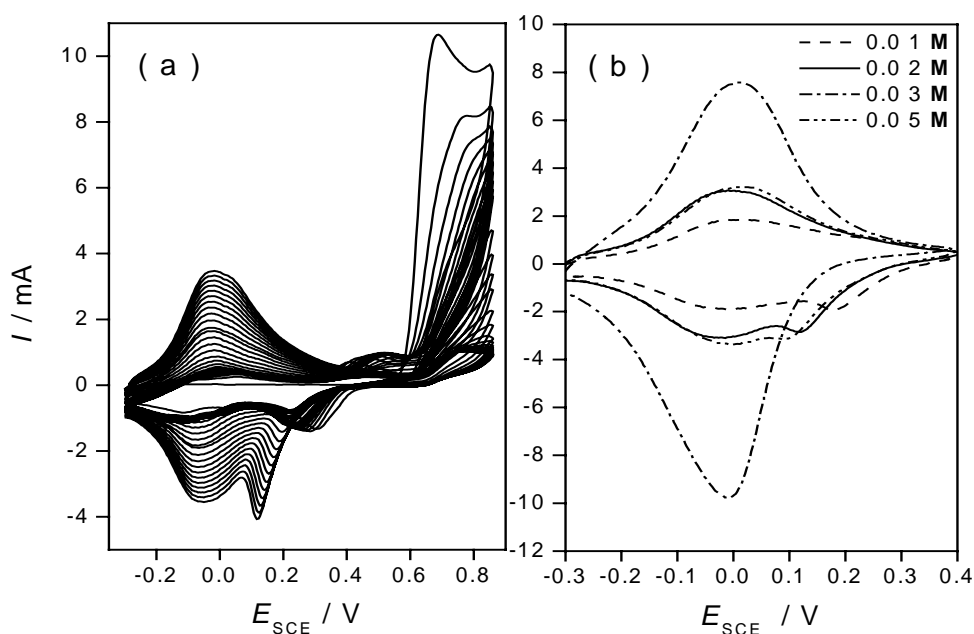
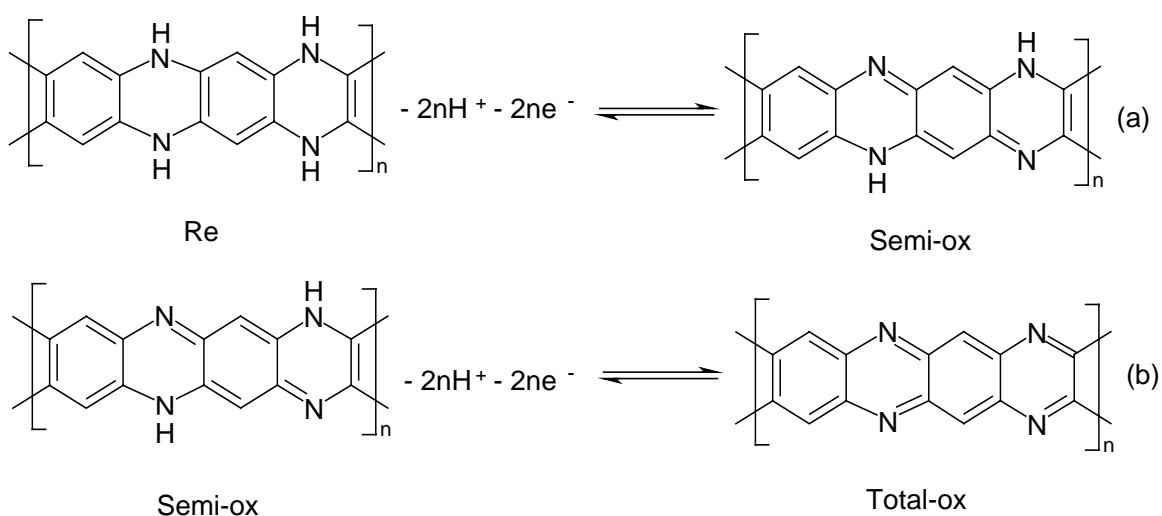


Fig. 3.2 (a) CVs recorded during the growth of POPD film (210 cycles) and (b) CVs of POPD films in 1.5 M H_2SO_4 , synthesized from solutions having different OPD concentrations as indicated, at a scan rate of 50 mV/s.

It was observed during electrolysis of OPD solutions having different concentrations that the anodic peak current of the monomer oxidation in the first cycle increases with increasing OPD concentration and reaches a maximum value with the 0.05 M solution. However, an enhanced and maximum polymer growth occurs from 0.03 M OPD solution. The cathodic shoulder is visible up to 100th cycle in this case and then merged into the main cathodic peak as the number of cycle increases for the polymerization of 0.03 M OPD solution. Above this concentration the polymer growth shows a sudden decrease and saturation.

Fig. 3.2 b shows CVs of POPD films, synthesized from solutions having different concentrations of OPD, in background electrolyte solution. The POPD film exhibits a major redox pair at $E_{\text{SCE}} = 0.00/-0.03$ and a cathodic shoulder at $E_{\text{SCE}} = 0.12$ V [179]. The existence of three redox states of POPD during its redox process has been proposed. The redox pair at $E_{\text{SCE}} = 0.00/-0.03$ V was assigned to the reversible oxidation and reduction of reduced and semioxidized forms (Scheme 3.3 a) and the one at $E_{\text{SCE}} = 0.00/0.12$ V to the oxidation and reduction of the semioxidized and highly unstable totally oxidized forms of POPD (Scheme 3.3 b), respectively [145, 147, 180].



Scheme 3.3 Reaction scheme for the electrochemical process of POPD film in strong acidic electrolyte solution.

3.3 Electrochemical Copolymerization of *o*-Phenylenediamine and *o*-Toluidine

Formation of the copolymer from mixed solutions of OPD and OT can be estimated by comparing the CVs of the electrolysis of mixed solutions with those of pure monomer solutions. CVs recorded during copolymerization were not only apparently different from those recorded for homopolymerization of OPD and OT, but significant differences were also observed with regard to peak potential, peak current values and other growth characteristics. Even among the copolymers, synthesized with different concentrations of OPD in the feed, differences were observed in peak current values and growth characteristics.

Fig. 3.3 a represents the CVs recorded during the electropolymerization of solution system OTB (0.02 M OPD + 0.1 M OT). In the first potential scan an anodic peak ap-

peared at $E_{\text{SCE}} = 0.69$ V, which indicates that OPD undergoes oxidation before OT [161]. However, the peak current value for this peak is much lower than for pure OPD. Unlike with the homopolymers already discussed, in the reverse scan three cathodic peaks centered at $E_{\text{SCE}} = -0.03$, 0.30 and 0.50 V can be observed. This indicates that subsequent to OPD oxidation, reaction with OT and/or OT cation radicals (at $E_{\text{SCE}} > 0.70$ V) results in dimer/oligomer formation [181]. In the second potential scan three anodic peaks at $E_{\text{SCE}} = 0.00$, 0.40 and 0.55 V with corresponding cathodic peaks were observed. On subsequent potential cycling these peaks grow at a slower rate than the peaks of the homopolymers (Fig. 3.1 a and 3.2 a). Up to the 100th cycle, anodic peaks at $E_{\text{SCE}} = 0.40$ and 0.55 V nearly merge into one and their corresponding cathodic peaks grow very slowly. After about 100 cycles a new redox pair appears at $E_{\text{SCE}} = 0.31/0.22$ V. The anodic and cathodic peaks of this pair shift into positive and negative directions, respectively, with further potential scans.

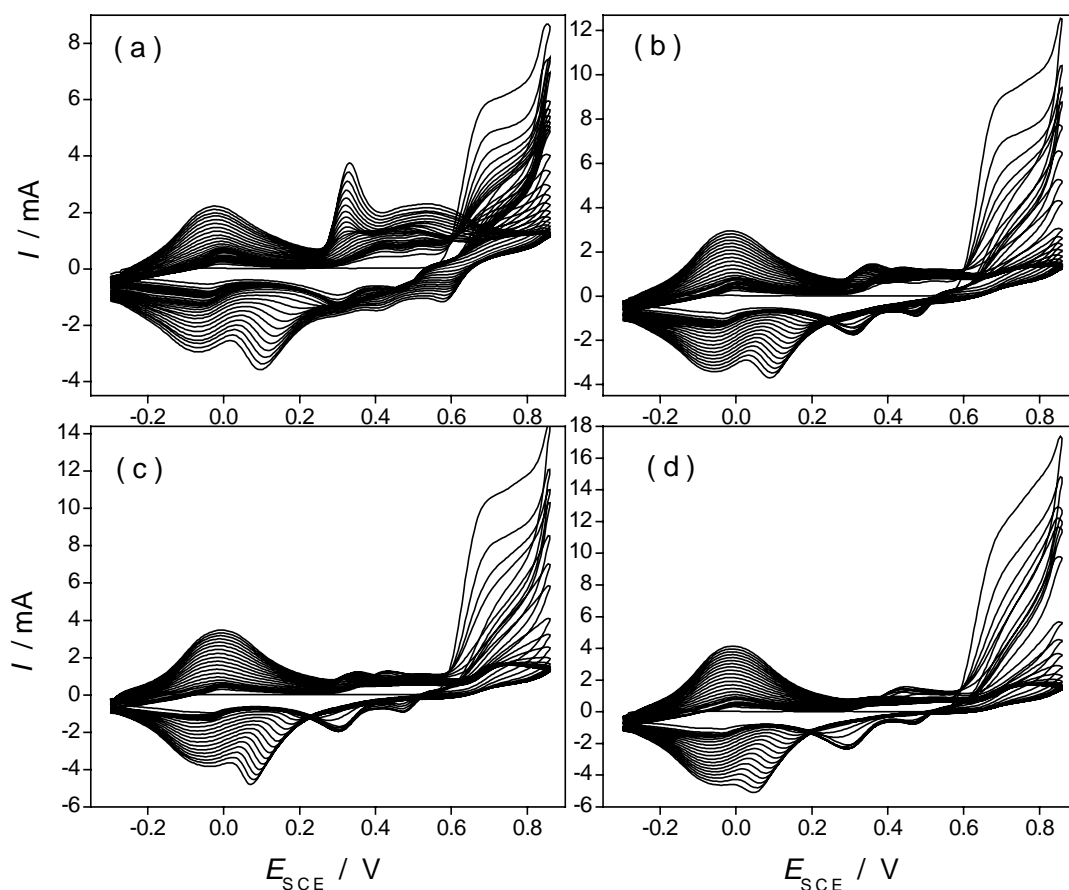


Fig. 3.3 CVs recorded with the growth of copolymer films (210 cycles) from solution system (a) OTB, (b) OTC, (c) OTD and (d) OTE, at a scan rate of 50 mV/s.

It is important to note that almost all anodic and cathodic peaks that appeared in the second cycle show a shift either to positive or negative potentials with subsequent cycling. Finally four redox pairs at $E_{\text{SCE}} = -0.03/-0.06$, $0.33/0.13$, $0.46/0.41$ and $0.55/0.58$ V, respectively, are observed. After electrolysis a light golden-brown deposit was observed on the electrode. Obviously peak potentials, number of redox pairs and overall growth process of the copolymer synthesized from solution system OTB are completely different from the growth process of the homopolymers synthesized from pure solutions of 0.02 M OPD and 0.1 M OT.

Fig. 3.3 b shows CVs recorded for solution system OTC (0.03 M OPD + 0.1 M OT). The peak current for monomer oxidation was lower than that of 0.03 M OPD alone but higher than that of the previous copolymer system (OTB) that may be due to increased concentration of OPD monomer in the feed. No prominent change in the peak potentials was noticed in the following cathodic scan. In the 70th cycle the oxidation peaks at $E_{\text{SCE}} = 0.40$ and 0.55 V merged into one peak to form a current plateau. After the 80th potential scan a redox pair appeared at $E_{\text{SCE}} = 0.31/0.22$ V. The anodic peak of this redox pair grows slowly and shifts to positive potentials in subsequent scans. In contrast the cathodic peak grows rapidly and shifts into negative direction. At the end of electrolysis three redox pairs centered at $E_{\text{SCE}} = -0.01/-0.05$, $0.35/0.10$ and $0.55/0.58$ V were observed. It can be noticed that in the final picture the first redox process and anodic peak of the second redox process of this system show a little positive shift relative to the previous system studied (system OTB). A golden-brown film was observed on the working electrode as the electrolysis was stopped.

Fig. 3.3 c depicts a series of CVs recorded for solution system OTD (0.04 M OPD + 0.1 M OT). The anodic peak current of the monomer oxidation peak was higher than in the previous cases. At the end of electrolysis three redox processes at $E_{\text{SCE}} = -0.01/-0.05$, $0.35/0.10$ and $0.55/0.58$ V were observed. Apparently the overall picture of this system seems to be similar to that of a previous one (OTC). Nevertheless, differences can be observed with regard to the peak current values. The anodic as well as the cathodic peak current values for the first redox pair were slightly higher as compared to copolymer OTC. Similarly in the second redox process, the anodic peak current was lower while the corresponding cathodic peak current was higher in comparison with the polymerization of solution system OTC. Differences were observed in the peak currents of the third redox processes of both systems. The film color observed on the working electrode for copolymer OTD was slightly darker than the film color of copolymer OTC. In addition to this it was

also observed that the anodic peak current of the first redox process of this system was higher than that of POPD synthesized from 0.04 M monomer solution.

CVs recorded for solution system OTE (0.05 M OPD + 0.1 M OT) are shown in Fig. 3.3 d. The peak current of the monomer oxidation peak is increased further but still lower than that of 0.05 M OPD alone. Unlike other copolymer systems discussed above, there are only two anodic peaks appearing at $E_{\text{SCE}} = -0.01$ and 0.40 V and three cathodic peaks at $E_{\text{SCE}} = -0.05$, 0.30 and 0.50 V, respectively, in the second potential scan. After completion of the 30th cycle, peak currents of the redox process at $E_{\text{SCE}} = 0.40/0.50$ V and reduction peak at 0.30 V decrease. After the 80th cycle a new redox pair appeared at $E_{\text{SCE}} = 0.31/0.22$ V and the peaks shift to positive and negative potentials, respectively, with potential cycling. The peak currents of the first redox process ($E_{\text{SCE}} = -0.01/-0.05$ V) continue to increase as the cycling progressed. Finally two redox processes centered at $E_{\text{SCE}} = -0.01/-0.05$ V and 0.35/0.05 V and a negligible redox current plateau at $E_{\text{SCE}} = 0.55/0.58$ V were observed. For the second redox process the anodic peak current value is very small as compared to its cathodic counter part. At the end of the experiment a dark golden-brown film was formed on the electrode. Although system OTE has the highest OPD concentration (0.05 M) in the comonomer feed, however, still the peak currents of the first redox process and the overall growth process during electrolysis is different from that of the corresponding pure OPD solution.

The copolymer synthesized from solution system OTA (0.01 M OPD + 0.1 M OT) showed growth features different from those of the other copolymers discussed above. In this case the copolymer growth characteristics were identical to those of copolymer OTB up to 60 cycles and showed four redox processes at $E_{\text{SCE}} = 0.00/-0.04$, 0.33/0.31, 0.44/0.40 and 0.52/0.47 V, respectively (Fig. not shown). However, after 60 cycles the peak currents of the redox pair at 0.00/ -0.04 remain nearly constant while the other three redox processes grow very quickly and the CV pattern becomes similar to that of POT. The growth rate of the polymer from solution system OTA was faster in comparison with the growth rate of the polymers from the other solution systems studied but was much lower than that of POT.

The CVs during electropolymerization of mixtures of OPD and OT strongly suggest the deposition of new materials (copolymers). The growth characteristics of these materials depend on monomer concentration. During continuous potential scanning, the peak currents of the redox processes show a gradual increase with potential cycling in all the systems studied (Fig. 3.3 a-d). This indicates the buildup of electroactive material (copolymer)

on the surface of the working electrode. When the concentration of OPD was increased in the feed the peak currents of the first redox process showed an increasing trend at any given cycle number as evident from Fig. 3.4 a that shows the dependence of the first anodic peak current on the number of cycles for different solution systems studied. Furthermore, the peak current value of the first anodic peak of the copolymer was highest for the highest concentration of OPD (0.04 and 0.05 M) in the feed. In case of pure OPD it reaches to a maximum at 0.03 M concentration and then decreases as discussed earlier. Fig. 3.4 b shows relationships between the first anodic peak current at 210th cycle and the concentration of OPD, for the electropolymerization of mixed solution and OPD alone. The anodic peak of the second redox pair also grows slowly with potential cycling but its growth is very much decreased with an increase in OPD concentration in the feed. Similarly the growth of the anodic peak of the third redox process is strongly inhibited by an increase in the OPD concentration in the feed.

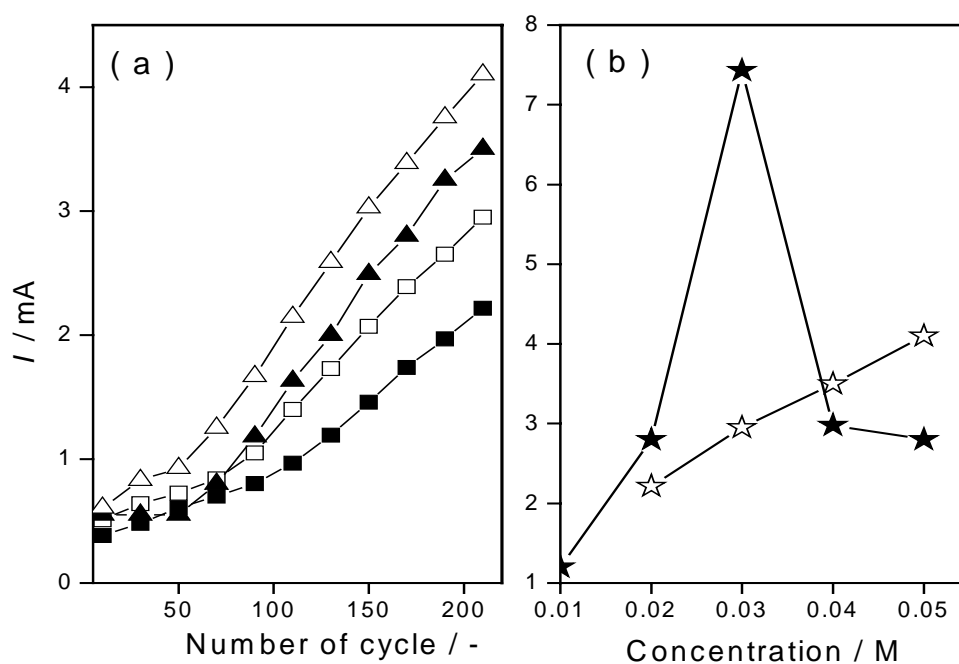


Fig. 3.4 Dependence of peak current of (a) first anodic peak on cycle number for copolymer growth deposited from solution system (■) OTB (□) OTC (▲) OTD and (△) OTE and (b) first anodic peak at 210th cycle on the concentration of OPD in pure monomer (★) and mixed solution (☆).

These observations imply the formation of new materials with electrochemical properties different from those of POT and POPD. As the OPD concentration increases in the feed, this factor seems to play a principal role in determining the redox response and characteristics of the copolymers.

3.3.1 Electrochemical Behavior of Poly(*o*-phenylenediamine-co-*o*-toluidine)

Potentiodynamic electrolysis of a 1.5 M H₂SO₄ solution containing both OPD and OT results in the deposition of a thin well adherent film. When transferred into supporting electrolyte solution the modified electrode shows its characteristic electrochemical activity in comparison with the homopolymers. Fig. 3.5 a shows CVs, recorded in the same potential range in monomer free electrolyte solution, for the electrodes modified with POPD (0.02 M), POT (0.1 M) and copolymer films from solution system OTA and OTB, respectively.

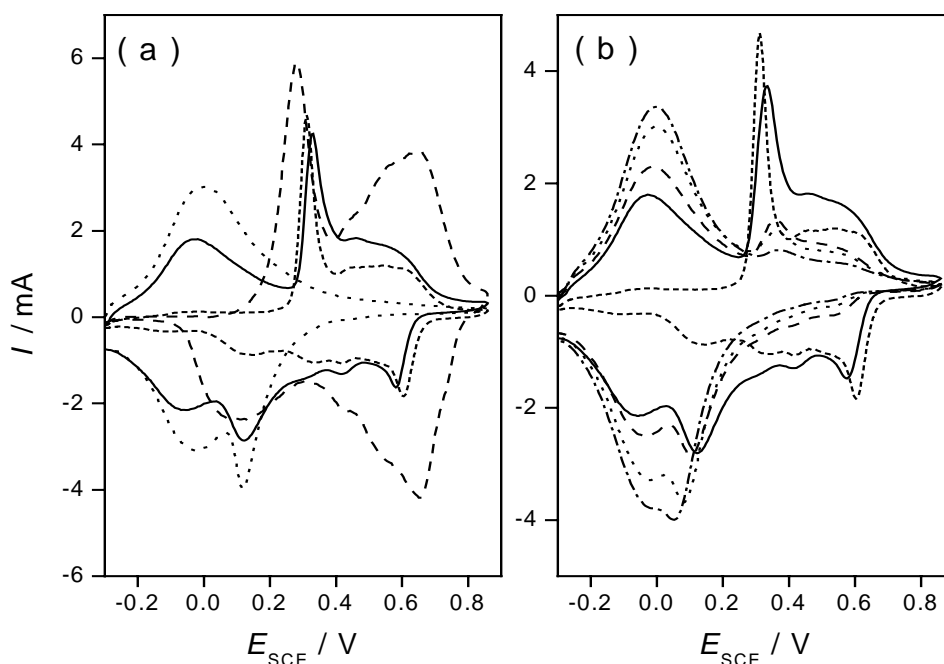


Fig. 3.5 CVs of (a) (.....) POPD, (---) POT and copolymer films deposited from solution system (---) OTA and (—) OTB and (b) copolymer films deposited from solution system (---) OTA, (—) OTB, (---) OTC, (.....) OTD and (---) OTE, in 1.5 M H₂SO₄ at a scan rate of 50 mV/s.

The main difference between the four curves in Fig. 3.5 a is that for POPD there is only one oxidation peak at $E_{\text{SCE}} = 0.00$ V and a main reduction peak at $E_{\text{SCE}} = -0.03$ V with a pre-peak at $E_{\text{SCE}} = 0.12$ V. On the other hand CV of POT film shows two redox

processes at $E_{\text{SCE}} = 0.28/0.15$ and $0.65/0.62$ V but there is no redox pair in the negative potential region. The CV of copolymer OTA shows resemblance to that of POT. The two main redox processes are shifted to $E_{\text{SCE}} = 0.31/0.13$ and $0.60/0.60$ V in comparison with POT, while a very negligible redox process in the negative potential region can also be observed. These differences in the CV of copolymer OTA relative to that of POT can be envisaged as being due to the incorporation of OPD units in the copolymer backbone.

The CV of copolymer synthesized from solution system OTB shows some promising characteristics. There are four redox processes at $E_{\text{SCE}} = -0.03/-0.06$, $0.33/0.13$, $0.46/0.41$ and $0.55/0.58$ V, respectively, in the CV of copolymer OTB. Obviously the CV of this copolymer film is not simply a superposition of the CVs of the individual POPD and POT films. It is clear that the copolymer has a wider useful potential range of redox activity than the homopolymers. These results suggest that the molecular structure of the copolymer OTB is different from those of POPD and POT and the formation of a genuine copolymer can be assumed. Fig. 3.5 b shows CVs of the copolymer films in the background electrolyte solution. The effect of increasing OPD concentration can be observed very clearly. Table 3.1 summarizes the redox peak potentials of the homopolymers POT and POPD and copolymers of OPD and OT, in the background electrolyte solution.

Table 3.1 Summary of the redox peak potentials of the polymers in Fig. 3.5

Polymer	Peak potentials of redox process (V) (vs. SCE)			
	1 st	2 nd	3 rd	4 th
POT	0.28/0.15	0.65/0.62	—	—
POPD	0.00/– 0.03	—	—	—
OTA	–0.03/–0.08	0.31/0.13	0.60/0.60	—
OTB	–0.03/–0.06	0.33/0.13	0.46/0.41	0.55/0.58
OTC	–0.01/–0.05	0.35/0.10	0.55/0.58	—
OTD	–0.01/–0.05	0.35/0.10	0.55/0.58	—
OTE	–0.01/–0.05	0.35/0.05	0.55/0.58	—

CVs of copolymer OTB at various scan rates in $1.5 \text{ M H}_2\text{SO}_4$ solution are shown in Fig. 3.6 a. The shape conveys that the copolymer is electroactive and surface confined. In order to evaluate the mechanism controlling the charge transport in the copolymer films the anodic peak currents were plotted as a function of scan rate (Fig. 3.6 b). A linear relation-

ship between peak currents and scan rate was found, which indicates the surface-bound transport characteristics of the copolymer films [182].

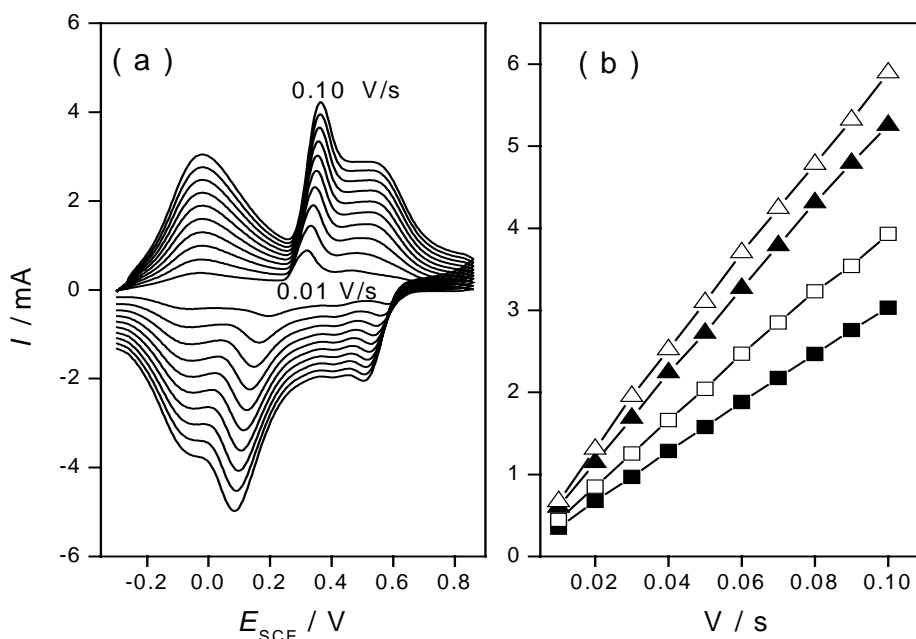


Fig. 3.6 (a) CVs of copolymer OTB film at different scan rates in 1.5 M H₂SO₄ and (b) Dependence of first anodic peak current on scan rate for copolymer films deposited from solution system (■) OTB, (□) OTC, (▲) OTD and (△) OTE.

3.3.2 Stability of Poly(*o*-phenylenediamine-co-*o*-toluidine)

A stable electroactive polymer film is of primary importance for such practical applications as in rechargeable batteries and in potential switching [183, 184, 185]. Many of the known conducting polymers undergo electrochemical degradation. A higher rate of electrochemical degradation of PANI in comparison with POPD, within the range of relatively high electrode potential, has been reported [186, 187]. The stability of some polymer films has been evaluated by applying continuous potential scans in monomer free electrolyte solution and after that comparing the CV of the initial and final potential scans. Stability for more than 100 cycles is required for applications of ICPs in batteries [185]. An improved stability of PANI by the addition of another monomer to ANI solution has been reported [183, 188, 189]. In the present study 110 continuous scans between $E_{\text{SCE}} = -0.30$ to 0.85 V were used in the stability test of the copolymer obtained at optimum feed concentration of OPD and OT (solution system OTB). The respective CVs are presented in Fig. 3.7. It can be observed that repeated scanning of the copolymer film does not result in substantial decrease

in the peak currents, which indicates good electrochemical stability of the copolymer film in this potential range. The change in the peak height of the first anodic peak is less obvious than in the second and third anodic peak. Furthermore, the first and second anodic peak shift into positive direction during repeated scanning. The observed changes indicate a gradual but slow decomposition of copolymer OTB on continuous potential cycling.

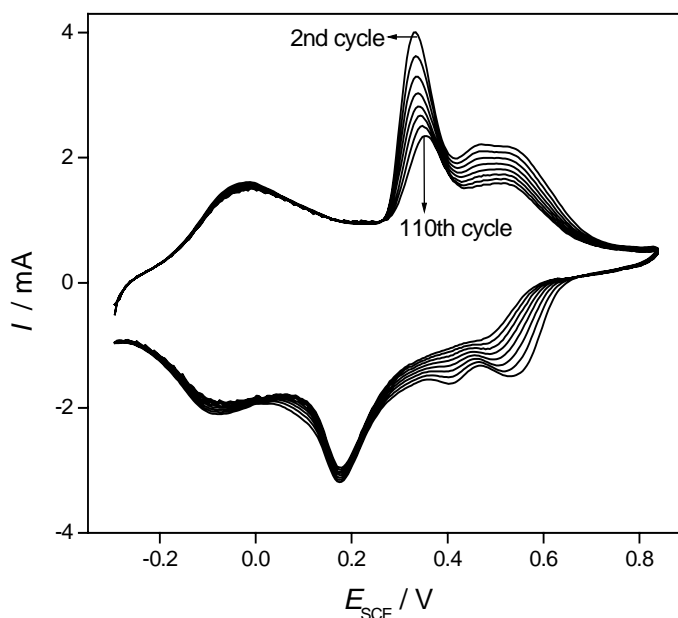


Fig. 3.7 CVs obtained by continuous potential cycling (110 cycles) between $E_{\text{SCE}} = -0.30$ to 0.85 V for copolymer OTB, in monomer free electrolyte solution, at a scan rate of 50 mV/s.

3.3.3 Effect of pH on the Electrochemical Activity of Poly(*o*-phenylenediamine-co-*o*-toluidine)

CVs of the homo-/copolymer films recorded in strong acidic solution have already been discussed (see Fig. 3.5). In order to gain further insight into the electrochemical activity of poly(OPD-co-OT), CVs of POPD, POT and copolymer OTB were recorded in an aqueous solution of 0.2 M Na_2SO_4 with different pH values. It was observed that redox activity of POPD is greatly diminished and the anodic and cathodic waves shifted to negative direction with increasing pH values (Fig. 3.8). This means that POPD shows good electrochemical activity only in acidic medium and its redox activity is rapidly lost if the pH of the solution is increased. In case of POT and the copolymer film the redox activity also decreased rapidly when the pH of the solution was increased stepwise from 1.0 to 3.0 (figures not shown).

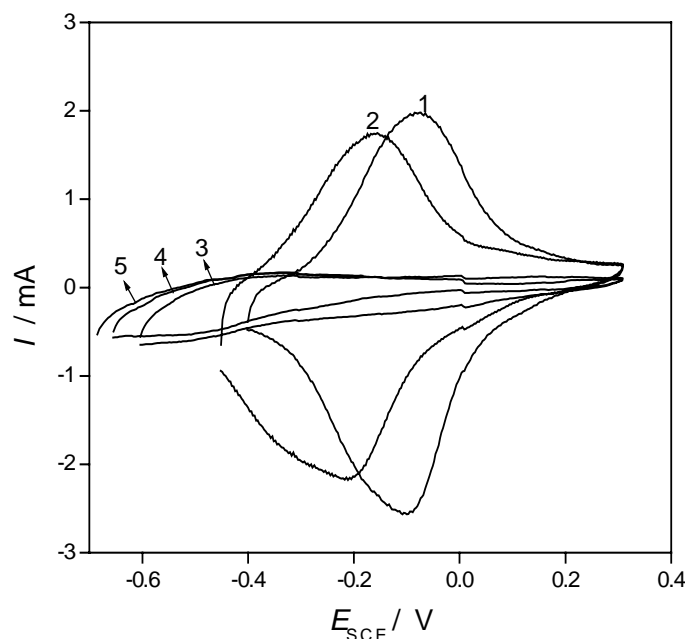


Fig. 3.8 CVs of POPD, deposited from 0.02 M OPD solution, in 0.2 M Na₂SO₄ with different pH values (1) 2.0, (2) 3.0, (3) 4.0, (4) 5.0 and (5) 6.0, at a scan rate of 50 mV/s.

Fig. 3.9 a shows CVs recorded for POT film in 0.2 M Na₂SO₄ with different pH values ranging from 4.0 to 7.0. At pH 4.0, there is only one broad anodic peak at $E_{\text{SCE}} = 0.25$ V with a cathodic peak at 0.05 V. Although there is no observable oxidation peak on the curve at pH 5.0, a cathodic peak can still be observed in the potential region between $E_{\text{SCE}} = -0.10$ to 0.10 V but this peak vanishes very rapidly as the pH is increased from 5.0 to 7.0. According to the changes as a function of pH value the electrochemical activity of POT decreases more quickly as the pH of the electrolyte solution is increased from 5.0 to 7.0. Results shown in Fig. 3.8 and Fig. 3.9 a indicate that both of the homopolymers POPD and POT have little electrochemical activity at pH > 3.0.

On the other hand the CV of the copolymer shows two anodic peaks at about $E_{\text{SCE}} = -0.15$ V and 0.60 V with a cathodic peak at $E_{\text{SCE}} = 0.05$ V and a cathodic current plateau in the region between $E_{\text{SCE}} = -0.30$ V and -0.05 V at pH 4.0 as shown in Fig. 3.9 b. Interestingly, it can be observed that the anodic and cathodic peak currents in Fig. 3.9 b decrease very slowly with increase in pH value from 5.0 to 9.0. This indicates the slow decay in the electrochemical activity of poly(OPD-co-OT) with increasing pH in the presently studied pH range. Thus on the basis of these results one can judge very easily that electrolysis of a mixed solution of OPD and OT resulted in copolymer. Moreover, copolymerization has not only increased the useful potential range of the redox activity of the polymer but also the

resulting copolymer shows considerable redox activity at higher pH values as compared with the homopolymers.

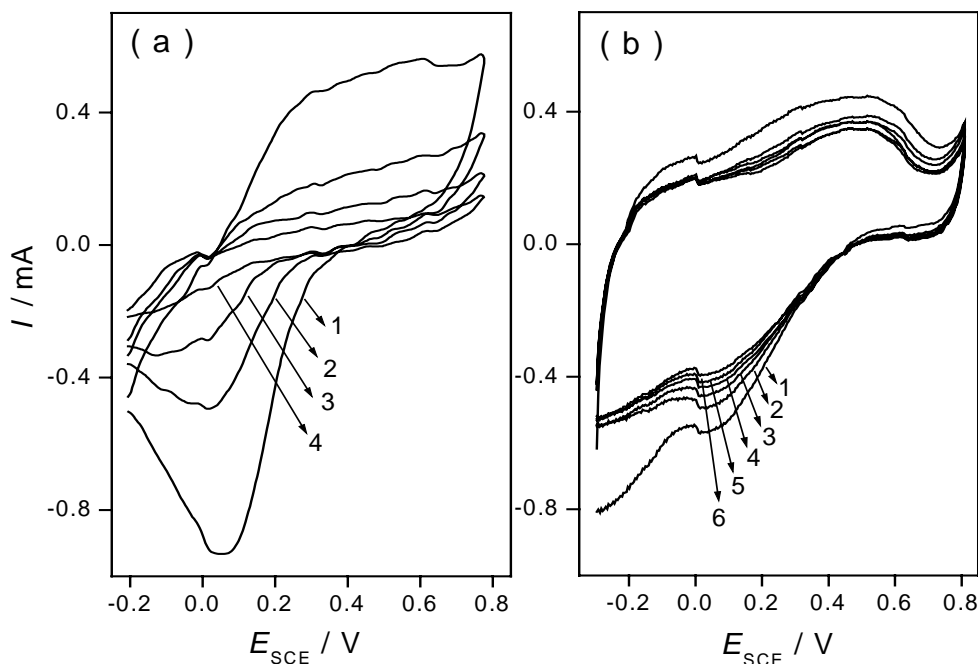


Fig. 3.9 CVs of (a) POT and (b) copolymer deposited from solution system OTB in 0.2 M Na_2SO_4 with different pH values (1) 4.0, (2) 5.0, (3) 6.0, (4) 7.0, (5) 8.0 and (6) 9.0, at a scan rate of 50 mV/s.

3.4 Electrochemical Copolymerization of *o*-Phenylenediamine and *m*-Toluidine

The electrolysis of MT solution results in a polymer showing electrochemical properties similar to POT, except the difference in the initial growth rate, as discussed in section 3.1. However, interestingly, the tendency of MT monomer towards copolymerization with OPD was lower and different from that of OT monomer. No evidence for copolymerization was observed when electrolysis of mixed solutions, having 0.1 M MT in the comonomer feed, was carried out. The CV pattern of the polymer growth was similar to the growth of POPD. This may be regarded as due to steric effect of $-\text{CH}_3$ substituent on the *meta* position, which decreases the probability of the reaction of MT units with that of OPD units. However, the polymer from mixed solutions of OPD and MT showed growth characteristics different from the homopolymers when the concentration of MT solution was doubled (0.2 M) in the comonomer feed. Consequently, further electrochemical and spectroelectrochemical studies on the homopolymerization of MT were performed with 0.2 M solution in

order to compare the properties of the PMT with those of the polymers synthesized from the mixed solutions containing 0.2 M MT and various concentrations of OPD.

A broad anodic peak at about $E_{\text{SCE}} = 0.70$ V and two cathodic peaks centered at 0.45 and 0.34 V, respectively, appeared on the first potential scan during the electrolysis of solution system MTA (Fig. not shown). Up to 90 cycles there was only one redox process at $E_{\text{SCE}} = 0.40/0.34$ V that show a slow increase in the peak currents. After 90 cycles three redox processes were observed. The peak currents of these redox pairs increase quickly with further potential scans and the CVs acquire the shape of PMT with three redox processes at $E_{\text{SCE}} = 0.34/0.34$, 0.48/0.50 and 0.56/0.64 V, respectively. A bluish colored film was observed on the surface of the working electrode when the electrolysis was stopped. Fig. 3.10 a depicts the CVs recorded during electrolysis of solution system MTB. The growth characteristics of the polymer from this solution system were closely similar to those of copolymer OTB with slight differences in the potentials of the redox peaks and are, therefore, not discussed here in detail. The copolymer showed three redox pairs at $E_{\text{SCE}} = -0.01/-0.04$, 0.32/0.05 and 0.53/0.55 V, respectively, and a light reddish-brown deposit was formed on the electrode, as the electrolysis was completed. The growth features of the polymer from solution system MTC (Fig. 3.10 b) were somewhat different from those of the homopolymers and copolymers, discussed in the preceding sections. An anodic peak at $E_{\text{SCE}} = 0.69$ V and two cathodic peaks at $E_{\text{SCE}} = 0.31$ and -0.03 V, respectively, appear on the first scan. At the 80th cycle a new redox pair appear at $E_{\text{SCE}} = 0.29/0.16$ V. The anodic peak of this redox pair grows slowly and shifts to positive potentials in the subsequent scans. In contrast the cathodic peak grows rapidly and shifts into negative direction. At the end of electrolysis two redox pairs centered at 0.00/ -0.01 , 0.34/0.06 and a negligible redox current plateau at $E_{\text{SCE}} = 0.57/0.58$ V, respectively, were observed. A reddish-brown film was observed on the working electrode when the electrolysis was stopped.

Fig. 3.10 c and d display a series of CVs recorded for solution systems MTD and MTE, respectively. The growth behavior and CVs recorded for these two systems have much resemblance with those recorded for POPD. However, the monomer oxidation peak currents are lower than those for pure OPD solutions (0.04 and 0.05 M). During potential cycling the cathodic shoulder merges into the main cathodic peak. At the end of electrolysis there is only one redox process at $E_{\text{SCE}} = 0.00/0.03$ V. The peak currents of this redox process are almost the same for both system MTD and MTE but higher than those of POPD synthesized from 0.04 and 0.05 M pure OPD solution.

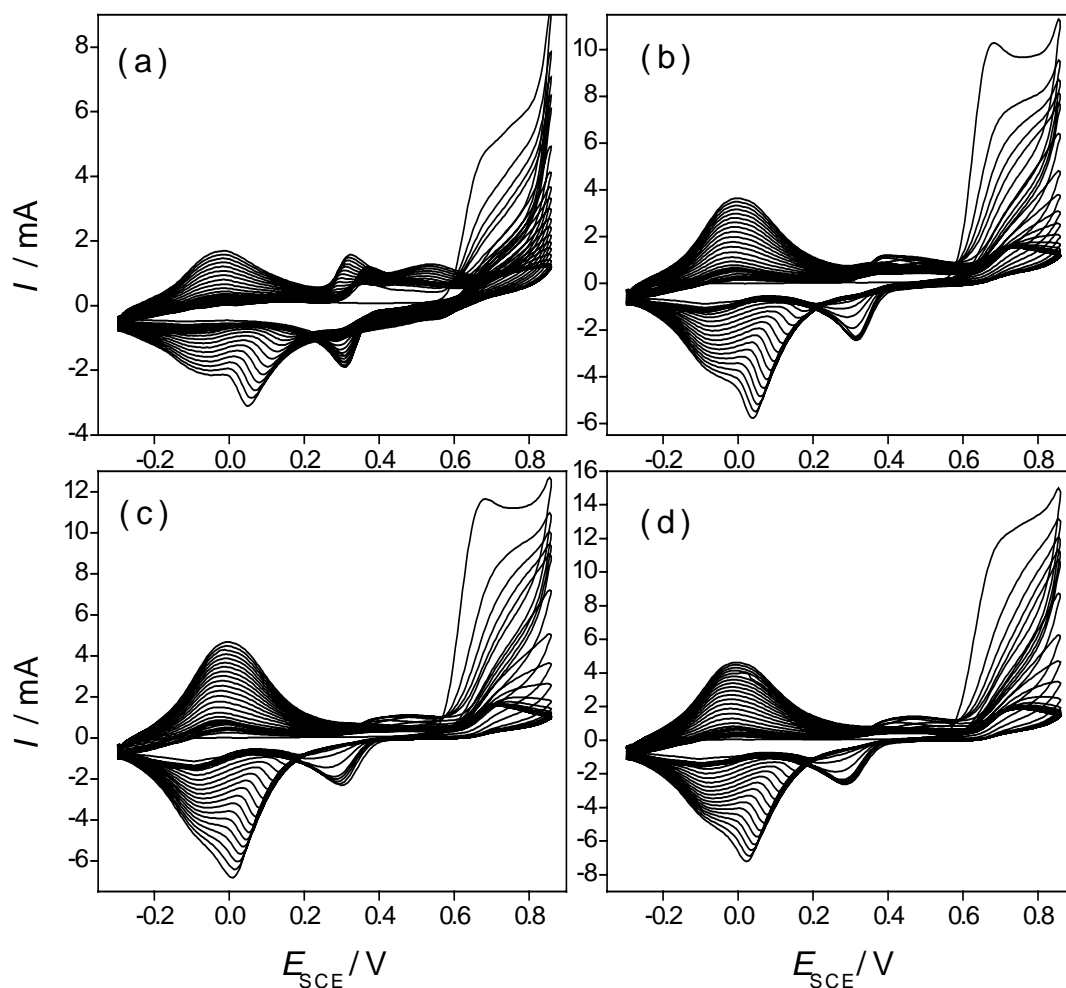


Fig. 3.10 CVs recorded with the growth of copolymer films (210 cycles) from solution system (a) MTB, (b) MTC, (c) MTD and (d) MTE, at a scan rate of 50 mV/s.

Thus on the basis of these results it can be assumed that the electrolysis of mixtures of OPD and MT results in the deposition of copolymer. The peak currents of the main redox processes of these copolymers showed an increasing trend at any given cycle number. Fig. 3.11 a shows the dependence of the first anodic peak on cycle number for different solution systems studied. The final peak current value of the first anodic peak at the end of electrolysis of mixed solutions increases with increasing OPD feed concentration and shows saturation above 0.03 M OPD feed concentration. This behavior is different from that of OPD polymerization from solution of varying concentrations (discussed earlier in section 3.2.) This difference can be clearly observed from Fig. 3.11 b that shows relationships between the first anodic peak current at 210th cycle and the concentration of OPD, for electropolymerization OPD alone and for mixed solutions of OPD and MT.

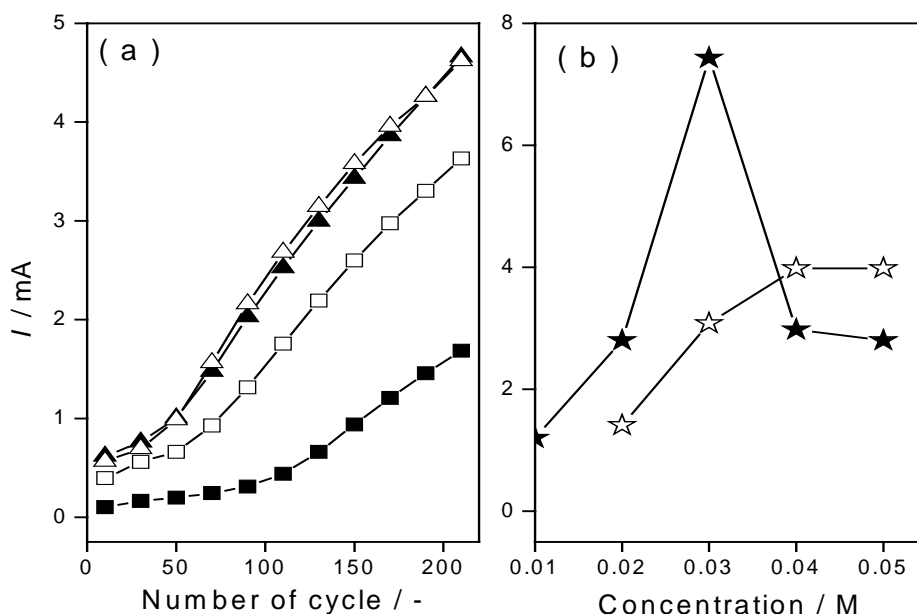


Fig. 3.11 Dependence of peak current of (a) first anodic peak on cycle number for copolymers growth deposited from solution system (■) MTB (□) MTC (▲) MTD and (△) MTE and (b) first anodic peak at 210th cycle on concentration of OPD in pure monomer (★) and mixed solution (☆).

For the copolymerization of OPD with MT, the peak currents of the second and third redox processes are strongly affected by increasing OPD feed concentration above 0.02 M. The differences between the growth processes of the homopolymers and copolymers suggest that electrolysis of a mixed solution of MT and OPD led to copolymer formation and the concentration of OPD in the feed seems to be very crucial for the properties of the resulting material from these mixed solutions.

3.4.1 Electrochemical Behavior of Poly(*o*-phenylenediamine-co-*m*-toluidine)

Further evidence for the formation of copolymer from the mixed solutions of OPD and MT can be gleaned from CVs of the respective polymers in background electrolyte solution. Fig. 3.12 a shows CVs of POPD (0.02 M), PMT (0.2 M), copolymer MTA and MTB, respectively, in 1.5 M H₂SO₄ solution. One main redox process at $E_{\text{SCE}} = 0.00/-0.03$ V and two redox processes at $E_{\text{SCE}} = 0.29/0.16$ and $0.56/0.53$ can be seen for POPD and PMT, respectively.

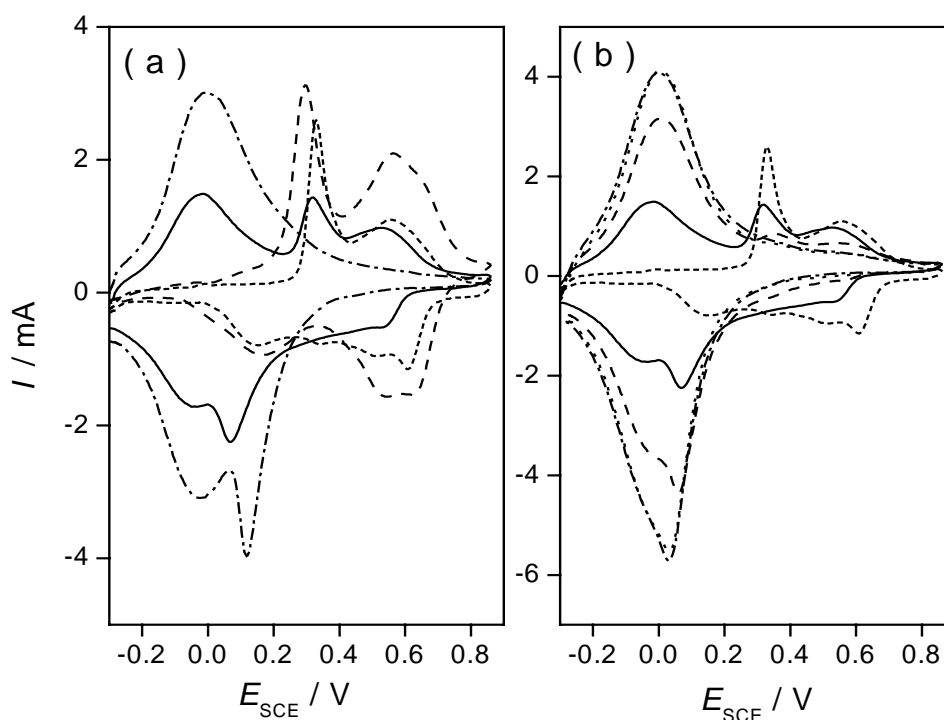


Fig. 3.12 CVs of (a) (---) POPD, (--) PMT and copolymer films deposited from solution system (----) MTA and (—) MTB and (b) copolymer films deposited from solution system, (----) MTA, (—) MTB, (--) MTC, (.....) OTD and (---) MTE, in 1.5 M H₂SO₄ at a scan rate of 50 mV/s.

In case of copolymer MTA, two main redox processes at $E_{\text{SCE}} = 0.32/0.13$ and $0.56/0.61$ are observed and the CV is closely similar to that of PMT. The little shift in the peak potentials of copolymer MTA in comparison with PMT may be caused by the incorporation of OPD units in the polymer chain. Instead the CV of the copolymer MTB is different from either homopolymers and shows three redox processes at $E_{\text{SCE}} = -0.01/-0.04$, $0.32/0.05$ and $0.53/0.55$ V, respectively. The CV of copolymer MTB shows resemblance with that copolymer OTB (Fig. 3.5 a) and shows a broader useful potential range of the redox activity. In order to find out whether both OTB and MTB also have the same molecular structure, a comparison between the properties of these copolymers will be made from time to time in the coming sections. Fig. 3.12 b shows CVs of poly(OPD-co-MT)s, in the background electrolyte solution. A summary of the redox peak potentials of the CVs in Fig. 3.12 is presented in Table 3.2.

Table 3.2 Summary of the redox peak potentials of the polymers in Fig. 3.12

Polymer	Peak potentials of the redox process (V) (vs. SCE)		
	1 st	2 nd	3 rd
PMT	0.29/0.16	0.56/0.53	—
POPD	0.00/−0.03	—	—
MTA	0.32/0.13	0.56/0.61	—
MTB	−0.01/−0.04	0.32/0.05	0.53/0.55
MTC	0.00/−0.01	0.34/0.06	0.57/0.58
MTD	0.00/0.03	—	—
MTE	0.00/0.03	—	—

Representative CVs of copolymer MTB at various scan rates in 1.5 M H₂SO₄ solution are shown in Fig. 3.13 a. A linear relationship between peak currents and scan rate was found for the copolymers of OPD with MT (Fig. 3.13 b), which indicates the surface-bound transport characteristics of the copolymer films [182].

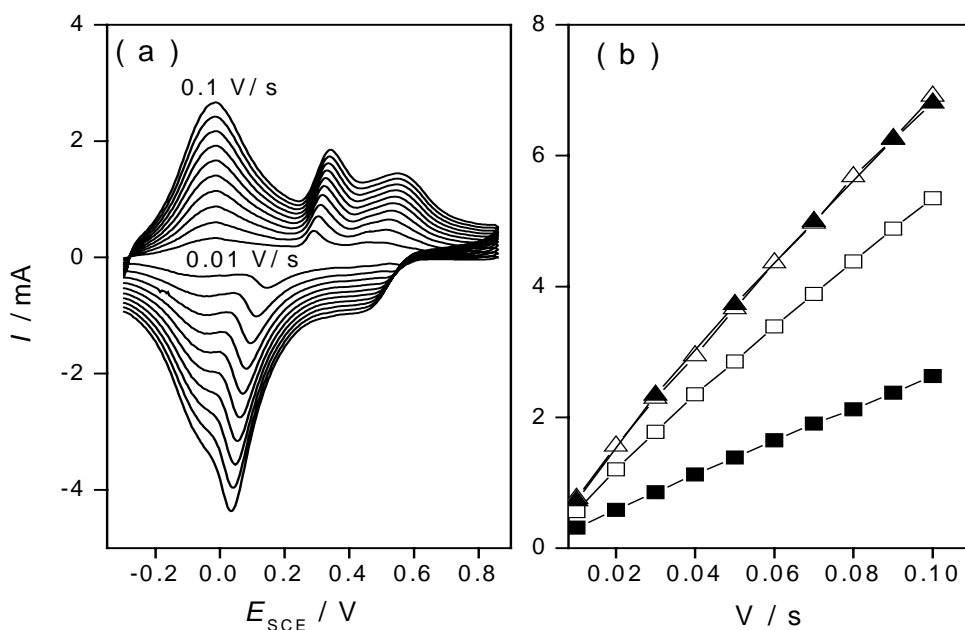


Fig. 3.13 (a) CVs of copolymer MTB film at different scan rates in 1.5 M H₂SO₄ and (b) Dependence of first anodic peak current on scan rate for copolymer films deposited from solution system (■) MTB, (□) MTC, (▲) MTD and (△) MTE.

3.4.2 Stability of Poly(*o*-phenylenediamine-co-*m*-toluidine)

Copolymer MTB, which showed improved electrochemical properties as compared with the homopolymers, was tested for electrochemical stability. Fig. 3.14 shows the CVs of copolymer MTB, recorded continuously for 110 potential scans between $E_{\text{SCE}} = -0.30$ to 0.85 V in the monomer free electrolyte solution. The slight decrease in the peak currents of the copolymer film with repeated scanning indicates good electrochemical stability of poly(OPD-co-MT) film in this potential range. The peak current of the first anodic peak decreases very slowly in comparison with the decrease in the peak current of the second and third anodic peak, suggesting the very slow decomposition of the copolymer film on continuous potential cycling.

Importantly, the first and second anodic peaks shift to positive and negative directions, respectively, during repeated scanning. This behavior of copolymer MTB, during continuous potential scanning, is different from that of copolymer OTB (Fig. 3.7) where the second anodic peak shifts positively. Thus it can be assumed that a polymer of somewhat different nature or structure can be deposited if one of the monomer (OT) is replaced by its isomer (MT) in the comonomer feed while keeping all the other experimental conditions constant.

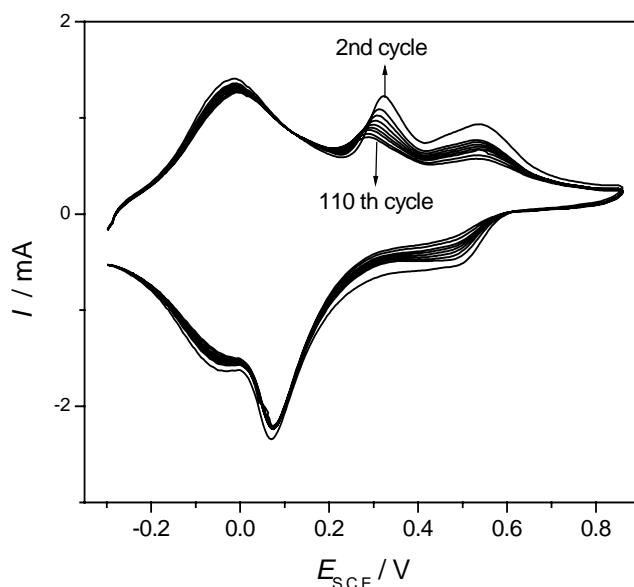


Fig. 3.14 CVs obtained by continuous potential cycling (110cycles) between $E_{\text{SCE}} = -0.30$ to 0.85 V for the copolymer MTB, in monomer free electrolyte solution, at a scan rate of 50 mV/s.

3.4.3 Effect of pH on the Electrochemical Activity of Poly(*o*-phenylenediamine-co-*m*-toluidine)

In order to see the effect of solution pH on the electrochemical activity of poly(OPD-co-MT), CVs of copolymer MTB were recorded in an aqueous solution of 0.2 M Na₂SO₄ with different pH values and were compared with those of the homopolymers. As stated in section 3.3.3, that POPD shows good electrochemical activity only in acidic medium and its redox activity is rapidly lost if the pH of the solution is increased. In case of PMT and the copolymer film the redox activity also decreased rapidly when the pH of the solution was increased stepwise from 1.0 to 3.0 (figures not shown).

Fig. 3.15 a shows CVs recorded for PMT film in 0.2 M Na₂SO₄ with different pH values ranging from 4.0 to 7.0. At pH 4.0, there is only one broad anodic peak at $E_{\text{SCE}} = 0.40$ V with a cathodic peak at $E_{\text{SCE}} = 0.09$ V. At pH 5.0, a cathodic peak can be observed in the potential region between $E_{\text{SCE}} = 0.01$ to 0.12 V but this peak vanishes very rapidly as the pH is increased from 5.0 to 7.0. This indicates that the electrochemical activity of PMT further diminishes as the pH of the electrolyte solution is increased from 5.0 to 7.0. Thus like POPD homopolymer, PMT also has little electrochemical activity at pH > 3.0.

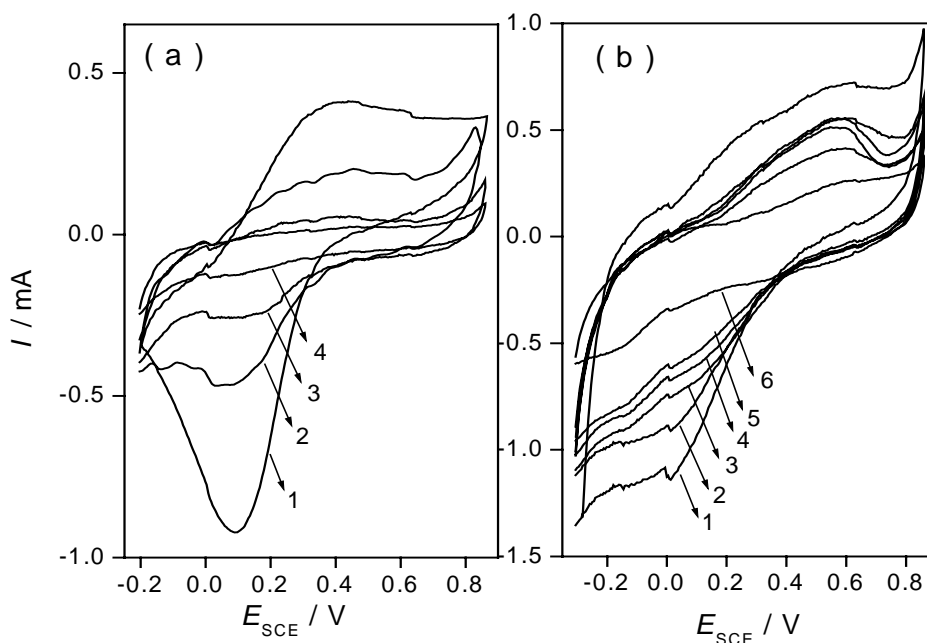


Fig. 3.15 CVs of (a) PMT and (b) copolymer MTB, in 0.2 M Na₂SO₄ with different pH values (1) 4.0, (2) 5.0, (3) 6.0, (4) 7.0, (5) 8.0 and (6) 9.0, at a scan rate of 50 mV/s.

In contrast the CV of the copolymer shows two broad anodic peaks at $E_{\text{SCE}} = -0.07$ V and 0.57 V with a cathodic peak at 0.02 V and a cathodic current plateau in the region between $E_{\text{SCE}} = -0.17$ V and -0.01 V at pH 4.0 as shown in Fig. 3.15 b. It is observable that the anodic and cathodic peak currents in Fig. 3.15 b decrease slowly with increase in pH value above 4.0 until the pH of the solution reaches to 9.0 where the decrease in peak current values is more obvious. This indicates that relative to the homopolymers, the decay in the electrochemical activity of poly(OPD-co-MT) with increasing pH, in the presently studied pH range, is slow. Additionally, these results suggest that electrolysis of a mixed solution of OPD and MT at appropriate feed concentration of the monomers resulted in a copolymer, which has not only a broader useful potential range of the redox activity than the homopolymers but also the resulting copolymer shows considerable redox activity at higher pH values as compared with the homopolymers.

On the other hand, a comparison of the CVs recorded for copolymer OTB (Fig. 3.9 b) and copolymer MTB (3.15 b) in solutions of different pH values shows that the electrochemical activity of copolymer OTB at higher pH values is better than that of copolymer MTB. This again reveals the probable differences in the structure of copolymer OTB and MTB, although the growth process and the CVs of the two polymers in the strong acidic solution are very similar.

4 In situ Conductivity Measurements

Electroactive polymers are usually classified into electron-conducting and redox polymers. Both classes feature different conductivity mechanisms. Generally the presence of charge carriers and good interchain interactions is considered crucial for good electrical conductivity [190]. In case of electron-conducting polymers conductivity is related to charge carriers delocalized in the extended π -network of the polymer. In case of redox polymers conductivity is accomplished by hopping mechanism [190], as a result the conductivity of the redox polymers is much lower than that of electron-conducting polymers [138, 191]. The homopolymers studied in this work belong to different classes. POT and PMT belong to electron-conducting polymers while POPD belongs to redox polymers. Therefore, the conductivity values and the trend of variations in conductivity with applied potential is expected to be different for POT/PMT and POPD. Consequently it can be assumed that conductivity values of the polymers synthesized from mixed solutions and the dependence of conductivities on applied potential will be strongly affected by the number of monomer units (OPD and OT or MT) incorporated in the polymer backbone. Hence, it will be interesting to measure the conductivities of the copolymers and compare with those of the homopolymers in order to get further evidence for copolymer formation and to see the effect of monomer feed concentration on the conductivities of the copolymers. For this purpose, the polymers were deposited potentiodynamically, in their respective potential ranges, from the corresponding solutions on a double-band gold electrode. *In situ* conductivity measurements of the deposited polymer films were carried out in 1.5 M H_2SO_4 .

4.1 In situ Conductivity Measurements of Poly(*o*-/*m*-toluidine)

Fig 4.1 a shows the plot of resistivity of POT versus applied electrode potential in an aqueous solution of 1.5 M H_2SO_4 . When the applied potential is increased the resistivity of POT decreases sharply by 3.5 orders of magnitude beyond $E_{\text{SCE}} = 0.10$ V reaching a minimum value at $E_{\text{SCE}} = 0.30$ V, remains nearly constant up to $E_{\text{SCE}} = 0.55$ V and then increases beyond $E_{\text{SCE}} = 0.55$ V. Minimum resistivity is observed in the potential range between $E_{\text{SCE}} = 0.30$ and 0.55 V where POT is present in its half oxidized emeraldine form (when radical cations are present and can act as charge carriers) [192]. When the applied potential is reversed the resistivity of POT decreases slowly up to 0.55 V, remains constant and after $E_{\text{SCE}} = 0.15$ V increases sharply. Similar observations have been reported elsewhere [107].

In case of PMT (Fig. 4.1 b) the plot of resistivity versus applied potential is similar to that of POT. A sharp decrease in the resistivity occurs as the potential is increased beyond $E_{\text{SCE}} = 0.10$ V followed by a sharp increase after $E_{\text{SCE}} = 0.55$ V. Minimum resistivity is observed in the potential range between $E_{\text{SCE}} = 0.30$ and 0.55 V. The behavior of the POT and PMT films regarding the changes in resistivity with changing applied potential is closely similar to that of parent PANI [18, 191]. However, the resistivity of POT and PMT is higher than that of PANI. This was attributed to the steric effect of the methyl group that could result in an increase in the torsional angle between the adjacent phenyl rings that consequently decrease the π -conjugation of the polymer backbone and hence the electrical conductivity.

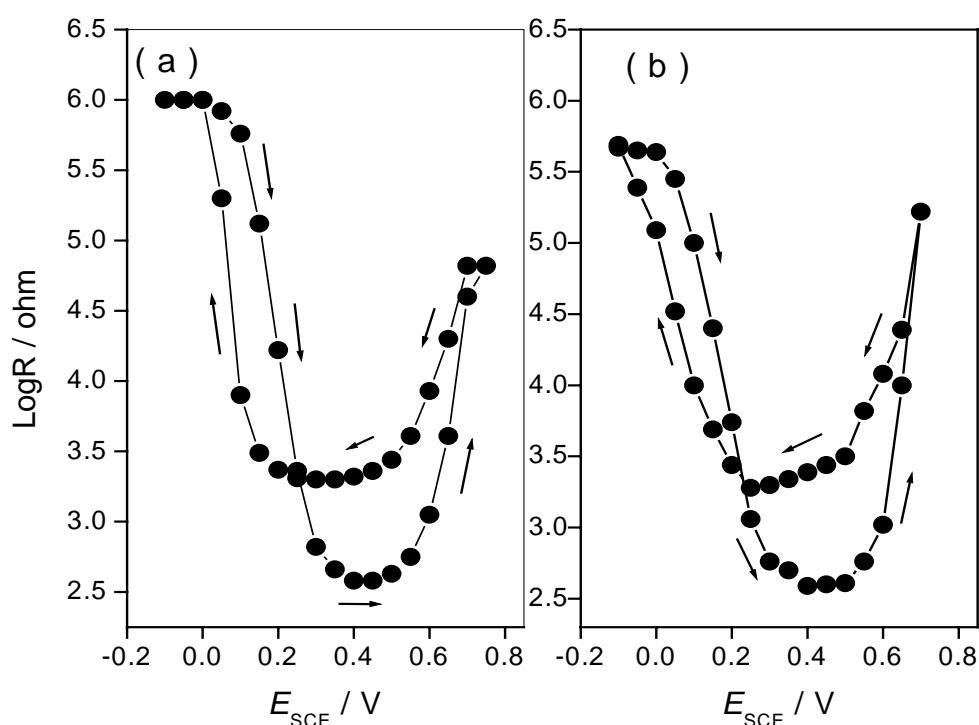


Fig. 4.1 Plots of resistivity versus applied electrode potential for (a) POT and (b) PMT in 1.5 M H_2SO_4 .

4.2 In situ Conductivity Measurements of Poly(*o*-phenylenediamine)

Fig. 4.2 shows plots of resistivity versus applied potential for POPD. As can be observed, the shape of the plot of resistivity versus applied potential for POPD is different from that of POT/PMT. Moreover, the resistivity of POPD is higher by about 3 orders of magnitude in comparison with POT/PMT that could be due to the lack of charge carriers

on its main structure. The minimum resistivity value or in other words conductivity maximum occurs in the range of the formal redox potential of the POPD.

Similar results have been reported for poly(2,3-diaminotoluene) (PDT), an analogue of POPD with one broad redox process. PDT has been reported to exhibit relatively low electrical conductivity with a maximum value at the formal redox potential of the polymer (where the polymer was supposed to be in the partially oxidized form) [190]. It was assumed that some protonated imines may exist in the partially oxidized PDT and these species might act as charge carriers to generate some electrical conductivity. Thus in the case of POPD protonated imines could also act as charge carriers. A maximum at the formal redox potential was also observed for the intensity of the absorption band characterizing conductivity [193] and for the other electrochemical and physiochemical characteristics of POPD [194]. However, such species cannot be created in the fully oxidized form of these redox polymers and as a result the conductivities were extremely low in the fully oxidized state.

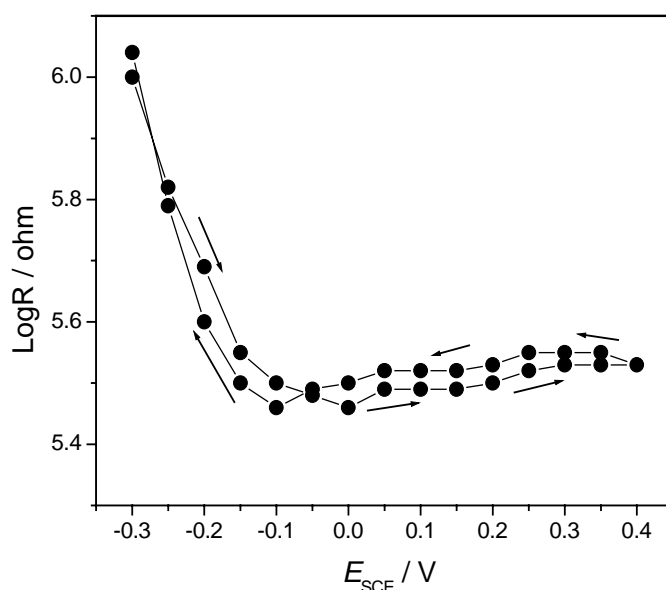


Fig. 4.2 Plot of resistivity versus applied electrode potential for POPD in 1.5 M H_2SO_4 .

4.3 In situ Conductivity Measurements of Poly(*o*-phenylenediamine-co-*o*-toluidine)

Fig. 4.3 a-d depicts dependencies of resistivity on the applied potential for the copolymer films deposited from the solution system OTA, OTB, OTC and OTD, respectively.

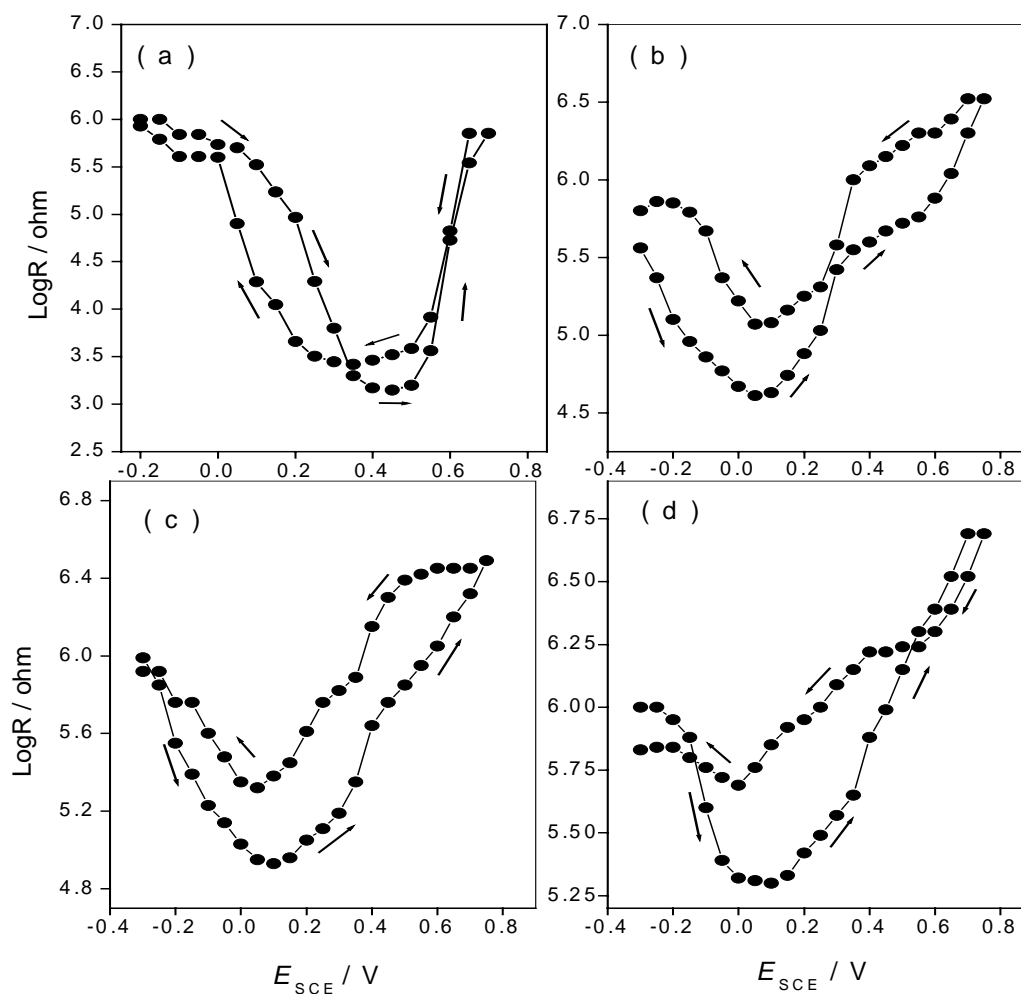


Fig. 4.3 Plots of resistivity versus applied electrode potential for copolymer (a) OTA, (b) OTB (c) OTC and (d) OTD in 1.5 M H_2SO_4 .

The resistivity plot of copolymer OTA (Fig. 4.3 a) is closely similar to that of POT in Fig. 4.1 a indicating that both polymers have similar conducting nature. The minimum resistivity is observed in the region between $E_{\text{SCE}} = 0.35$ to 0.45 V. The resistivity values of copolymer OTA are higher approximately by half an order of magnitude than that of POT, which can be attributed to the incorporation of OPD units in the copolymer backbone. It is well known that the extent of conjugation of π -orbital is responsible for conductivity in polymers and the presence of substituents in the polymer chain causes perturbation of the coplanarity of the π -system, which results in lowering of the degree of conjugation [39, 40] and ultimately the conductivity. The presence of two different substituents will induce additional deformation along the copolymer backbone that will result in a more sterically

hindered polymer in comparison with POT. Therefore, the resistivity of the copolymer appears to be more than that of POT.

In case of copolymer OTB (Fig. 4.3 b), there is a slow decrease in the resistivity from $E_{\text{SCE}} = -0.30$ V up to -0.10 V and gradual increase after 0.20 V. Minimum resistivity is observed in the potential range between $E_{\text{SCE}} = -0.10$ and 0.20 V for this system. Interestingly POT has minimum resistivity between 0.30 and 0.55 V (a potential window of 250 mV) while for the copolymer the conductive potential range is between $E_{\text{SCE}} = -0.10$ to 0.20 V (with the potential window of 300 mV). This information reveals that copolymer OTB has an extended conducting potential range. However, the resistivity of copolymer OTB is higher by 2 orders of magnitude than that of POT, which may be due to more complicated structure or relatively low level of conjugation in the copolymer.

In order to explain the conductivity mechanism or structure of copolymer OTB one can consider several possibilities. Firstly, if it is assumed that the copolymer is possibly of electron conducting nature even then a reduction in the conductivity of the copolymer in comparison with POT should be expected. The incorporation of more OPD units in the copolymer backbone will result in more sterically hindered copolymer structure. Secondly, one can also assume that the copolymer may probably be a mixture of copolymer chains with different monomer contents and has significant number of block segments resulting from the complexity of polymerization [195]. Considering the poor conjugation of POPD units the block copolymer can be poorly conjugated because the POPD blocks will isolate POT blocks that will ultimately result in a decrease in the number of the charge carriers and the conjugation length along the polymer backbone. However, this difference in conductivity between the homopolymers and copolymer cannot be explained only by the variations of conjugation length but the extent of interchain interaction could also play an important role in determining the resistivity values [196].

The resistivity curve for copolymer OTC, shown in Fig. 4.3 c is closely similar to that of copolymer OTB. But in this case the resistivity is higher by approximately 2.3 orders of magnitude as compared to that of POT. The plot of resistivity versus potential for the copolymer film synthesized from solution system OTD (Fig. 4.3 d) shows a trend somewhat different from the other copolymers in Fig. 4.3. In this case the resistivity is higher by 2.7 orders of magnitude than POT. This increase in the resistivity with increasing OPD feed concentration indicates the formation of copolymer with increasing number of OPD/POPD units in the backbone.

4.4 In situ Conductivity Measurements of Poly(*o*-phenylenediamine-co-*m*-toluidine)

The plot of resistivity versus applied potential for copolymer MTA is presented in Fig. 4.4 a. The shape of the plot is closely similar to that of PMT (Fig. 4.1 b). Minimum resistivity is observed in the potential region between $E_{SCE} = 0.35$ and 0.50 V. The resistivity of copolymer MTA is higher by one order of magnitude as compare with PMT.

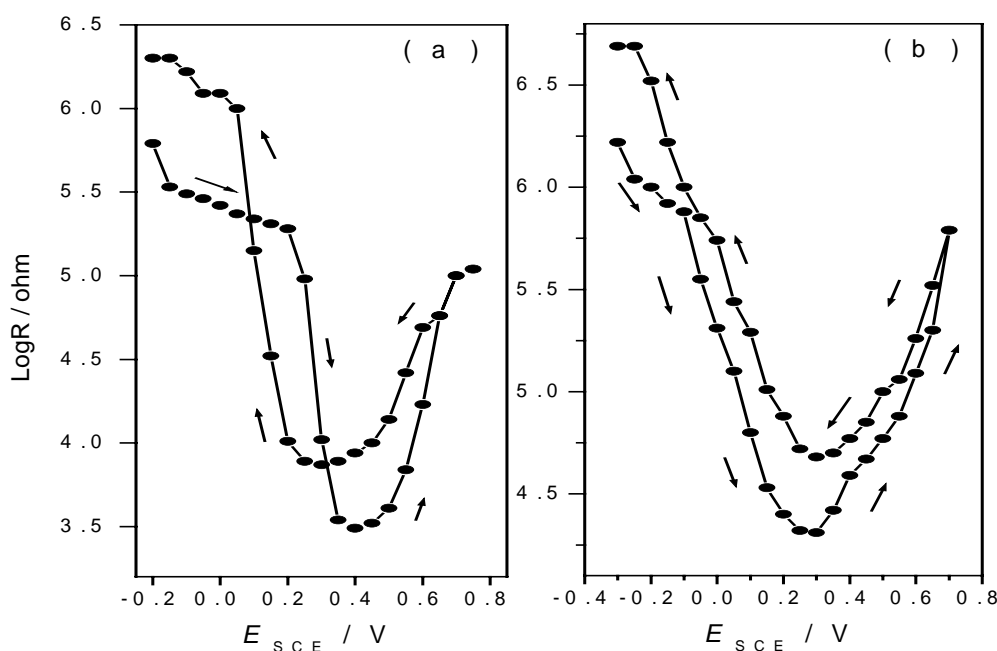


Fig. 4.4 Plots of resistivity versus applied electrode potential for copolymer (a) MTA and (b) MTB in $1.5 \text{ M H}_2\text{SO}_4$.

Fig. 4.4 b depicts dependencies of resistivity on the applied potential for the copolymer film deposited from solution system MTB. The resistivity decreases gradually, with increasing potential into the positive direction, reaching a minimum at $E_{SCE} = 0.30$ V. After $E_{SCE} = 0.30$ V the resistivity increases with increasing potential. Minimum resistivity is observed in the potential range between $E_{SCE} = 0.10$ and 0.40 V for this system. It can be noticed that the potential range of minimum resistivity for copolymers MTB is different from that of PMT which shows minimum resistivity in the potential range between $E_{SCE} = 0.30$ and 0.55 V. However, the resistivity of copolymer MTB is higher by 2.1 orders of magnitude than that of PMT.

Thus *in situ* conductivity measurements further suggest the deposition of copolymer from the electrolysis of mixed solutions containing OPD and OT or MT, because the copolymers have conductivity values and electrode potential region for maximum conductiv-

ity different from those of the respective homopolymers. The results also indicate strong dependence of resistivities of the copolymers on the monomer feed concentration. The observed increase in the resistivity values of the copolymers with increasing OPD feed concentration can be attributed to an increase in the number of OPD/POPD units in the copolymer backbone. Moreover, a comparison of plot of resistivity of copolymer OTB (Fig. 4.3 b) and copolymer MTB (Fig. 4.4 b) indicates that the two plots are different from one another, which might be due to differences in the structure and properties of two copolymers.

5 UV-Vis Spectroelectrochemical Measurements

5.1 Spectroelectrochemical Studies of Homopolymerization of *o*-/*m*-Toluidine

It is frequently assumed that during electropolymerization process of ANI and its derivative highly reactive intermediates are produced [197]. These intermediates react subsequently with solution species giving oligomers/polymers, which are finally deposited on the electrode surface. In the present study *in situ* UV-Vis spectroscopy was used to detect any intermediates formed during the electrochemical homo-/copolymerization and for the characterization of the homo-/copolymer films. UV-Vis spectra recorded at various time intervals for OT initial stages of polymerization (Fig. 5.1 a), at an applied potential of $E_{\text{SCE}} = 1.0$ V on an ITO electrode, show characteristic absorption bands at about $\lambda = 300$, 400 and 700 nm, respectively.

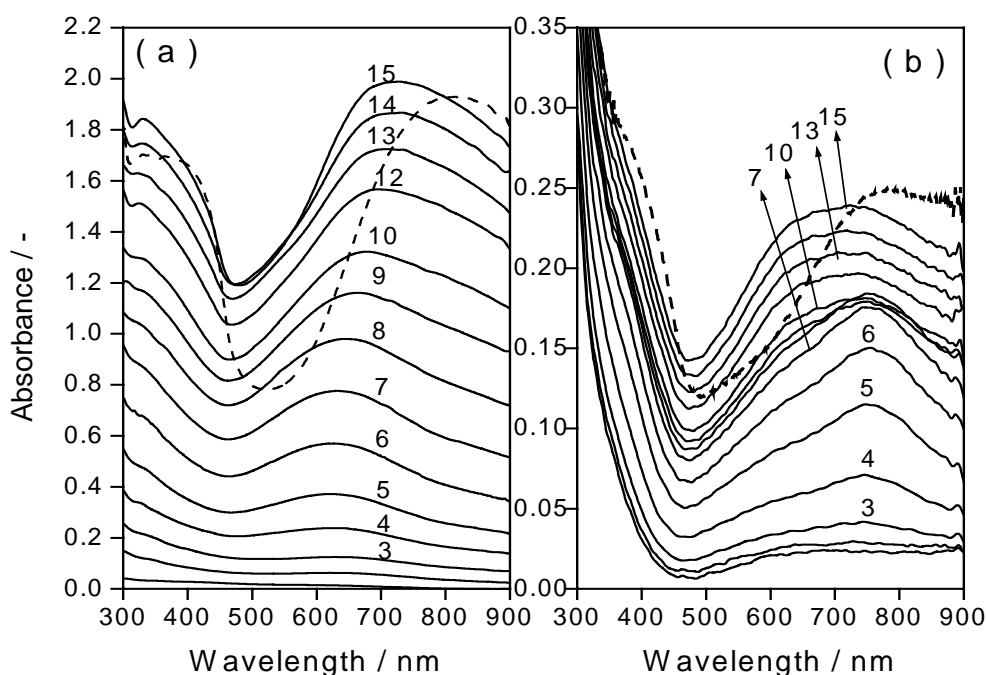


Fig. 5.1 UV-Vis spectra collected at different time intervals (as indicated, in minutes) during constant potential electropolymerization of solution containing (a) 0.1 M OT and (b) 0.2 M MT. Dashed lines show the spectra obtained after 7 min after interruption of electrolysis.

The absorption at $\lambda = 300$ nm corresponds to the $\pi \rightarrow \pi^*$ electronic transition of neutral species. The band at $\lambda = 400$ nm is due to PPD type radical cation and/or oxidized ben-

zidine type dimer, formed as the intermediate during the polymerization. The band in the red region of the spectra is due to dictationic form of the PPD type intermediates [176]. Two transient absorbance bands at $\lambda = 450$ and 750 nm were observed earlier by Malinauskas et al. [47] during the initial stages of electropolymerization of OT and assigned to an intermediate and its end product, respectively. After seven minutes of polymerization another absorption in the form of a shoulder around $\lambda = 335$ nm can be seen. The appearance of this shoulder around $\lambda = 335$ nm has been assigned to the electronic transition of quinoid rings [198].

The dashed line in Fig. 5.1 a represent the spectra recorded after seven minutes after interruption of electrolysis. It was observed that after interruption of electrolysis, the growth of the absorbance increases in the following 60 seconds and after that it decreases and a nearly constant value of the absorbance is attained in the next four or five minutes (spectra not shown). The relatively high growth of the absorbance after interruption of electrolysis than after the initial anodic step has been reported to be a characteristic of ring-substituted anilines [47]. The increase in the absorbance after switching off electrolysis and the observed red shift of the bands in the dashed line may be due to further chemical reactions of oxidized intermediate species with monomers, adsorbed on the surface of the electrode, resulting in oligomer/polymer formation [199, 200].

In case of MT, no well-defined transient absorbance bands for the intermediates are observed in the spectra recorded during the electrooxidation of MT solution (Fig. 5.1 b). Instead the spectra show a poorly defined absorption between 380 and 450 nm and a broad absorption band at $\lambda > 600$ nm, respectively. Moreover, the absorbance intensity is lower than that of OT. A similar picture of absorbance growth with an MT solution after an anodic potential switch has been reported elsewhere [47]. In this study the authors followed the course of electrooxidation of MT at fixed wavelengths. An absorbance transient at $\lambda = 450$ nm was assigned to an intermediate, whereas a transient at $\lambda = 750$ nm was assigned to an end product of electrooxidation of MT. The dashed line in Fig. 5.1 b shows the spectrum recorded after seven minutes after switching off electrolysis.

5.2 Spectroelectrochemical Studies of Homopolymerization of *o*-Phenylenediamine

Representative spectra for the initial stages of electrooxidation of an OPD solution are shown in Fig. 5.2 a. After switching the electrode potential to $E_{\text{SCE}} = 1.00$ V, two bands at $\lambda < 300$ nm and $\lambda = 492$ nm are observed. Soon afterwards a band at $\lambda = 462$ nm appears

followed by the appearance of a shoulder at $\lambda = 420$ nm and a band at $\lambda = 600$ nm. The band at $\lambda = 492$ nm diminishes after some time while the band initially observed at $\lambda = 462$ nm becomes the principal band in the corresponding spectra as the electrolysis proceeds. The peak assignment of the UV-Vis spectra in Fig. 5.2 a can be attempted by considering the electropolymerization mechanism of OPD (Section 1.11.2, Scheme 1.4) and by comparing the spectral characteristics reported for PANI-like and phenazine-like structures taking into account the electronic transitions arising from these structures.

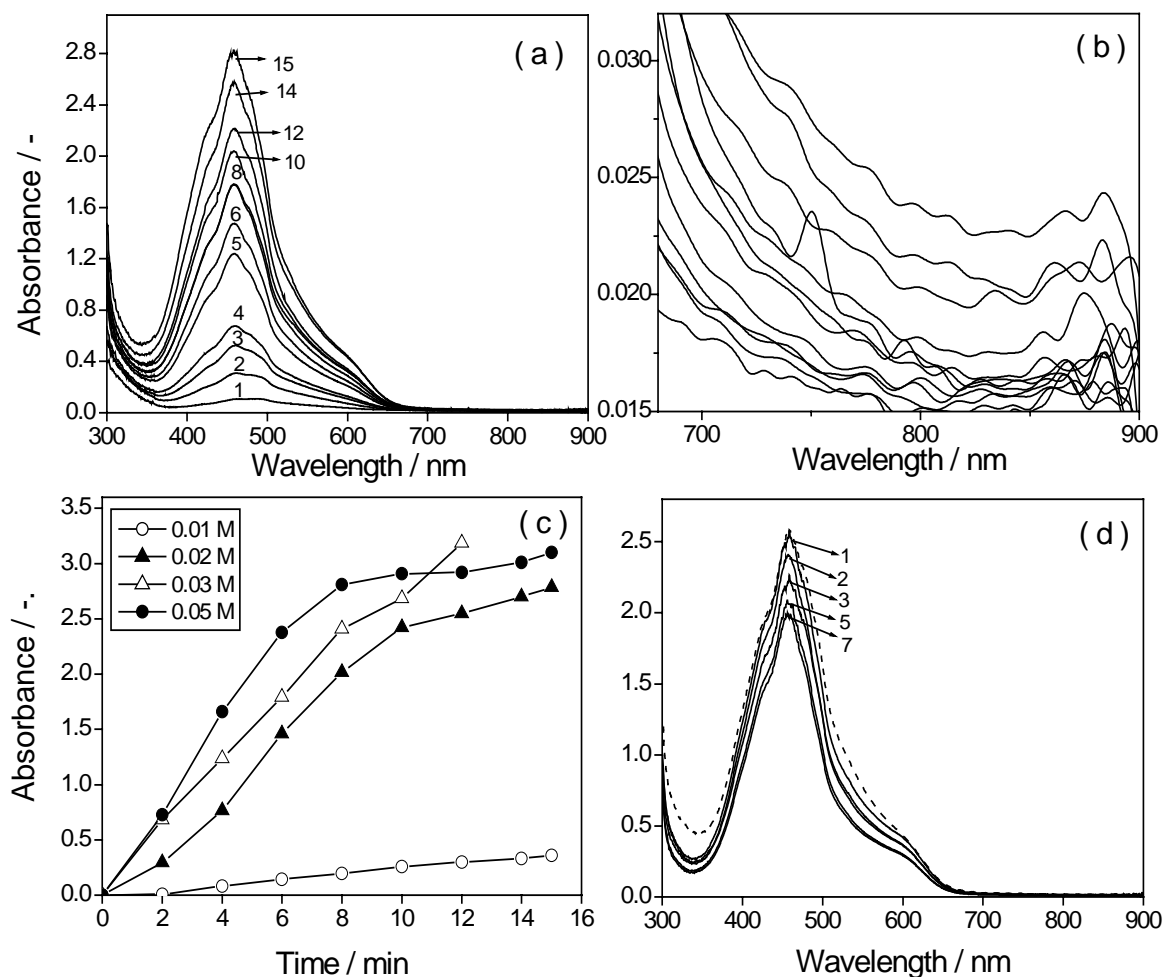


Fig. 5.2 (a and d) UV-Vis spectra collected at different time intervals (as indicated, in minutes) during constant potential electropolymerization and after interruption of electrolysis, respectively, for 0.02 M OPD solution, the dashed line in (d) shows a spectrum obtained at 15th minute during electrolysis, (b) The long wave length part of (a) and (c) Time dependence of the absorbance at $\lambda = 462$ nm after stepping the electrode potential to $E_{SCE} = 1.00$ V in solutions containing OPD in various concentrations (as indicated).

It should be kept in mind that in the present case spectroelectrochemistry is performed on a minute time scale, in addition the optical spectra recorded during the initial stages of polymerization of OPD are intense thus making it difficult to assign the observed peaks to the presence of monomeric radical cations or short lived intermediates. Basically there might be a low stationary concentration of the monomer cation radicals near the electrode surface, but presumably during oxidation their optical absorption would be overwhelmed by the absorptions of much more stable dimeric, trimeric and even longer oligomeric structures that are immediately formed on the electrode surface. Therefore, it can be assumed that the spectra recorded during oxidation of OPD belong to these relatively stable intermediates. Generally, two absorption bands at $\lambda = 330$ and $\lambda = 440$ nm and a broad absorption band at $\lambda > 600$ nm have been reported in the early stages of aniline polymerization. The peaks at $\lambda = 440$ and $\lambda > 600$ nm have been assigned, respectively, to the cationic and dicationic radicals resulting from head to tail coupling (PPD type of dimer) [176]. The dimeric or oligomeric species containing phenazine type structure have been reported to give absorption bands at $\lambda = 451$ or $\lambda = 420$ nm [139, 201].

In the light of the preceding discussion it is possible to make assignments for the absorption bands in Fig. 5.2 a. The appearance of the band at $\lambda = 492$ nm in the first scan of the spectra may corresponds to radical cations of PPD type dimer whose dicationic form absorbs in the red region with very low intensity (Fig. 5.2 b). The appearance of the band at $\lambda = 462$ nm followed by the shoulder at $\lambda = 420$ nm indicates the subsequent formation of phenazine type dimer/oligomer. The band at $\lambda = 492$ is visible only up to 4 minutes and then disappears or is overlapped by the band corresponding to phenazine type intermediates. Variations in the absorption intensity of the spectra were observed when electrolysis was performed for OPD solutions having different concentrations. Consequently, a plot of the absorption intensity of the major band at $\lambda = 462$ nm as a function of time, obtained at constant potential electrolysis for solutions of different OPD concentrations, shows an increasing trend with increasing concentration (Fig. 5.2 c). Initially up to 10 minutes there is a fast increase in the absorption intensity of the band at $\lambda = 462$ nm with increasing concentration and progressing electrolysis. After 10 minutes this increase becomes slower except in case of 0.03 M OPD solution where the absorbance continues to increase quickly. This trend is consistent with our cyclic voltammetric results on the growth of POPD films on a gold electrode (Section 3.2).

The spectra recorded after switching off the potential (Fig. 5.2 d) did not show any shift in the peak position and were similar to those recorded during electrolysis. This was attributed to the stable nature of the intermediates [50]. No polymer film was observed on the ITO glass electrode during the electrolysis of OPD solution (15 min) with various concentrations studied. This suggests that all the spectra recorded during the electrolysis are caused by solution species only [47]. A very similar spectrum was obtained from the solution after the removal of the ITO electrode whereas the ITO electrode itself did not give any spectrum in the monomer free electrolyte solution.

5.3 Spectroelectrochemical Studies of Copolymerization of *o*-Phenylenediamine and *o*-Toluidine

Interesting features in the spectroelectrochemical studies were observed for the mixtures of solutions containing a constant OT and varying OPD concentrations. It is, therefore, worthwhile to compare the UV-Vis spectral characteristics of the polymerization of OPD or OT alone and the polymerization of mixtures of OPD and OT in order to deduce any conclusion about the spectral results obtained from mixed solutions.

Fig. 5.3 a exemplifies the UV-Vis spectra recorded during constant electrode potential polymerization at $E_{SCE} = 1.00$ V for solution system OTA. It can be seen that the spectra recorded for solution system OTA are different from those recorded during the polymerization of homopolymers. The band corresponding to PPD type cationic radicals, observed at $\lambda = 492$ nm in the case of OPD polymerization, appears around $\lambda = 497$ nm for mixed solution. Moreover, unlike OPD polymerization, there are definite variations in the growth features of the peak around $\lambda = 497$ nm for the mixed solution. Obviously, the incorporation of OT units in the growing units, when electrolysis is performed with a mixture of OPD and OT, results in the red shift and alteration of the growth characteristics of the $\lambda = 497$ nm band.

For instance the band observed at $\lambda = 492$ nm during OPD polymerization (Fig. 5.2 a) disappears after some minutes, in case of mixed solution the band at $\lambda = 497$ nm not only persists till the end of electrolysis but also appears as the main band of the spectra for solution system OTA. Presumably, PPD type cation radicals are predominantly formed when electrolysis of OPD is performed in the presence of OT. As the OPD concentration increases in the feed the peak at $\lambda = 497$ nm is dominated by the high energy band at $\lambda = 462$ nm.

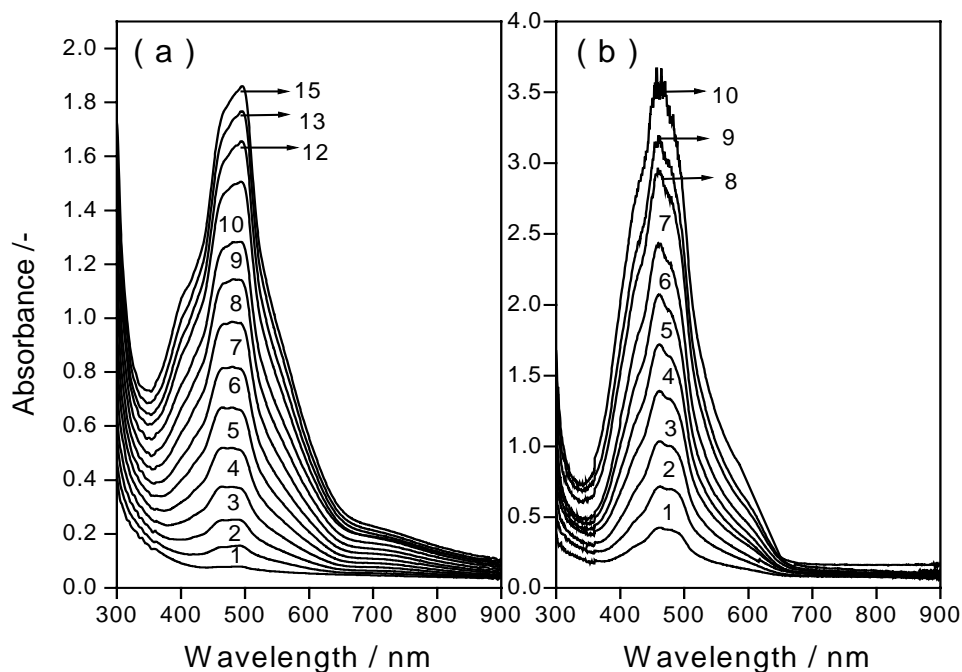
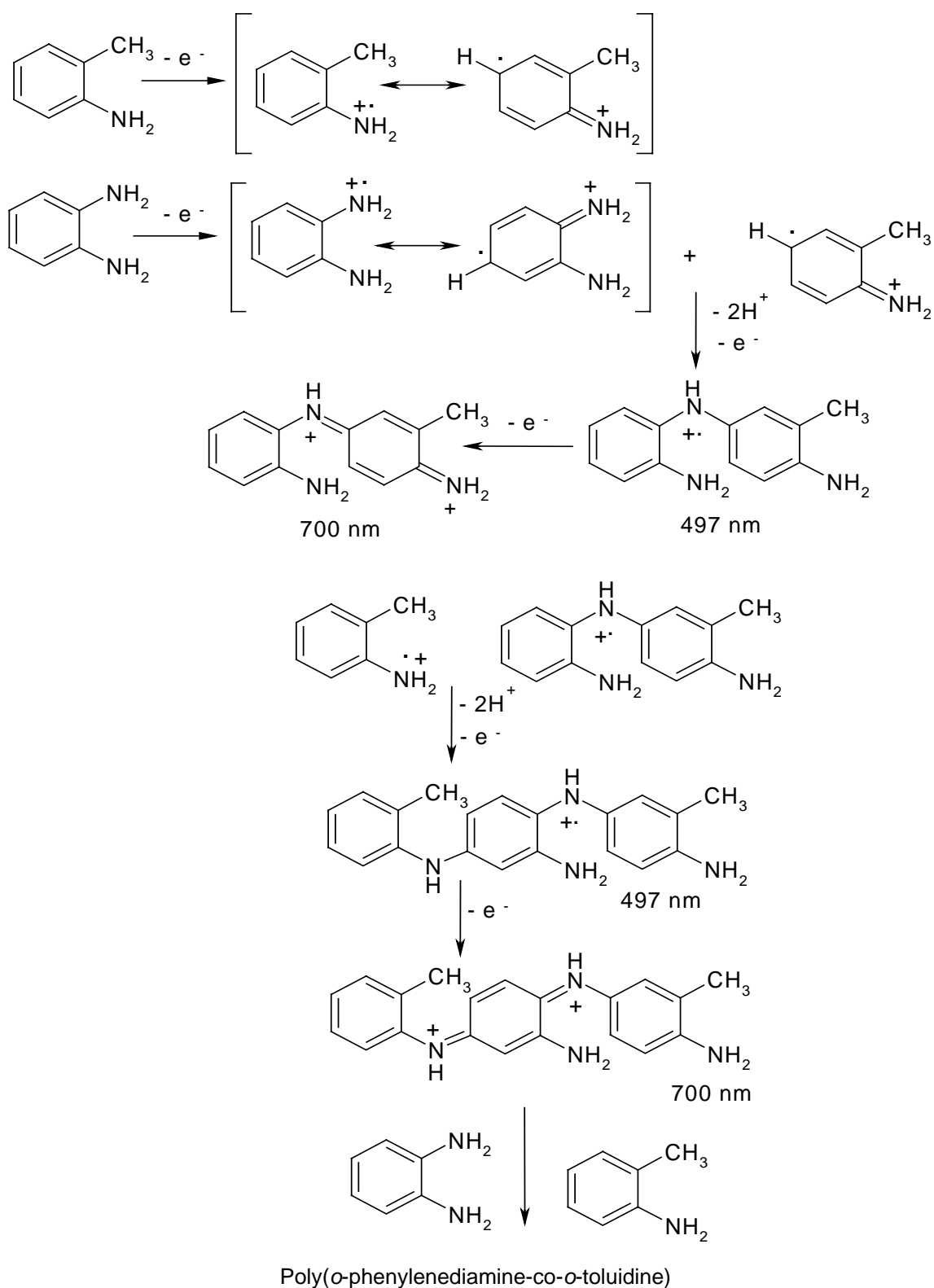


Fig. 5.3 UV-Vis spectra collected at different time intervals (as indicated, in minutes) during constant potential electropolymerization of solution system (a) OTA and (b) OTE.

Likewise, the absorption intensity of the band at $\lambda > 650$ nm also shows clear dependence on the OPD feed concentration and decreases with increasing OPD feed concentration. But even at 0.05 M OPD feed concentration (solution system OTE), this band is more prominent than the respective absorption for OPD polymerization (Fig. 5.3 b). In addition, the overall absorption of the spectra for mixed solutions increases abruptly with increasing OPD feed concentration, as can be seen from Fig. 5.3 b. This behavior is in contrast to the polymerization of pure OPD solution having different concentrations. These differences between the spectral response of the pure monomers and mixed solutions can be envisaged as being due to the participation of both monomers in the electropolymerization process when electrolysis of mixed solution containing OT and OPD is carried out.

Thus it may be inferred that at the applied potential of $E_{\text{SCE}} = 1.00$ V, OPD and OT can be oxidized to produce their corresponding cation radicals that undergo cross reaction resulting in aniline type mixed intermediates (dimer/oligomer) [181] that can lead to copolymer formation in the later stages of polymerization (Scheme 5.1). Therefore, the band observed at $\lambda = 497$ nm for mixed solution can now be assigned for the formation of PPD type intermediate dimer/oligomer, formed by the dimerization of OPD and OT cation radicals. The absorption at the red end of the spectrum beyond $\lambda = 650$ nm is assigned to the dicationic form of the mixed dimer/oligomer [191].



Scheme 5.1 Electrocopolymerization of OPD and OT.

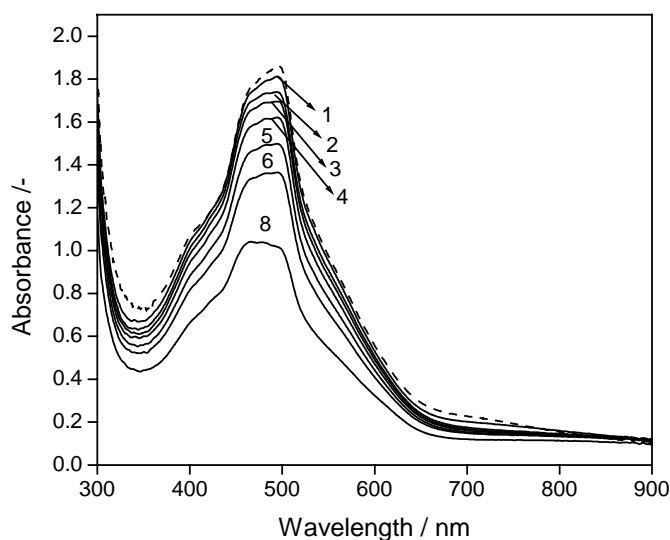


Fig. 5.4 UV-Vis spectra collected at different time intervals (as indicated, in minutes) after interruption of electrolysis for solution system OTA. Dashed line shows spectrum obtained at 15th minute during the electrolysis.

An analysis of the spectroscopic behavior of the mixed solutions after switching off the electrode potential was also made in order to support the assignment to the mixed cation radicals. In Fig. 5.4, the spectra recorded at different time intervals after interruption of electrolysis for solution system OTA are presented as an example. It is observable that the spectra in Fig. 5.4 do not match those recorded during electrolysis of the corresponding mixed solution. The absorbance value of the band at $\lambda = 497$ nm, assigned to the cation radical presumably resulting from the cross reaction of OPD and OT, shows a significant decrease in absorbance in comparison with the neighboring band at $\lambda = 462$ nm. The ratio of the absorbance of the band at $\lambda = 497$ to the band at $\lambda = 462$ nm, at the end of electrolysis (15th minute) and at the 8th minute after interruption of electrolysis changes from 1.076 to 0.971. Obviously the intermediate cation radical observed at $\lambda = 497$ nm undergoes a chemical reaction with neutral OPD or OT resulting in oligomer formation. Such a decrease of the absorbance of the band corresponding to an intermediate has been noticed in the polymerization of *N*-alkylsubstituted anilines [47, 48].

Similarly, the spectra in Fig. 5.4 also support our assignment of the band in the red region to the dicationic form of the mixed intermediate. One may suspect that during electrolysis of mixed solutions the band at $\lambda > 650$ nm is caused by POT only. But it can be seen from the spectra in Fig. 5.4 that contrary to OT the intensity of this band decreases with time without showing any band maximum or red shift, when the electrolysis is

stopped. This indicates that in case of mixed solution the red region band is caused by species different from those found with pure POT (presumably the dicationic form of the aniline type mixed dimer/oligomer).

5.4 Spectroelectrochemical Studies of Copolymerization of *o*-Phenylenediamine and *m*-Toluidine

The presence of mixed intermediates during the initial stages of copolymerization of OPD with MT was detected when electrolysis of mixed solutions having a constant MT and various OPD feed concentrations, was followed by UV-Vis spectroscopy. Fig. 5.5 a and b, respectively, present UV-Vis spectra registered during electropolymerization of mixed solutions of OPD and MT containing the lowest (0.01 M, system MTA) and highest (0.05 M, system MTE) OPD feed concentration, studied in the present work.

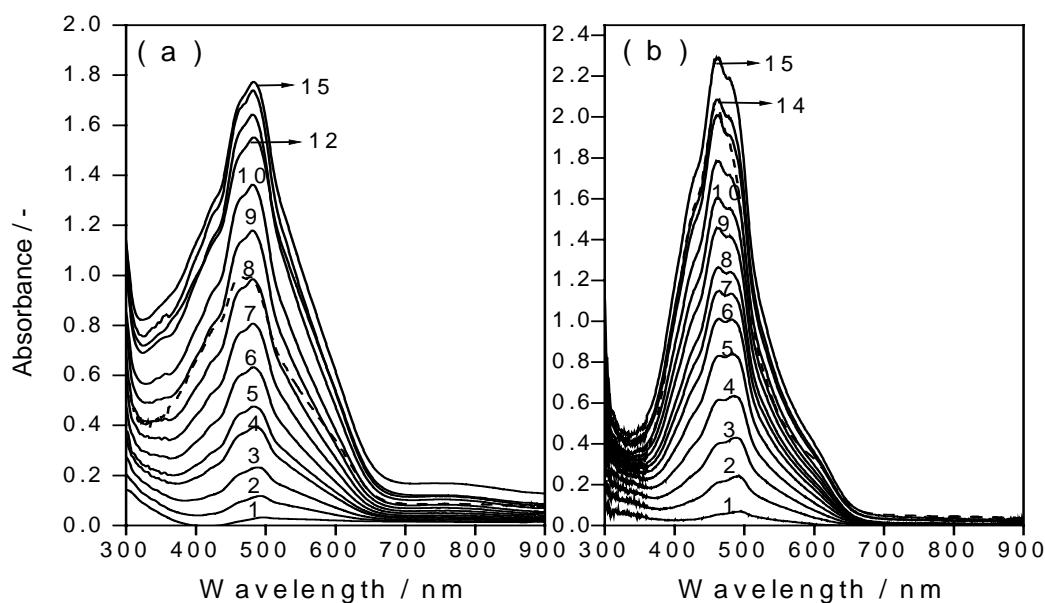


Fig. 5.5 UV-Vis spectra collected at different time intervals (as indicated, in minutes) during constant potential electropolymerization of solution system (a) MTA and (b) MTE. Dashed lines show spectra obtained at 7th minute after interruption of electrolysis.

The spectra registered in Fig. 5.5 present essentially the same picture (both during and after interruption of electrolysis) as those presented in Fig. 5.3 for the copolymerization of OPD with OT. The alteration of the growth characteristics of the band at $\lambda = 497$ nm or the red region band, with varying OPD feed concentration, is similar to the copolymerization

of ortho and meta isomers of toluidine with OPD. However, differences were observed in the absorption intensity of the bands. Contrary to the mixed solutions of OPD and OT, the absorption increases steadily with increasing OPD feed concentration for the mixed solutions of OPD and MT. The reason may lay in the difference of the substituent position between OT and MT. Probably the formation of dimeric/oligomeric species is more facilitated when OT is present in the feed as one of the monomer. It seems that initially similar intermediates are produced during the copolymerization of OPD with OT or MT. However, substantial differences, between optical response of the finally deposited poly(OPD-co-OT) and poly(OPD-co-MT) on the electrode surface, were observed when the spectra of the respective polymer coated electrodes were recorded at different applied potentials in the blank solution and will be discussed in the coming sections.

5.5 Spectroelectrochemistry of Poly(*o/m*-toluidine)

No noticeable polymer film was deposited on the electrode during the electrolysis (15 minutes) of OT or MT, therefore, the electrode was held approximately for 30 minutes more in the respective monomer solution at $E_{\text{SCE}} = 1.00$ V until a bluish green colored film was deposited on the electrode surface. The polymer film was reduced to its leucoemeraldine form by holding it at $E_{\text{SCE}} = -0.20$ V.

Fig. 5.6 a shows UV-Vis spectra of the POT-coated ITO electrode obtained at different electrode potentials ranging from $E_{\text{SCE}} = -0.20$ to 0.70 V in $1.5 \text{ M H}_2\text{SO}_4$. Spectra obtained at $E_{\text{SCE}} = -0.20$ to 0.10 V correspond to the reduced leucoemeraldine form of POT. The spectra show an absorbance maximum at $\lambda = 300$ nm and two low intensity bands at $\lambda = 425$ and $\lambda = 850$ nm, respectively. The absorbance band at $\lambda = 300$ nm corresponds to $\pi \rightarrow \pi^*$ transition of the benzoid rings in the reduced leucoemeraldine form of POT [107, 108, 202]. The extent of conjugation of π -orbital is believed to affect the position of the band for $\pi \rightarrow \pi^*$ transition. Any decrease or increase in the conjugation of the polymer will results, respectively, in a hypsochromic or bathochromic shift of this band [38, 39, 40].

The band at $\lambda = 425$ nm shows a maximum absorption value at $E_{\text{SCE}} = 0.40$ V followed by a steady decrease with an increase in the applied potential in the anodic direction. This band has been assigned to an intermediate state (polaron) formed during electrooxidation of the leucoemeraldine state of POT [203].

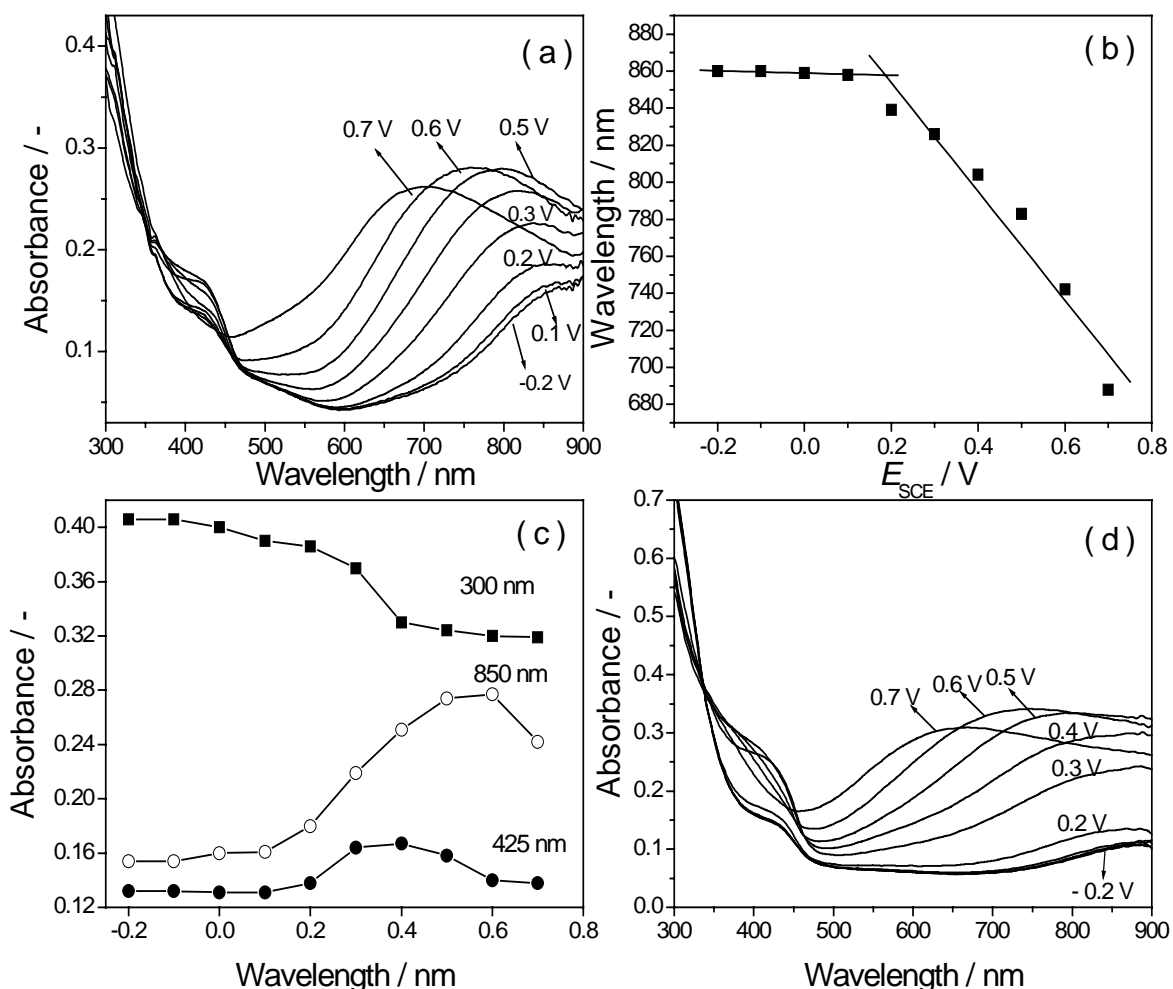


Fig. 5.6 (a and d) UV-Vis spectra of a POT and PMT-coated ITO glass electrode, respectively, obtained at different electrode potential values ranging from $E_{SCE} = -0.20$ to 0.70 V at every 0.10 V, in 1.5 M H_2SO_4 (b) Variations in the position of the POT band beyond $\lambda = 650$ nm with applied potentials and (c) Absorbance vs potential plot for three selected wavelengths, derived from spectra displayed in (a).

The main absorbance band in the red region of the spectra corresponds to the conducting emeraldine state of POT. The intensity of this band increases, with the potential shifted to higher values, simultaneously with a decreasing intensity of the band at $\lambda = 300$ nm. This indicates a progressive oxidation of POT film from the reduced leucoemeraldine state to its half oxidized emeraldine state. This band can be observed even at $E_{SCE} = -0.20$ V. This suggests that electrochemical reduction at $E_{SCE} = -0.20$ V is obviously incomplete and some charge remains in the sample [204]. A drastic blue shift and decrease in the intensity of this band can be observed as the potential passes $E_{SCE} = 0.60$ V, which corresponds to the conversion of emeraldine state of POT to its pernigraniline state [18, 205]. Two isobes-

tic points exist in Fig. 5.6 a at $\lambda = 370$ nm between the bands at $\lambda = 300$ and 425 nm and at around $\lambda = 460$ nm between the bands at $\lambda = 425$ and 850 nm, respectively. This indicates that a fixed ratio of oxidized to reduced form exists when the film is oxidized consecutively by applying increasing potential [41, 206]. These observations are in close agreement with those reported recently for the interconversion of the totally reduced leucoemeraldine, half oxidized emeraldine and the totally oxidized pernigraniline states of PANI [207].

The band at $\lambda = 850$ nm shows a blue shift with increasing potential in the anodic direction as evident from Fig. 5.6 b. For potentials lower than $E_{\text{SCE}} = 0.10$ V this band can be observed at round about $\lambda = 850$ nm and its position remains nearly unchanged. As the potential exceeds $E_{\text{SCE}} = 0.10$ V, a linear decrease in the absorption wavelength as a function of electrode potential can be observed and the band moves to approximately $\lambda = 681$ nm, corresponding to the applied potential of $E_{\text{SCE}} = 0.70$ V. The plot in Fig. 5.6 b is similar to the one reported by Brandl and Holze [204] for the shift in the absorption energy of the red region band in the UV-Vis spectra of PANI as a function of electrode potential. They have provided an explanation for the hypsochromic shift of the red region band with increasing potentials, which is based on the assumption of a distribution of chain segments of different effective conjugation length. According to the authors, the linear increase in the absorption energy (or a linear decrease in position maximum of the red region band in the present case) as a function of electrode potential suggest that a decreasing average conjugation length is responsible for the absorption energy or wavelength shift. No change in the absorption energy of the band was observed at lower electrode potentials that was assigned to the maximum conjugation length. It was supposed that only one charge exist per undisturbed coplanar polymer segment and there are charges only on the longest of these segments, as these have the lowest oxidation potentials. The increase in potential abstract more electrons from the polymer and the higher potentials allow the oxidation of shorter coplanar segments. As a result the absorption energy shifts to higher values i.e. the absorption wavelength decrease.

Elsewhere, the gradual blue shift of the red region band in the UV-Vis spectra of chemically synthesized PANI has been attributed to the formation of compact coil structure due to incorporation of SO_4^{2-} anions [18]. Dominis et al. [208] observed that the absorption maximum of redoped PANI in two different solvents is different. They have attributed this

difference to the compact and extended coil conformation of the PANI where the compact coil form shows absorption maximum at higher energies.

The absorption variation of the three main bands of POT with the applied potential can be well seen by plotting the value of absorbance as a function of applied potential (Fig. 5.6 c). It is observable that the absorption value of the band at $\lambda = 300$ nm decreases with increasing potential implying that the leucoemeraldine form of the POT is decreased with an increase in the potential. The absorbance band at $\lambda = 850$ nm increases with the increase of potential indicating a progressive oxidation of the POT film. A decrease in the absorption intensity of this band can be observed when the potential passes $E_{\text{SCE}} = 0.60$ V. It was suggested that at high potentials, pernigraniline sites are produced and irreversible processes like hydrolysis take place [204]. Such processes cause defects in the polymer backbone, which result in the decrease of the effective conjugation length. The chains with the highest effective conjugation length will be the first to suffer from the defect state, as these are the ones that are oxidized first if the potential is increased. Since they are responsible for absorption at the longest wavelengths, this wavelength region is where decrease in the absorption will be observed, first.

Fig. 5.6 d shows UV-Vis spectra of the PMT-coated ITO electrode obtained at different electrode potentials ranging from $E_{\text{SCE}} = -0.20$ to 0.70 V in 1.5 M H_2SO_4 . PMT exhibits optical properties essentially similar to that of POT, with the three corresponding bands at $\lambda = 300$, 420 and 850 nm, respectively, while two isobestic points at $\lambda = 338$ and 460 nm can also be observed, respectively. Both POT and PMT change color from pale yellow in the reduced form to bluish green in the oxidized form.

5.6 Spectroelectrochemistry of Poly(*o*-phenylenediamine)

Fig. 5.7 depicts the UV-Vis spectra of an ITO electrode, covered with POPD, at different potentials in the anodic direction ranging from $E_{\text{SCE}} = -0.30$ to 0.60 V. In the reduced form of the polymer low intensity absorption was observed beyond $\lambda = 600$ nm, which decreased slowly with the increase in potential. Maximum variations in the absorption intensity of the band around $\lambda = 482$ nm were observed at $E_{\text{SCE}} = 0.00$ V, close to the oxidation potential of POPD. The intensity of this band increases with the rise of potential up to $E_{\text{SCE}} = 0.40$ V and then remains nearly constant. The film changes its color from pale yellow in the reduced form to reddish brown in the oxidized form.

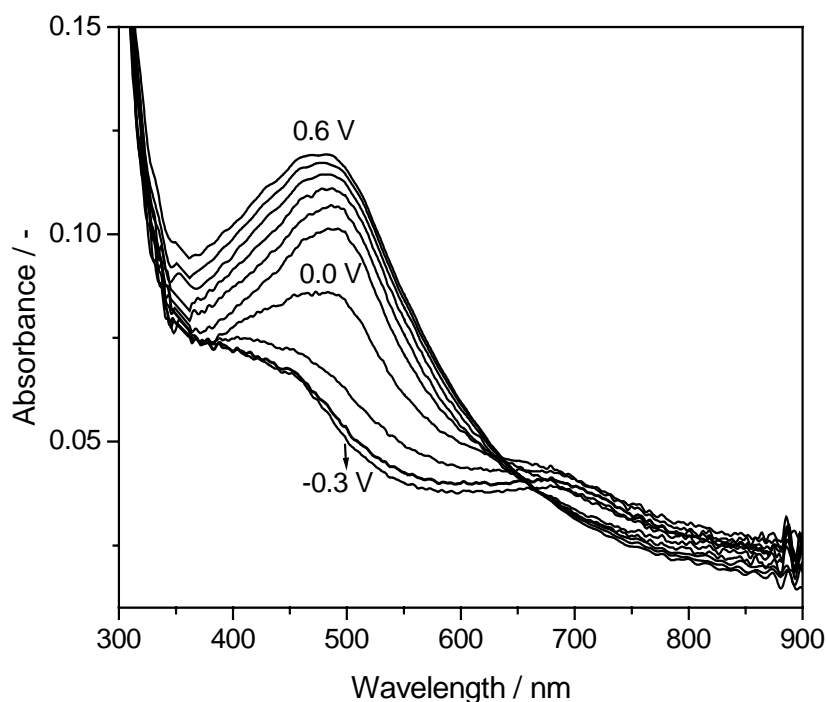


Fig. 5.7 UV-Vis spectra of a POPD-coated ITO glass electrode, obtained at different electrode potential values ranging from $E_{\text{SCE}} = -0.30$ to 0.60 V at every 0.10 V, in 1.5 M H_2SO_4 .

5.7 Spectroelectrochemistry of Poly(*o*-phenylenediamine-co-*o*-toluidine)

The spectroelectrochemical properties of the copolymer films were followed and compared with the homopolymers in order to identify the modifications in the spectral properties of the copolymers as a result of incorporation of OPD and OT units in the backbone of the copolymers. After holding the ITO electrodes for at least 70 minutes in the mixed solutions, respective copolymer films were deposited on the electrode, which display following characteristics (electrochromism). A copolymer film synthesized from mixed solution having 0.01 M OPD concentration (solution system OTA) exhibits a bluish color in its oxidized form while copolymer films synthesized with other OPD feed concentration were reddish brown in color. The absorption spectra of the deposited copolymer films were recorded in 1.5 M sulfuric acid solution at different applied potentials. The spectral response of the copolymers was found to be different from that of POPD or POT. Besides that, the copolymers show variations in the spectral properties among them. These variations can be assigned to the formation of copolymers having different proportions of monomer units (OPD or OT) in it.

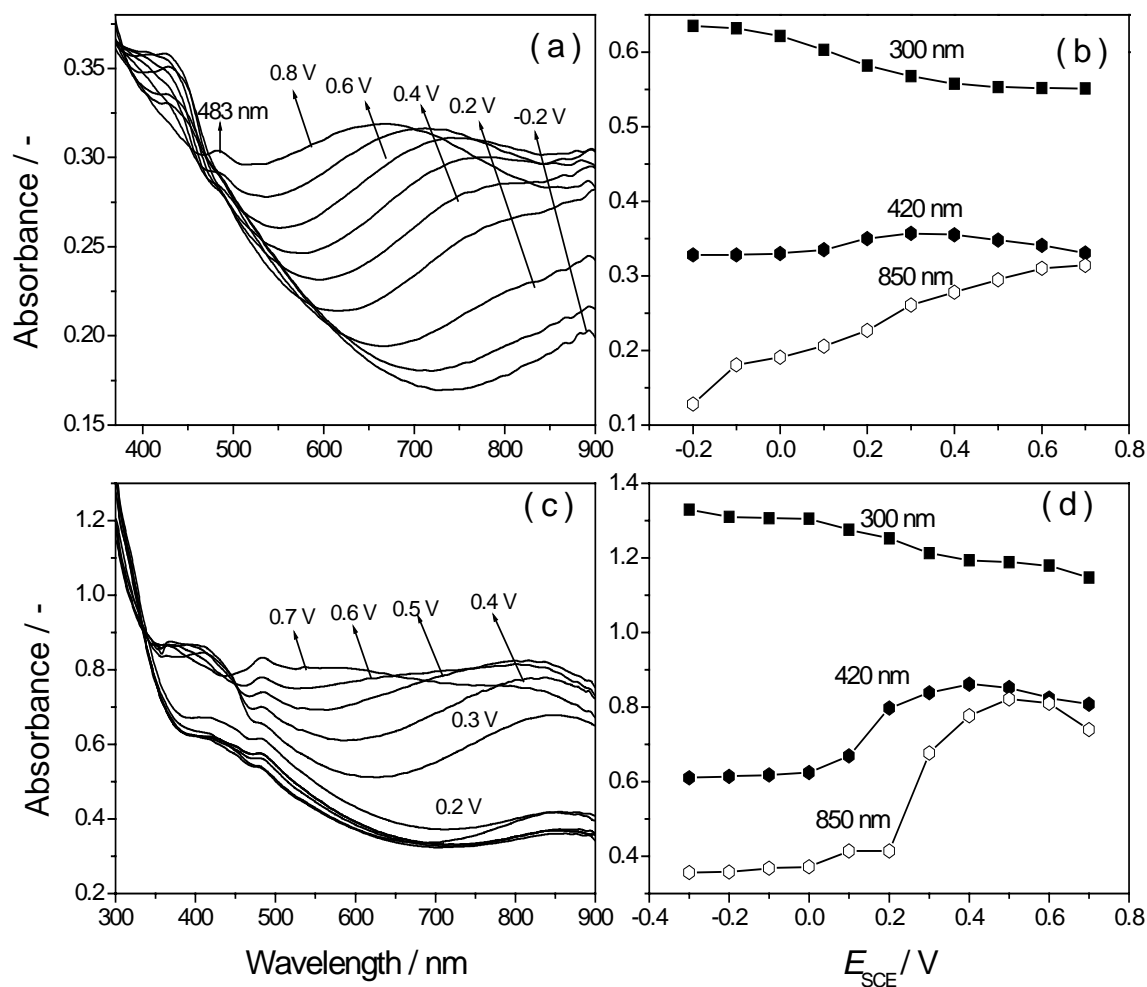


Fig. 5.8 UV-Vis spectra of copolymer-coated ITO glass electrodes, from solution system (a) OTA and (c) OTB, obtained at different electrode potential values ranging from $E_{SCE} = -0.30$ to 0.70 V at every 0.10 V, in 1.5 M H_2SO_4 . (b and d) Absorbance vs. potential plot for three selected wavelengths, derived from spectra displayed above in (a and c), respectively.

Fig. 5.8 a and c display the spectra recorded at different applied potentials for the copolymer films synthesized from solution systems OTA and OTB, respectively. Similar to POT, the spectra show three bands namely at about $\lambda = 300$, 420 and $\lambda > 650$ nm, respectively. Additionally another band at around $\lambda = 483$ nm can be observed which is absent in the spectra of POT alone. The origin of this feature may lie in the presence of OPD or POPD segments in the copolymer structure. The films show similar spectral response as that of POT with changing the applied potential in the positive direction. The intensity of the band at $\lambda = 420$ decreases after an applied potential of $E_{SCE} = 0.40$ V while the absorb-

ance of the band at $\lambda > 650$ nm increases with increasing potential, as evident from Fig. 5.8 b and d, respectively.

However, interestingly the electrochromic response of the above mentioned copolymer films is completely different from one another. The copolymer film in Fig. 5.8 a changes its color from pale yellow to blue upon oxidation while the copolymer film in Fig. 5.8 c does not show multiple color change characteristics of POT but show electrochromism like that of POPD. Chiba et. al have proposed that a polymer having an ideal conjugated aromatic structure should be black in its oxidized form but the copolymer OTB film was brown colored in oxidized form, so the possibility of an intermediate structure between the homopolymers cannot be excluded for this copolymer [209].

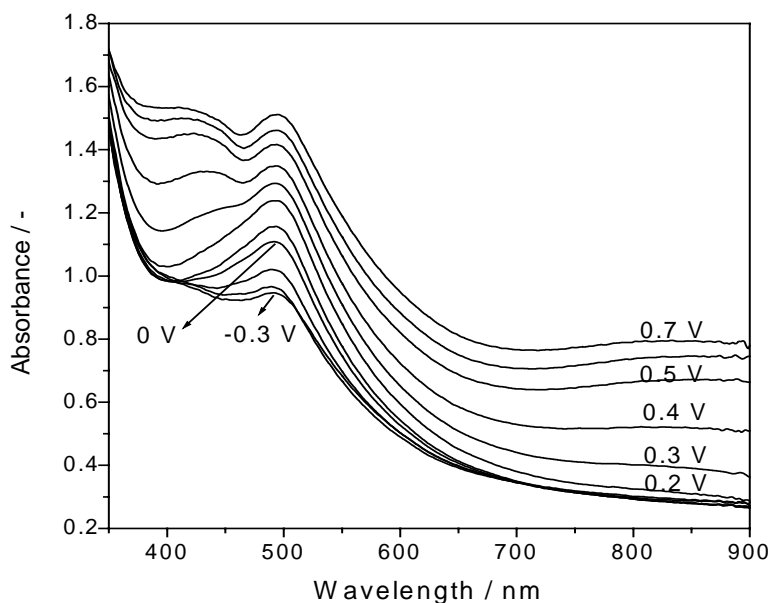


Fig. 5.9 UV-Vis spectra of copolymer OTC-coated ITO glass electrode, obtained at different electrode potential values ranging from $E_{\text{SCE}} = -0.30$ to 0.70 V at every 0.10 V, in 1.5 M H_2SO_4 .

The copolymer film synthesized from solution system OTC (Fig. 5.9) show spectral characteristics different from the either homopolymers, POPD and POT. Like copolymer OTA and OTB, the spectra of copolymer OTC also show three main bands upon oxidation but with a different scenario. These bands appear at $\lambda = 420$, 495 and $\lambda > 650$ nm, respectively. In the reduced state the absorption band at $\lambda = 495$ nm is prominent. Upon increasing the potential beyond $E_{\text{SCE}} = 0.20$ V new bands appear at ca. $\lambda = 420$ and $\lambda > 650$, respectively. All these bands grow in intensity with further increase in potential.

The copolymer films synthesized with higher OPD feed concentrations i.e. from solution system OTD and OTE, respectively, show spectral characteristics similar to POPD except that the main intensity band has shifted to longer wavelengths in comparison with POPD. This band appears at $\lambda = 498$ nm for the copolymer OTD (Fig. 5.10 a) while in case of copolymer film synthesized from solution system OTE the main band is observed at $\lambda = 492$ nm (Fig. 5.10 b). Therefore, it is highly probable that the OT units have been incorporated in the copolymer chain, as a result the copolymers synthesized even with highest OPD feed concentrations show some differences in spectral characteristics in comparison with POPD. The incorporation of OT units into POPD may result in more conjugated polymer than common POPD, which accounts for the bathochromic shift in the copolymer.

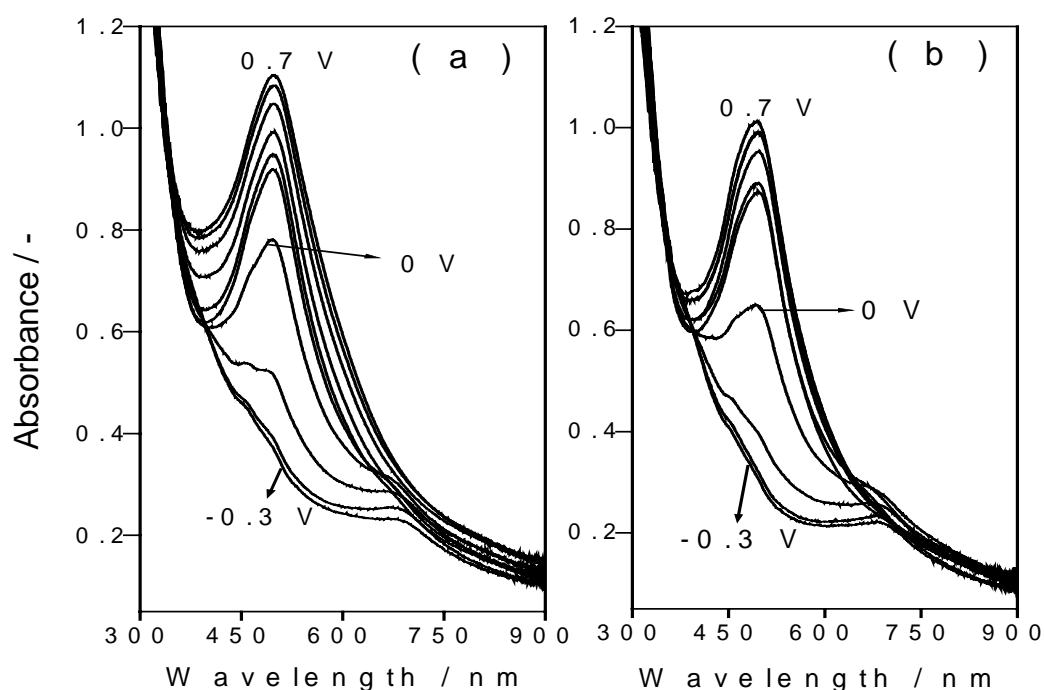


Fig. 5.10 UV-Vis spectra of copolymer (a) OTD and (b) OTE, obtained at different electrode potential values, ranging from $E_{\text{SCE}} = -0.30$ to 0.70 V at every 0.10 V, in 1.5 M H_2SO_4 .

On the basis of the spectroelectrochemical studies of poly(OPD-co-OT) it is reasonable to assume that the electrolysis of mixed solutions of OPD and OT result in different materials (copolymer). The spectroscopic results confirm that the properties of the copolymers strongly depend on the concentration of OPD in the feed and clear variations in the optical properties of the materials from mixed solutions can be observed just by varying the concentration of OPD in the feed. The UV-Vis results of poly(OPD-co-OT) further add

support to the assumption made in Section 4.3, that the structure of the copolymer is probably a mixture of copolymer chains with different monomer contents and has significant number of block segments of POPD or POT. When the OPD feed concentration exceeds 0.03 M the resulting copolymers show properties closely similar to those of POPD, which indicates an increase in the number of POPD block segments in the respective copolymers. Table 5.1 represents a comparison of the positions of the main bands observed in the UV-Vis spectra of POT, POPD and poly(OPD-co-OT).

Table 5.1 A comparison of the positions of the major bands in the UV-Vis spectra of POT, POPD and poly(OPD-co-OT)

Polymer	UV-Vis band position (nm)		
	Polaronic	OPD/POPD segments	Bipolaronic
POT	425	—	> 650
POPD	—	482	—
OTA	420	483	> 650
OTB	420	483	> 650
OTC	420	495	> 650
OTD	—	498	—
OTE	—	492	—

5.8 Spectroelectrochemistry of Poly(*o*-phenylenediamine-co-*m*-toluidine)

When the ITO electrode was held for a certain time (at least 70 minutes) in the mixed solutions containing OPD and MT, respective copolymer films were deposited on the electrode. The absorption spectra of the deposited copolymer films, recorded in 1.5 M sulfuric acid solution at different applied potentials, are compared in Fig. 5.11. The spectra of these copolymer films were not only different from those of respective homopolymers and poly(OPD-co-OT) but also show distinct variations among them especially at lower OPD feed concentration (system MTA and MTB, Fig. 5.11 a and b, respectively).

In the potential range of $E_{\text{SCE}} = -0.30$ to 0.20 V a broad band around $\lambda = 500$ nm can be observed in case of the copolymer synthesized from solution system MTA (Fig. 5.11 a). As observed with PMT (Fig. 5.6 d), the two absorptions corresponding to polaronic and bipolaronic forms of copolymer MTA appear at $\lambda = 417$ and $\lambda > 600$ nm at an applied potential of $E_{\text{SCE}} = 0.30$ V. However, unlike PMT the polaronic band disappears at potentials beyond $E_{\text{SCE}} = 0.40$ while the bipolaronic band continues to increase without any band

maximum and blue shift. As the electrode potential passes $E_{\text{SCE}} = 0.60$ V a major band in the region of $\lambda = 450 - 650$ nm, probably due to the fully oxidized form of the copolymer, occupies the spectra. This implies that the incorporation of OPD units in the copolymer backbone results in the change of the spectroelectrochemical response of the copolymer in comparison with PMT. Like PMT, the film changes its color from pale yellow in the reduced state to blue in the oxidized state.

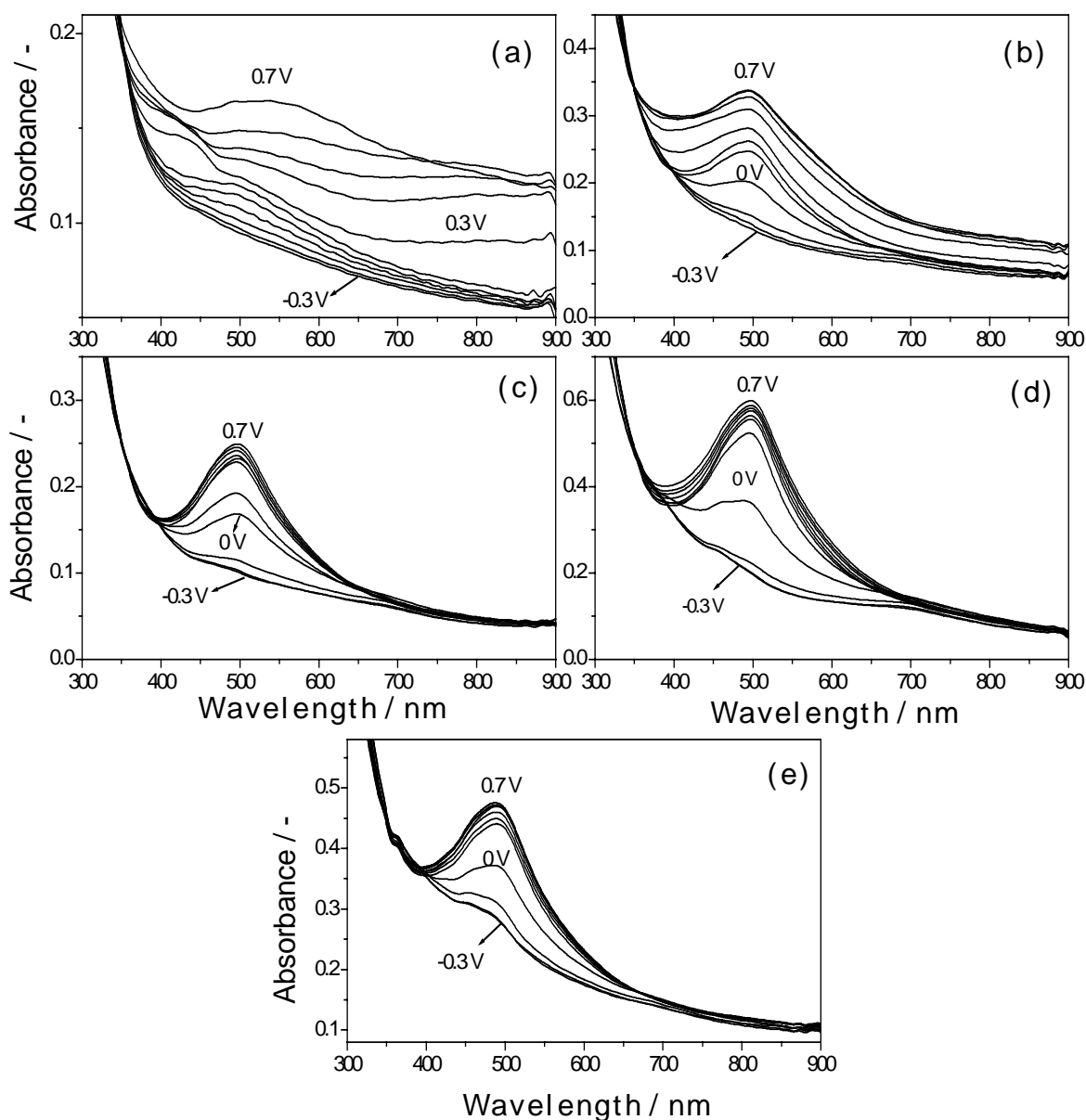


Fig. 5.11 UV-Vis spectra of copolymer-coated ITO glass electrodes, from solution system (a) MTA, (b) MTB, (c) MTC, (d) MTD and (e) MTE, obtained at different electrode potential values ranging from $E_{\text{SCE}} = -0.30$ to 0.70 V at every 0.10 V, in 1.5 M H_2SO_4 .

In case of copolymer MTB (Fig. 5.11 b), a maximum intensity band at $\lambda = 494$ nm and a broad absorption in the red region is observed. The presence of the broad absorption in the red region may be due to bipolaronic transitions of MT/PMT moieties in the copolymer. These observations also suggest that the structure of copolymer MTA and MTB is different from that of the homopolymers as well as from one another. Perhaps, a copolymer of varying composition of OPD/POPD or MT/PMT could be generated while performing electropolymerization with different feed ratios of OPD. Furthermore, UV-Vis spectra of copolymer MTB in Fig. 5.11 b are substantially different from those of copolymer OTB in Fig. 5.8 a, which support the assumption that the structure of the two polymers is very different from one another. For the polymers obtained from solution systems MTC, MTD, and MTE (Fig. 5.11 c, d and e, respectively) the spectra show close similarities with the spectra obtained for POPD alone. However, the maximum position of the band is shifted in comparison with POPD, which may be attributed to incorporation of MT/PMT units in these polymers. The main band appears at $\lambda = 498$, 497 and 488 nm for copolymer MTC, MTD and MTE, respectively. Table 5.2 shows a comparison of the positions of the main bands observed in the UV-Vis spectra of poly(OPD-co-MT) and the respective homopolymers.

Table 5.2 A comparison of the positions of the major bands in the UV-Vis spectra of PMT, POPD and poly(OPD-co-MT)

Polymer	UV-Vis band position (nm)		
	Polaronic	OPD/POPD segments	Bipolaronic
PMT	420	—	> 650
POPD	—	482	—
MTA	417	—	> 650
MTB	420	494	> 650
MTC	420	498	—
MTD	—	497	—
MTE	—	488	—

6 FT-IR Measurements

FT-IR spectroscopy helps in identifying the structure and/or types of chemical bonds in a material. This technique measures the absorption of various infrared light wavelengths by the material of interest. These infrared bands identify specific molecular components and structures. Absorption bands in the range of 4000-1500 cm^{-1} are typically due to functional groups, e.g. -OH , C=O , N-H etc. The region between 1500-400 cm^{-1} is referred to the fingerprint region. Absorption bands in this region are generally due to intra-molecular phenomena and are highly specific for each material. Vibrational spectra are directly related to structural features of molecules. The frequencies of the bond vibrations are determined by the electronic nature of the bonds and are therefore sensitive to changes in structure and environment.

FT-IR spectroscopy is used most often to study the structural properties of conducting polymers. Structure of PANI has been elucidated using this vibrational spectroscopy [210]. FT-IR spectroscopy of PANI reveals that PANI is formed by 1,4-coupling of aniline monomer [210]. *In situ* FT-IR spectroscopy has been effectively used to study the structural changes and modifications during the electrochemically induced insulator to metal transition of PANI [211, 212]. The metallic state of PANI has been reported to show a broad band above 4000 cm^{-1} . The band exhibits maximum intensity in the half oxidized state of the polymer and bleaches in the completely oxidized state and has been correlated with the presence of free charge carriers [107, 109, 213]. Formation of the intermediate product of polymerization has been characterized using this technique [44]. Infrared spectra of PANI films deposited on various substrates have also been studied *ex situ* [16, 214] and assignments of the vibrational modes of the polymer have been made by several groups [215, 216, 217, 218]. Moreover, formation of copolymers and presence of a functional group on the polymer backbone [51, 219, 220] as well as the anion content and degree of oxidation of a polymer can be deduced [211, 212] from the presence of corresponding bands and their intensities in the FT-IR spectrum. In this dissertation, the FT-IR spectra (*ex situ*) for the homo-/copolymers were recorded in order to roughly have an idea about the structural properties of the polymers. Moreover, the FT-IR spectra were helpful to trace both corresponding monomers in the respective copolymer backbone. The FT-IR measurements were performed with the completely oxidized form of the polymer, under the assumption that the washing and drying processes as well as contact with air did not alter the sample properties significantly.

6.1 FT-IR Measurements of Poly(*o*-/*m*-toluidine)

Fig. 6.1 represents the FT-IR spectrum of POT. The skeletal vibrations of the aromatic rings show two bands at 1635 and 1500 cm^{-1} , which are attributed to C=C stretching vibrations of quinoid and benzoid rings, respectively [216, 221]. The intensity of quinoid ring stretching vibrations relative to the intensity of benzoid ring stretching vibrations is considered to be a measure of the degree of oxidation of the polymer [211]. The intensity of the band at 1635 cm^{-1} is higher than that of the band at 1500 cm^{-1} indicating the presence of predominantly quinoid rings in POT (as the sample was collected in its completely oxidized state) [211, 212, 222]. The shoulder at 1325 cm^{-1} and a weak peak at 1288 cm^{-1} are assigned to C–N stretching vibrations of quinoid and benzoid rings, respectively, as reported elsewhere for PANI [223, 224]. A peak at 1068 cm^{-1} is due to SO_4^{2-} anions [223]. The FT-IR spectrum of POT shows the characteristic band of the $-\text{CH}_3$ functional group at about 1004 cm^{-1} [40, 225].

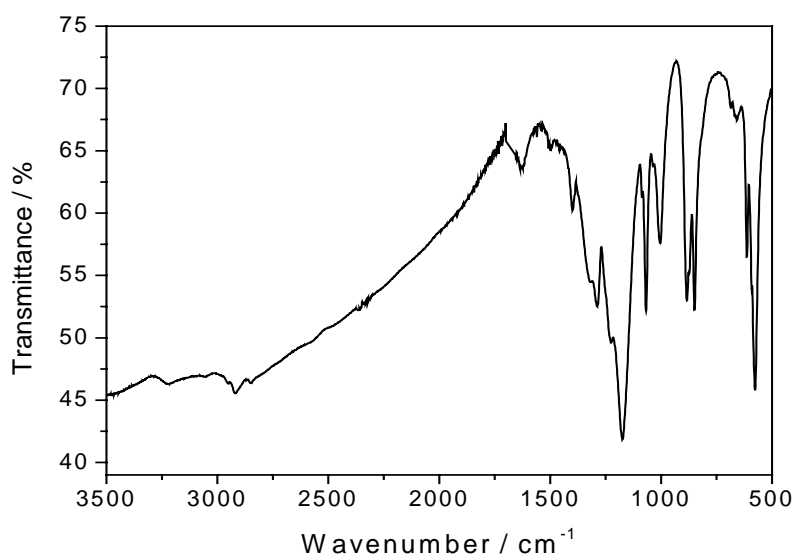


Fig. 6.1 FT-IR spectrum of POT.

The signal due to C–H in plane bending vibrations is observed at 1175 cm^{-1} . The peak at 883 cm^{-1} has been assigned to 1,2,4-trisubstituted aromatic rings indicating polymer formation [226]. The signal at 576 cm^{-1} is due to C–H out of plane bending vibrations

[227, 228]. The peak at 2922 cm^{-1} is caused by C–H stretch modes of the substituent methyl group [131].

Fig. 6.2 depicts the FT-IR spectra registered for PMT. The frequency peaks at 2922, 1557, 1486, 1305, 1246, 1150, 880 and 579 cm^{-1} are attributed, respectively, to C–H stretching of the substituent methyl group, C=C stretching vibrations of quinoid rings, C=C stretching vibrations of benzoid rings, C–N stretching vibrations of quinoid rings, C–N stretching vibrations of benzoid rings, C–H in plane bending vibrations, 1,2,4-trisubstituted aromatic rings and C–H out of plane bending vibration.

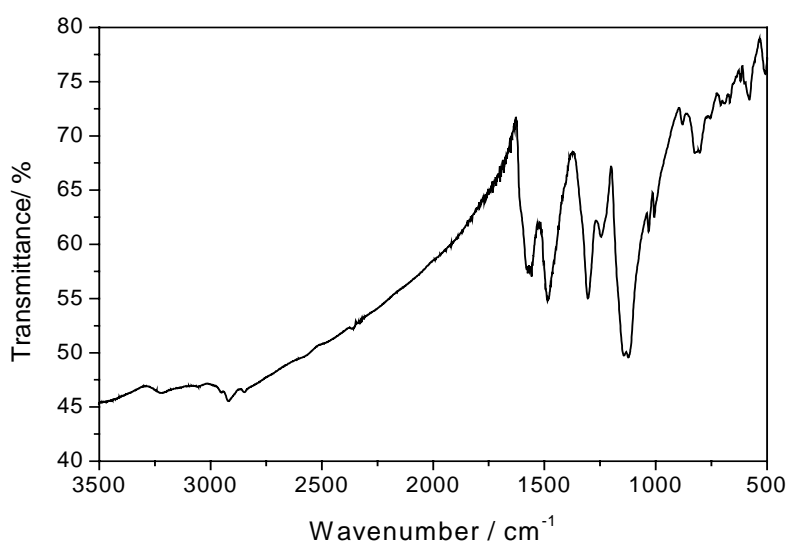


Fig. 6.2 FT-IR spectrum of PMT.

6.2 FT-IR Measurements of Poly(*o*-phenylenediamine)

The POPD spectrum shows a broad band in the region between $3700\text{--}3000\text{ cm}^{-1}$ generally assigned to primary and secondary amino groups present in the polymer [139, 229, 230]. The band at 1636 cm^{-1} is broad and can be assigned to C=C stretching vibrations the aromatic rings. Another band at 1400 cm^{-1} may corresponds to the ring stretching vibrations of the phenazine type structures in the POPD backbone [231, 232]. The bands assigned to C–N stretching vibrations of the quinoid and benzoid rings appear at 1319 and 1287 cm^{-1} , respectively. The peaks at 850 cm^{-1} are due to out of plane bending motion of the C–H bonds of the 1,2,4,5-tetrasubstituted benzene nuclei of phenazine units. The presence of the bands at 884 cm^{-1} due to in-plane bending motion of the C–H bonds of the 1,2,4-

trisubstituted benzene rings indicates the presence of open rings in the phenazine units [233]. The signal at 614 cm^{-1} is assignable to ring deformation. The peak at 578 cm^{-1} is due to C–H out of plane bending vibration.

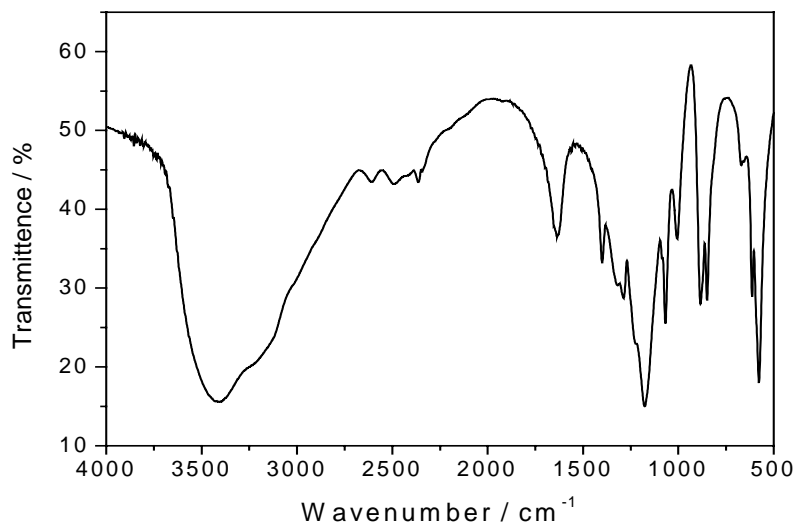


Fig. 6.3 FT-IR spectrum of POPD.

6.3 FT-IR Measurements of Poly(*o*-phenylenediamine-co-*o*-toluidine)

Fig. 6.4 compares the FT-IR spectra recorded for poly(OPD-co-OT). The diversity in the nature of the copolymers with changing OPD feed concentration was observed with the FT-IR study. Most of the bands show variations in the intensity and position.

The spectra of all the copolymers show the main bands corresponding to N–H stretching vibrations and ring stretching vibrations of quinoid and benzoid structures. The intensity of the N–H stretching vibrations in the region between $3700\text{--}3000\text{ cm}^{-1}$ increases with increasing OPD feed concentration indicating an increase in the number of primary and secondary amino groups in the copolymer structure. The stretching vibrations of quinoid rings show a blue shift for the copolymers. The corresponding band appears at 1600 cm^{-1} for copolymer OTA (Fig. 6.4 a), while for copolymer OTB (Fig. 6.4 b) and OTC (Fig. 6.4 c) this signal is shifted to 1618 and 1621 cm^{-1} , respectively. The band corresponding to benzoid stretching vibrations is observed at 1495 cm^{-1} for copolymer OTA and its intensity decreases for copolymer OT and OTC.

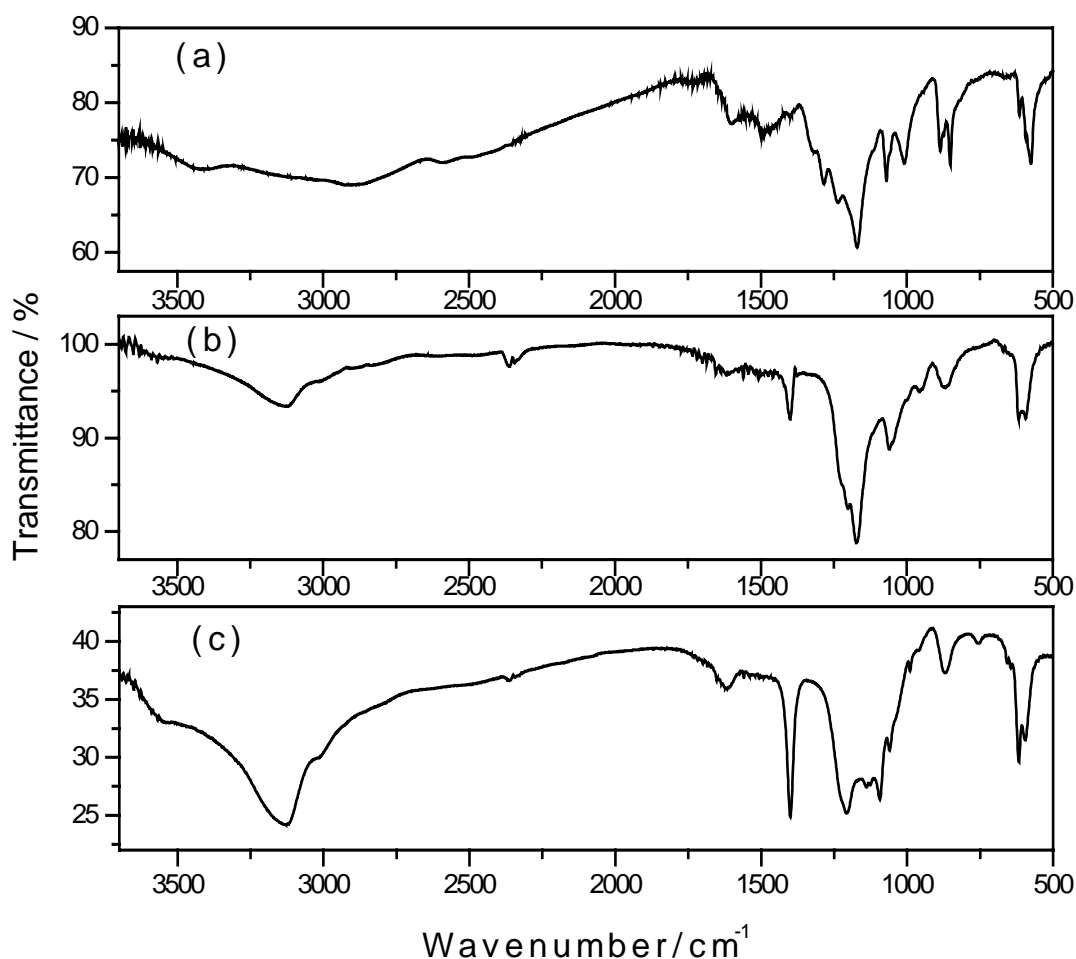


Fig. 6.4 FT-IR spectra of copolymer (a) OTA, (b) OTB and (c) OTC.

The intensity of the two bands centered at 1400 and 615-617 cm^{-1} greatly increases with increasing OPD feed concentration. The 1400 cm^{-1} band in the copolymer indicate the presence of phenazine type structures in the copolymer backbone. These cyclic structures in the copolymers could either be due to the presence of POPD blocks or may result from the cyclization of the adjacent OPD and OT unit in the copolymer chain. On the other hand the intensity of the band at 1007-958 cm^{-1} , due to $-\text{CH}_3$ bending vibrations, substantially decreases from copolymer OTA to OTC. This is indicative of the gradual decrease in the OT units in the copolymer structure with increasing OPD feed concentration. In addition, the later band shows a prominent blue shift from copolymer OTA to OTC. The occurrence of the band at 885-869 in all the copolymers in Fig. 6.4 indicates that the monomers are bonded head to tail [172], as expected from the UV-Vis study in Section 5.3. The major

FT-IR bands of poly(OPD-co-OT) and the respective homopolymers are listed along with their assignments in Table 6.1.

Table 6.1 A comparison of the major FT-IR bands and their assignments for POT, POPD and poly(OPD-co-OT)

Wavenumber (cm ⁻¹)					Description
POT	POPD	Cop OTA	Cop OTB	Cop OTC	
576	578	576	591	591	β (C–H)
—	614	615	617	617	Def(ring)
883	884/850	885/830	869	867	Head to tail coupling
1004	—	1007	959	958	β (–CH ₃)
1068	1068	1069	1060	1068	Due to sulfate anions
1288	1287	1235	—	1208	ν (C–N) B
1325	1319	1284	—	—	ν (C–N) Q
—	1400	1398	1401	1401	ν (Ring) P
1500	—	1495	1491	—	ν (C=C) B
1635	1636	1600	1618	1621	ν (C=C) Q
2922	—	—	—	—	ν (C–H) due to –CH ₃
3243	3700-3000	3700-3000	3700-3000	3700-3000	ν (N–H)

B: benzoid; Def: deformation mode; P: phenazine type structures; Q: quinoid type ring; β : bending mode; ν : stretching mode.

6.4 FT-IR Measurements of Poly(*o*-phenylenediamine-co-*m*-toluidine)

The FT-IR spectra of the poly(OPD-co-MT) are shown in Fig. 6.5. In general, with some exceptions, the spectral characteristics of the copolymers are very similar to those of POPD. The intensity of the broad band, in the region of 3700-3000 cm⁻¹, increases with increasing OPD feed concentration. Its position also changes with changing OPD concentration in the feed. The band corresponding to quinoid stretching vibrations occurs at 1618, 1627 and 1634 cm⁻¹ for copolymer MTA, MTB and MTC (Fig. 6.5 a, b and c), respectively. The intensity of this band was also found to increase with increasing OPD feed concentration. The incorporation of MT moiety in the copolymer was indicated by the appearance of the characteristic C–H stretching of the substituent methyl group which was observed as a very weak band at 2922 cm⁻¹ in the spectra of the copolymer MTB (Fig. 6.5 b). This band cannot be observed in the spectra of the copolymer MTA and MTC, which is probably due to its masking by the strong and broad peak in the region 3700-3000 cm⁻¹.

The major FT-IR bands of poly(OPD-co-MT) and the respective homopolymers are listed along with their assignments in Table 6.2.

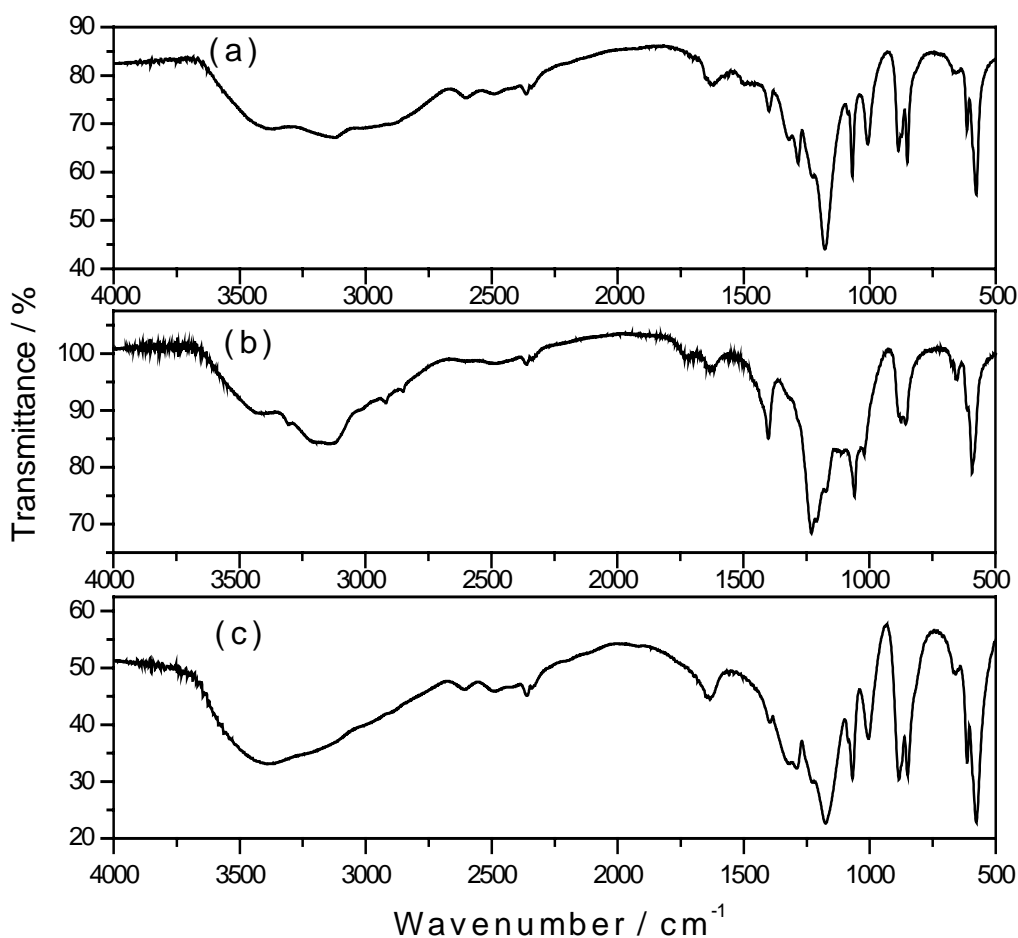


Fig. 6.5 FT-IR spectra of copolymer (a) MTA, (b) MTB and (c) MTC.

The FT-IR spectra of the polymers synthesized from the mixture of OPD and OT or MT further establish that the electrolysis of mixed solution of OPD and OT or MT results in copolymers. The spectra also reveal the structural differences between the homo-/copolymers as well as between poly(OPD-co-OT) and poly(OPD-co-MT) and it can be inferred that polymers with different structural properties are deposited if the OT monomer is replaced by the MT monomer in the comonomer feed with OPD.

Table 6.2 A comparison of the major FT-IR bands and their assignments for PMT, POPD and poly(OPD-co-MT)

Wavenumber (cm ⁻¹)					Description
PMT	POPD	Cop MTA	Cop MTB	Cop MTC	
579	578	577	593	576	β(C–H) out of plane
—	614	658	656	651	Def(ring)
880	884/850	886/851	856	884/850	Head to tail coupling
1068	1068	1068	1068	1068	Due to sulfate anions
1246	1287	1284	1230	1289	ν(C–N) B
1305	1319	1322	—	1338	ν(C–N) Q
—	1400	1400	1400	1396	ν(Ring) P
1486	—	1499	—	—	ν(C=C) B
1557	1636	1618	1627	1634	ν(C=C) Q
2922	—	—	2922	—	ν(C–H) due to –CH ₃
3241	3700-3000	3700-3000	3700-3000	3700-3000	ν(N–H)

B: benzoid; Def: deformation mode; P: phenazine type structures; Q: quinoid type ring; β: bending mode; ν: stretching mode.

7 Raman Spectroelectrochemical Measurements

7.1 Raman Spectroelectrochemical Measurements of Poly(*o*-/*m*-toluidine)

The Raman spectra of POT recorded at different applied potentials are shown in Fig. 7.1 a. In the reduced state the spectra show two main bands at 989 and 1058 cm^{-1} corresponding to the internal modes of sulfate ions [18]. These bands are not affected by changing the potential to higher values. New bands appear upon oxidation of the polymer when the potential is gradually increased in the anodic direction. These bands observed, can be assigned to different vibrational modes based on the known assignments.

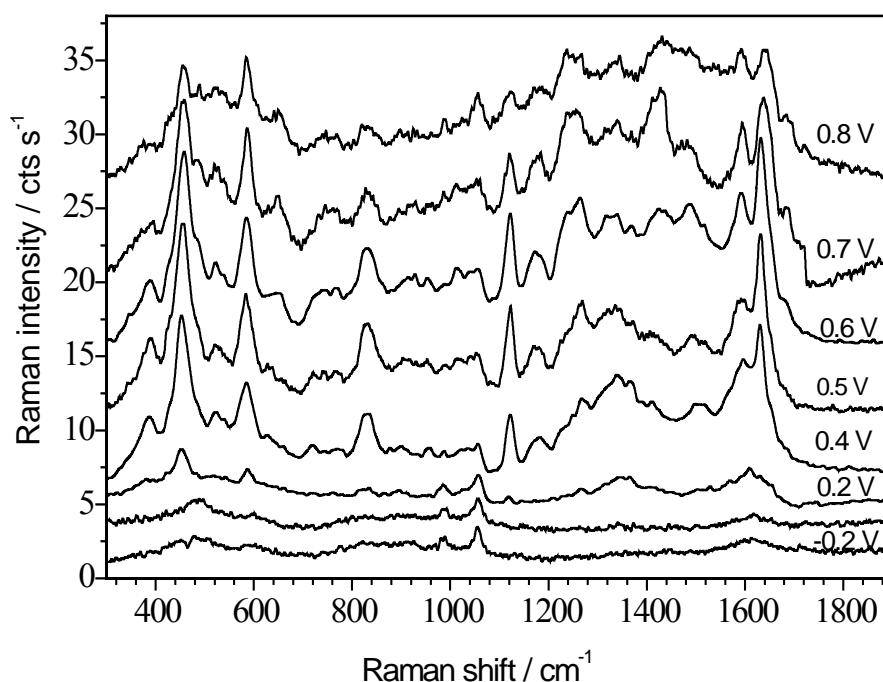


Fig. 7.1 *In situ* Raman spectra of POT, obtained at different electrode potentials ranging from $E_{SCE} = -0.20$ to 0.80 V, in 1.5 M H_2SO_4 .

A weak band appearing at 1122 cm^{-1} after $E_{SCE} = 0.20$ V grows in intensity up to $E_{SCE} = 0.60$ V and then decreases afterwards. This band corresponds to the C–C stretching vibration in the methyl substituted semiquinone and quinone rings [234]. Another band at 1177 cm^{-1} can be attributed to the C–H bending vibration mode of aromatic rings. Normally, at lower electrode potential, this band is considered to be the characteristic C–H bending vibration mode of benzoid rings [235, 236]. However, the absence of this band at

lower potentials in the present case and its appearance and gradual increase in intensity with the anodic sweep suggest this to be the feature of the quinoid like rings in the oxidized form of the polymer [237]. A medium intensity band at 1269 cm^{-1} has been assigned to the C–N stretching vibrations of semiquinoid and quinoid rings [234]

The low intensity signals appearing in the range of $1300\text{--}1400\text{ cm}^{-1}$ centered at 1338 and 1369 cm^{-1} , belong most probably to the stretching vibration of C–N⁺ of the polaronic part having an intermediate single-double bond order and being coupled to quinoid like rings [236]. The appearance of two bands in this region has been correlated with the two kinds of differently organized polarons [238]. The band located at 1338 cm^{-1} is present at all potentials above $E_{SCE} = 0.00\text{ V}$ in the presently studied potential range. In contrast, the band present at 1369 cm^{-1} diminishes after $E_{SCE} = 0.60\text{ V}$. During the anodic sweep a new band of weak intensity at round about 1490 cm^{-1} appears when extending the potential to $E_{SCE} = 0.40\text{ V}$. This signal is observed in the potential region between $E_{SCE} = 0.20$ to 0.60 V where the emeraldine state of POT exists and thus can be assigned to the C=N stretching of the semiquinone structure. Similar observations have been reported elsewhere [236, 239]. At $E_{SCE} = 0.80\text{ V}$ the intensity of this band greatly diminishes.

The Raman spectra of POT seems to consist of very weak overlapping bands in the region of $1580\text{--}1650\text{ cm}^{-1}$ at an applied potential of $E_{SCE} = 0.20\text{ V}$. On extending the potential to $E_{SCE} = 0.40\text{ V}$ two signals centered at 1597 and 1630 cm^{-1} , respectively, can be observed. The band at 1597 cm^{-1} grows in intensity with increasing potential showing a shift to 1592 cm^{-1} at the highest potential tested and has been assigned to the C=C stretching vibrations of quinoid like rings [237, 239]. The very striking feature of the Raman spectra of POT is the strong band at 1630 cm^{-1} and needs special attention. This band becomes prominent as the applied potential passes $E_{SCE} = 0.20\text{ V}$. After $E_{SCE} = 0.20\text{ V}$ its intensity greatly increases with increasing potential and attains a maximum at $E_{SCE} = 0.60\text{ V}$. Further increase in potential above $E_{SCE} = 0.60\text{ V}$, results in a decrease in the intensity of this band. A very prominent blue shift to 1639 cm^{-1} is observed at the highest potential applied.

A band in the spectral region of $1610\text{--}1630\text{ cm}^{-1}$ has usually been reported for PANI and its derivatives, using blue or green excitation laser, and is repeatedly assigned to ring C–C stretching vibrations of benzoid rings, characteristic of the reduced form of the polymer. As the enhancement of Raman modes is directly correlated to the UV-Vis-NIR absorption, the blue and red lasers are expected to enhance, respectively, the “reduced” and “oxidized units” of the polymer.

Shreepathi and Holze [18] observed a strong band at 1628 cm^{-1} in the reduced leucoemeraldine form of PANI with blue laser light ($\lambda_{\text{ex}} = 476.5\text{ nm}$) and have assigned it to the ring C–C stretching vibrations of benzoid rings. The same band at 1627 cm^{-1} has been observed with green laser light ($\lambda_{\text{ex}} = 514.5\text{ nm}$) for the reduced form of PANI and was again assigned to benzoid rings [240]. Malinaukas et al. [146] have observed a strong band at 1620 cm^{-1} with green light ($\lambda_{\text{ex}} = 514.5\text{ nm}$) in the Raman spectra of poly(ANI-co-OPD). This band showed an increase in the intensity with increasing potential until the potential was made more positive than the first anodic wave of the copolymer, after which the intensity of this band diminished. They have attributed this feature to be due to a benzoid mode. Berrada et al. [241] observed a band in the range of $1612\text{--}1620\text{ cm}^{-1}$ during their experimental and theoretical studies of PANI and POT. They have used two different lasers, blue ($\lambda_{\text{ex}} = 457.9\text{ nm}$) and red ($\lambda_{\text{ex}} = 647.1\text{ nm}$) for their study, and assigned this band to C–C stretching vibration of benzoid rings.

In a comparative study of electrochemically prepared PANI, it was observed with the use of three different excitation wavelengths, that this band shows strong intensity with blue and green excitations. However, with red laser light, the intensity of this band was very low at less positive potentials (where the number of benzoid structures should be high in the reduced state of the polymer) [237]. It was assumed that because the red laser does not enhance the bands for the reduced segments, therefore, the intensity of this band remains low when red excitation laser is used. In contrast to this Quillard et al. [235] have reported, in their study of PANI with red laser light ($\lambda_{\text{ex}} = 647.4\text{ nm}$), an increasing intensity of this band at potentials between $E_{\text{SCE}} = -0.15$ to 0.65 V , where the amount of benzoid rings should generally decrease due to the conversion of benzoid to quinoid units.

The main feature in our spectra of POT, obtained with red laser light ($\lambda_{\text{ex}} = 647.1\text{ nm}$), is the unusual intensity dependence of the band located at 1630 cm^{-1} on the applied potential and notable upshift in frequency of the band from 1630 to 1640 cm^{-1} when the potential passes $E_{\text{SCE}} = 0.60\text{ V}$. Rather similar observations have recently been reported by Wei et al. [239] for the band at 1616 cm^{-1} in the Raman spectra of poly(*N*-methylaniline) in the range of $E_{\text{Ag/AgCl}} = 0.42$ to 0.82 V , studied with ($\lambda_{\text{ex}} = 780\text{ nm}$) laser. However, they did not provide any explanation for this tendency of the band. Likewise, a band at 1628 cm^{-1} , in the Raman spectra of the copolymer of aniline with 2-aminonaphthalene-6,8-disulfonate obtained with red laser light ($\lambda_{\text{ex}} = 632.8\text{ nm}$), has been reported to show a maximum of intensity at an applied potential of $E_{\text{Ag/AgCl}} = 0.40$ or 0.50 V [242]. The corresponding band at

1628 cm^{-1} was ascribed to the C=N–C of the half oxidized state (with maximum polaron concentration) of the copolymer containing heterocyclic rings in its backbone. Cintra et al. have observed a corresponding band at 1640 cm^{-1} , with red laser light ($\lambda_{\text{ex}} = 632.8\text{ nm}$) but not with the blue one ($\lambda_{\text{ex}} = 488\text{ nm}$), for the eletrosynthesized films of poly(5-amino-1-naphthol). This was ascribed to C–N–C bonds of the ladder structure of the polymer containing phenazine-like molecular fragments [243].

Thus the elucidation of the band at 1630 cm^{-1} in our Raman spectra of POT seems to be a complicated task. One possibility is to correlate this band to the red region band in the UV-Vis spectra of POT. *In situ* UV-Vis spectra shows that during an anodic potential sweep, an absorbance band beyond $\lambda = 650\text{ nm}$ corresponding to half oxidized emeraldine state of POT, shows an increase in the absorption intensity till the potential reaches $E_{\text{SCE}} = 0.60\text{ V}$. At an applied potential higher than $E_{\text{SCE}} = 0.60\text{ V}$, the absorbance of this band decreases with a clear blue shift, giving an indication of transformation of POT into fully oxidized pernigraniline state at a potential higher than $E_{\text{SCE}} = 0.60\text{ V}$.

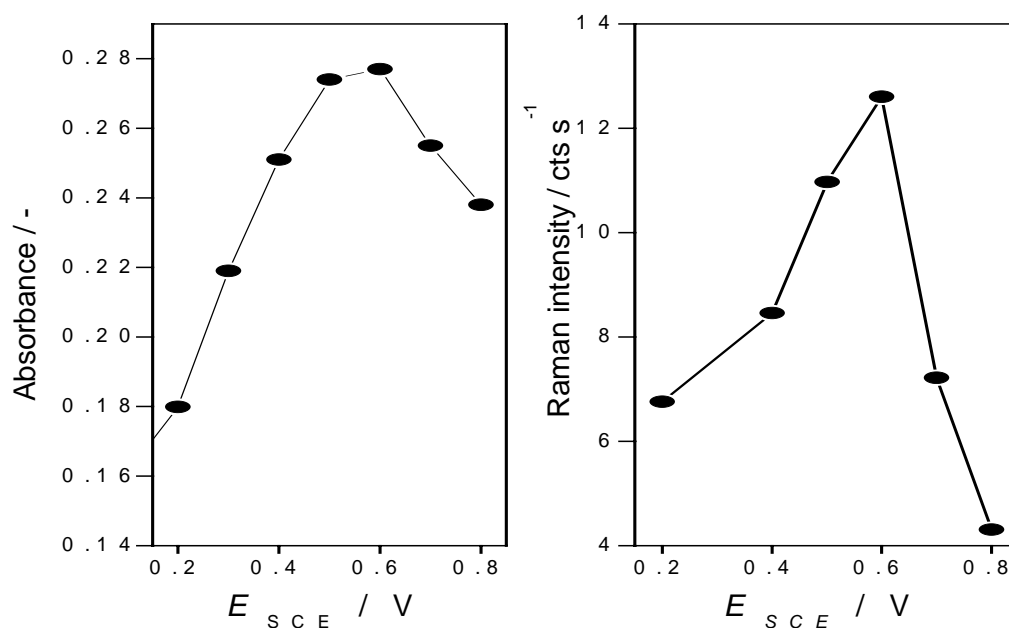


Fig. 7.2 Dependence of the (a) absorbance intensity of the band at $\lambda > 650\text{ nm}$ in UV-Vis spectra and (b) Raman intensity of the band at 1630 cm^{-1} in the Raman spectra of POT, on the applied electrode potential.

The laser excitation wavelength used in the present study approximately falls in the range of the red region of UV-Vis absorption band of POT. Hence, enhancement due to

resonance Raman effect is expected for the half oxidized or fully oxidized form of POT. When plotted as a function of potential, the trend of potential dependence of absorption intensity for the UV-Vis band at $\lambda > 650$ nm (Fig. 7.2 a) is very similar to the potential dependence of the Raman intensity of the band at 1630 cm^{-1} (Fig. 7.2 b) in the corresponding spectra of POT. Thus it may be inferred that the band located at 1630 cm^{-1} in the Raman spectra of POT and the behavior of this band during an anodic sweep probably belongs to the emeraldine to pernigraniline transition of POT. In addition to the above-mentioned major bands, several bands in the lower frequency region appear in the Raman spectra of POT upon oxidation. All the major bands observed in the Raman spectra of POT are summarized in Table 7.1.

Table 7.1 Major band assignments of Raman spectra of POT obtained with $\lambda_{\text{ex}} = 647.1\text{ nm}$

Wavenumbers (cm^{-1}) at electrode potential (V) (vs. SCE)				
0.20	0.40	0.60	0.80	Description
–	387	387	–	$\delta(\text{C-H})$
450	452	458	458	$\gamma(\text{C-H})$
584	584	584	584	$\delta(\text{Ring})$
–	830	830	830	$\gamma(\text{C-H})$
1122	1122	1122	1123	$\nu(\text{C-C})$ of $-\text{CH}_3$ substituted SQ/Q
–	1177	1175	1173	$\beta(\text{C-H})$ Q
1269	1267	1264	1264	$\nu(\text{C-N})$ SQ/Q
1355	1340/1370	1340/1370	1344	$\nu(\text{C-N}^+)$ SQ
–	1490	1488	–	$\nu(\text{C=N})$ QI
–	1597	1592	1592	$\nu(\text{C=C})$ SQ/Q
–	1630	1632	1640	–

B: benzoid; SQ: semiquinone; Q: quinoid type ring; QI: quinoneimine; β : bending mode; δ : in-plane deformation mode; γ : out-of-plane deformation mode; ν : stretching mode.

Fig. 7.3 shows the Raman spectra of a PMT film at different applied potentials. No well resolved Raman spectra were obtained for PMT with red laser excitation despite of several efforts.

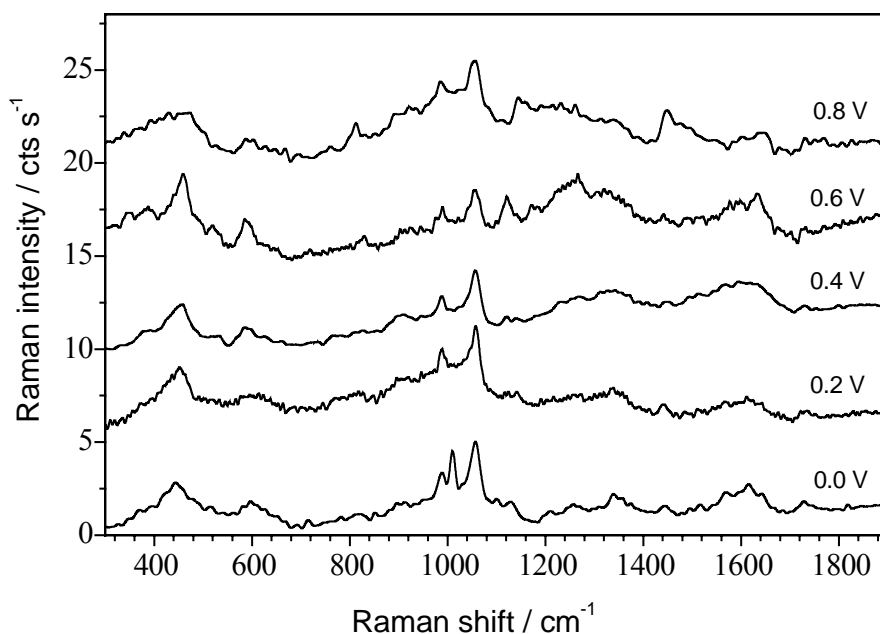


Fig. 7.3 *In situ* Raman spectra of PMT, obtained at different electrode potentials ranging from $E_{SCE} = 0.00$ to 0.80 V, in 1.5 M H_2SO_4 .

7.2 Raman Spectroelectrochemical Measurements of Poly(*o*-phenylenediamine)

Fig. 7.4 depicts the Raman spectra of POPD film. The major Raman bands are given in Table 7.2. The dominating bands observed at an electrode potential of $E_{SCE} = -0.20$ V, are located at 1248 , 1390 , 1471 , 644 and 603 cm^{-1} . The strong band located at 1248 cm^{-1} undergoes a decrease in the intensity with increase in the electrode potential in the positive direction. Elsewhere, a Raman band at 1248 cm^{-1} with similar tendency has been assigned to the C–N stretching vibration [242]. The substantial decrease in the intensity of this band after $E_{SCE} = 0.00$ V indicates the decrease in the number of C–N bonds due to oxidation of the polymer. Another band that undergoes strong decrease in the intensity, with the increasing potential, is the one located at 1471 cm^{-1} . This band prevails over other bands at an applied potential of $E_{SCE} = -0.20$ V. As the potential steps to more positive potentials the band 1471 cm^{-1} shows a decrease in the intensity and vanishes after $E_{SCE} = 0.10$ V.

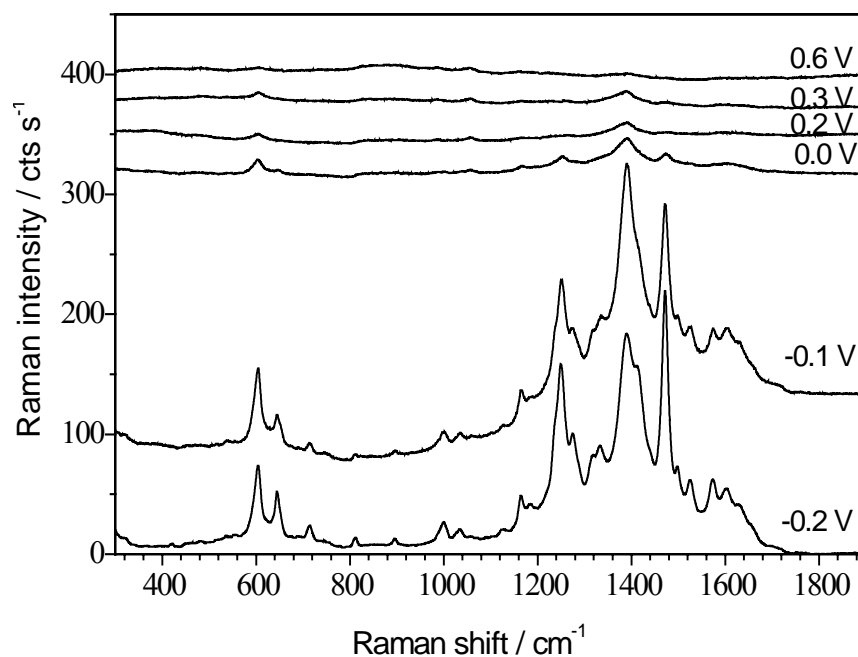


Fig. 7.4 *In situ* Raman spectra of POPD, obtained at different electrode potentials ranging from $E_{SCE} = -0.20$ to 0.60 V, in 1.5 M H_2SO_4 .

Table 7.2 Major band assignments of Raman spectra of POPD obtained with $\lambda_{ex} = 647.1$ nm

Wavenumbers (cm^{-1}) at electrode potential (V) (vs. SCE)					
-0.20	0.00	0.10	0.20	0.30	Description
603	603	603	603	603	Def (ring)
644	647	649	—	—	Def (ring)
1164	1166	1170	—	—	β (C-H)
1248	1248	1252	1252	—	ν (C-N)
1390	1390	1392	1388	1388	—
1471	1473	1474	1474	—	ν (Ring) P
1575	—	—	—	—	ν (C=C) B
1603	1606	1606	—	—	ν (C=C) SQ

B: benzoid; Def: deformation mode; P: phenazine type structures; Q: quinoid type ring; SQ: semiquinone; β : bending mode; ν : stretching mode.

In literature the assignment of the band at 1480-1495 cm^{-1} to the C=N mode is well established for PANI [237, 191, 242, 244]. Similarly Jiang et al. [245] have observed a band at 1485 cm^{-1} in the Raman spectra of OPD-fibers and assigned this band to the stretching vibrations of C=N groups. However, an attempt to assign this band, in the present case, to C=N groups of POPD must be discarded due to decreasing trend of its intensity with potential. The presence of this band in the reduced form indicates that this mode is in resonance condition with red line and that it is not necessarily related to oxidized species. In a recent study of phenazine by Li et al. [232], using green laser excitation ($\lambda_{\text{ex}} = 526 \text{ nm}$), a medium intensity band at 1474 cm^{-1} was observed at an electrode potential of $E_{\text{SCE}} = -0.20 \text{ V}$ which becomes very weak when the electrode potential is moved to $E_{\text{SCE}} = 0.00 \text{ V}$ and has been assigned to the ring stretching vibrations. Following this study, the band observed at 1476 cm^{-1} in the Raman spectra of POPD can be assigned to the ring stretching vibration of the phenazine like structures in its backbone.

The most important band that shows dependence on the applied potential is the one appearing at 1390 cm^{-1} . This band attains maximum intensity at $E_{\text{SCE}} = -0.10 \text{ V}$ and decreases afterwards. In many cases a Raman band with such a behavior has been attributed to an intermediate state of the polymer. A band at 1415 cm^{-1} was observed in the Raman spectra of electrodes modified with POPD and PANI-POPD bilayer [146]. The band attained a maximum at $E_{\text{RHE}} = 0.00 \text{ V}$. This was attributed to the semi oxidized form of POPD that has maximum concentration of charge carriers at this electrode potential. Further increase in the potential caused a decrease in the intensity of the corresponding band.

It is noteworthy to mention that the CV of POPD shows only one broad redox process. However, a two-step electrooxidation process was proposed earlier for the phenazine-like structure of POPD [146, 246]. According to this the oxidation of a fully reduced to fully oxidized form of POPD proceeds via an intermediate state that present the half oxidized form of the polymer. Recently Shah and Holze [247] observed a band around 1645 cm^{-1} in the Raman spectra of poly(o-aminophenol), a structurally analogue of POPD, using red laser excitation ($\lambda_{\text{ex}} = 647.1 \text{ nm}$). The intensity of this band grows during a positive potential shift, attains a maximum at about $E_{\text{SCE}} = 0.30 \text{ V}$, and then decreases with further increase in potential. They have attributed this to the existence of intermediate species during the redox transformation of the polymer.

Thus it is conceivable that the band at 1390 cm^{-1} corresponds to the semi oxidized state of POPD, where the number of charge carriers is maximum. When the potential is increased further, the intensity of this band decreases drastically since the transition from the

semi oxidized to total oxidized state occurs. The assignment for the other bands appearing in the spectra of POPD is as follow. The bands at 603 and 644 cm^{-1} are assigned to ring deformation modes [232]. The intensity of the band at 603 cm^{-1} increases with increasing potential up to $E_{\text{SCE}} = -0.10$ V followed by a decrease with the further anodic sweep of potential. The band at 644 cm^{-1} shows a decrease in the intensity with the increasing potential and diminishes after $E_{\text{SCE}} = 0.00$ V. The medium intensity band appearing at 1164 cm^{-1} and a very weak shoulder at 1184 cm^{-1} is assigned C–H bending vibration modes [234, 236]. The band at 1164 cm^{-1} shifts to 1170 cm^{-1} and disappear after $E_{\text{SCE}} = 0.00$ V. The presence of weak intensity bands at 1575 and 1603 cm^{-1} indicates that POPD may contain benzoid and quinoid structures in its reduced state [146].

7.3 Raman Spectroelectrochemical Measurements of Poly(*o*-phenylenediamine-co-*o*-toluidine)

Fig. 7.5 represents the Raman spectra of copolymer OTB. The spectra are not so simple and show differences in many features and tendencies in comparison with the homopolymers and are, therefore, discussed in detail. At an applied potential of $E_{\text{SCE}} = -0.20$ V the copolymer film shows a broad band at 1615 cm^{-1} representing quinoid and benzoid like structures. Two bands of considerable intensity located at 1378 and 605 cm^{-1} can also be observed. Upon increasing the potential to $E_{\text{SCE}} = 0.00$ V new bands of weak intensity at 1508, 1473, 1295, 1245 and 1158 cm^{-1} appear. As the potential reaches $E_{\text{SCE}} = 0.10$ V the intensity of all the bands increases. Further increase in the potential induces a reduction in the intensity of the Raman bands until these bands nearly disappear at $E_{\text{SCE}} = 0.60$ V.

The broad band at about 1615 cm^{-1} grows in intensity and at $E_{\text{SCE}} = 0.10$ V splits into two well separated bands centered at 1629 and 1600 cm^{-1} , respectively. These bands shift to 1626 and 1597 cm^{-1} , respectively, with further increase in potential and at $E_{\text{SCE}} = 0.30$ V again merged into one to form a broad band with very low intensity. In addition to this a weak intensity band located at 1442 cm^{-1} is observed at in the Raman spectrum of copolymer OTB an applied potential of $E_{\text{SCE}} = -0.20$ V. No band was observed at this frequency in the Raman spectra of the corresponding homopolymers. This band grows in intensity with a maximum at $E_{\text{SCE}} = 0.10$ V and disappears after $E_{\text{SCE}} = 0.30$ V. It has been suggested that upon oxidation, the inner rings of the molecules loose their aromatic character. The pure C–C stretching vibrations are mainly affected by these changes and split into two well-separated components [248]. The C=C stretching of the semiquinone rings give rise to

a strong band at 1600 cm^{-1} while the C–C stretching of these units appear at 1442 cm^{-1} [248].

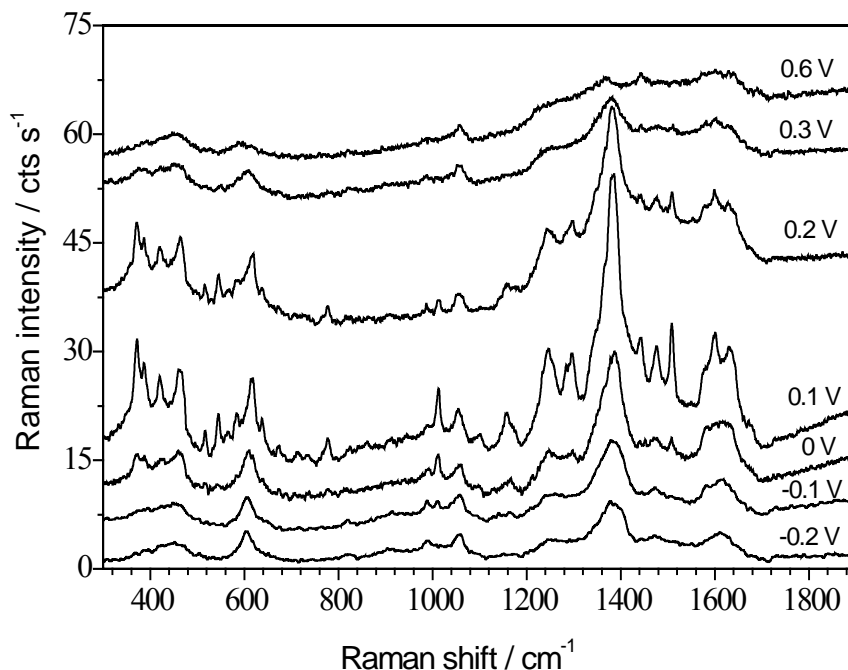


Fig. 7.5 *In situ* Raman spectra of copolymer OTB, obtained at different electrode potentials ranging from $E_{\text{SCE}} = -0.20$ to 0.60 V , in $1.5\text{ M H}_2\text{SO}_4$.

Another weak band at 1508 cm^{-1} , not observed in case of either homopolymer, appears at an applied potential of $E_{\text{SCE}} = 0.00\text{ V}$ and becomes strong and sharp when the potential is increased to $E_{\text{SCE}} = 0.10\text{ V}$. Upon further oxidation this band decreases and finally disappears at $E_{\text{SCE}} = 0.30\text{ V}$. It has been assigned to the stretching vibrations of quinoneimine fragments with a C=N bond coupled with quinoid like rings [237]. It should be noted that the very intense band at 1471 cm^{-1} , observed in the Raman spectra of POPD at lower potentials, is completely absent in the spectra of the copolymer. On the other hand a weak intensity band at 1473 cm^{-1} appears after $E_{\text{SCE}} = -0.10\text{ V}$ and grows in intensity, shifts to 1476 cm^{-1} and diminishes after $E_{\text{SCE}} = 0.20\text{ V}$. This band can be assigned to stretching vibrations of quinoneimine type C=N bond. The bands corresponding to C–N stretching of semiquinoid radicals appear at 1295 and 1245 cm^{-1} . These bands are observed in the potential region of $E_{\text{SCE}} = -0.10$ and 0.30 V with a maximum at $E_{\text{SCE}} = 0.10\text{ V}$. The medium intensity band at 1158 cm^{-1} showing an up shift to 1162 cm^{-1} with increasing potential is assigned to C–H bending vibrations of quinoid type rings. The band corresponding to C–C vibrations in the methyl substituted semiquinone rings give signal at 1105 cm^{-1} with a weak intensity between the applied potential of $E_{\text{SCE}} = -0.10$ and 0.20 V .

As observed with POPD, the dominating band appearing at 1378 cm^{-1} between the applied potentials of $E_{\text{SCE}} = -0.20$ and 0.50 V is attributable to the half oxidized state of the copolymer. In contrast to POPD, this band is downshifted and attains a maximum intensity at $E_{\text{SCE}} = 0.10\text{ V}$ (for POPD it was observed at 1390 cm^{-1} with maximum at $E_{\text{SCE}} = -0.10\text{ V}$). Furthermore, numerous bands of considerable intensities appear upon oxidation in the 300 to 600 cm^{-1} region. Such bands were absent in the Raman spectra of POPD but the spectra of POT showed signals of strong intensity in this region when the potential was increased beyond $E_{\text{SCE}} = 0.20\text{ V}$. The major bands observed in the Raman spectra of copolymer OTB are listed in Table 7.3 along with their assignments.

Table 7.3 Major band assignments of Raman spectra of copolymer OTB obtained with $\lambda_{\text{ex}} = 647.1\text{ nm}$

Wavenumbers (cm^{-1}) at electrode potential (V) (vs. SCE)					
-0.20	0.00	0.10	0.20	0.30	Description
–	370	372	372	371	$\delta(\text{C-H})$
–	427	420	419	–	$\gamma(\text{Ring})$
–	463	462	462	462	$\gamma(\text{C-H})$
–	–	545	544	–	$\delta(\text{Ring})$
605	610	617	619	605	Def(ring)
–	1105	1101	1101	–	$\nu(\text{C-C})$ of $-\text{CH}_3$ substituted SQ
–	1158	1160	1162	–	$\beta(\text{C-H})$ Q
–	1245	1245	1242	–	$\nu(\text{C-N})$ SQ
–	1295	1297	1297	–	$\nu(\text{C-N})$ SQ
1378	1389	1385	1382	1380	–
–	1442	1444	1444	–	$\nu(\text{C-C})$ SQ
–	1473	1475	1476	–	$\nu(\text{C=N})$ QI
–	1508	1508	1509	1511	$\nu(\text{C=N}) + \text{Q}$
1615	1600/1629	1600/1629	1597/1626	1615	$\nu(\text{C=C})$ SQ/ $\nu(\text{C=N})$ QI

B: benzoid; Def: deformation mode; Q: quinoid type ring; QI: quinoneimine; SQ: semiquinone; β : bending mode; δ : in-plane deformation mode; γ : out-of-plane deformation mode; ν : stretching mode.

The above discussion provides some useful information about the electrochemical properties of the copolymer. The Raman spectra of copolymer OTB suggest that during the redox process the copolymer passes through an intermediate state, which exists, in the potential range between $E_{SCE} = -0.10$ and 0.30 V. This is the same potential range, which covers the boundaries of first and second oxidation peaks in the CV of copolymer OTB or where the maximum conductivity values exist. The Raman spectra also suggest that the copolymer has a different structure from that of homopolymers having the properties of both homopolymers, which is in good accordance with cyclic voltammetric, conductivity or UV-Vis spectroelectrochemical data of copolymer OTB.

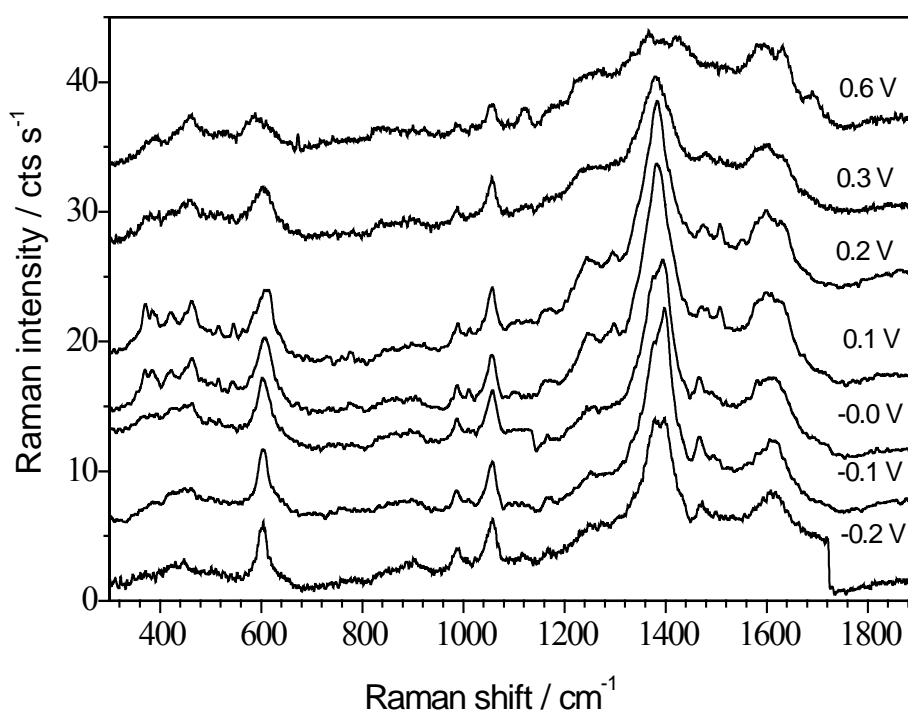


Fig. 7.6 *In situ* Raman spectra of copolymer OTC, obtained at different electrode potentials ranging from $E_{SCE} = -0.20$ to 0.60 V, in 1.5 M H_2SO_4 .

Fig. 7.6 demonstrates the Raman spectra registered at different applied potentials for copolymer OTC. At an applied potential of $E_{SCE} = -0.20$ V the spectrum shows a broad band around 1615 cm^{-1} and strong bands at 1386 and 605 cm^{-1} , respectively. As observed with copolymer OTB, these bands also grow in intensity with the increasing potential, reach a maximum at $E_{SCE} = 0.10$ V and decrease afterwards. New bands can be observed at 1507 , 1297 , 1245 and in the region between 300 and 600 cm^{-1} , when the applied potential is increased from $E_{SCE} = 0.00$ to 0.20 V. These bands disappear upon further oxidation.

However, in contrast to copolymer OTB the intensity of these bands was low. At an applied potential of $E_{\text{SCE}} = -0.20$ V a weak intensity band is observed at 1472 cm^{-1} . Unlike the corresponding band in the Raman spectra of copolymer OTB, its intensity decreases with increasing potential. However, the same tendency was observed with a band at 1476 cm^{-1} in the Raman spectra of POPD. Increasing concentration of OPD in the feed presumably induces some differences in the copolymer structure in comparison with copolymer OTB. In other words it may indicate an increase of OPD/POPD units in copolymer OTC. The major Raman bands of copolymer OTC and their assignments are listed in Table 7.4.

Table 7.4 Major band assignments of Raman spectra of copolymer OTC obtained with $\lambda_{\text{ex}} = 647.1\text{ nm}$

Wavenumbers (cm^{-1}) at electrode potential (V) (vs. SCE)					
-0.20	0.00	0.10	0.20	0.30	Description
—	—	376	372	371	$\delta(\text{C-H})$
—	—	420	419	—	$\gamma(\text{Ring})$
—	450	463	462	462	$\gamma(\text{C-H})$
—	—	543	546	—	$\delta(\text{Ring})$
605	605	606	606	606	Def(ring)
—	1169	1169	1162	—	$\beta(\text{C-H})$ Q
—	1253	1245	1244	—	$\nu(\text{C-N})$ SQ
—	—	1297	1297	—	$\nu(\text{C-N})$ SQ
1386	1397	1384	1381	1358	—
1472	1467	1467	—	—	$\nu(\text{C=N})$ QI / (Ring) P
—	—	1507	1507	—	$\nu(\text{C=N}) + \text{Q}$
1615	1616	1609	1607	1605	$\nu(\text{C=C})$

B: benzoid; Def: deformation mode; P: phenazine type structures; Q: quinoid type ring; QI: quinoneimine; SQ: semiquinone; β : bending mode; δ : in-plane deformation mode; γ : out-of-plane deformation mode; ν : stretching mode.

When the OPD feed concentration is further increased the Raman features show more similarities with POPD as evident from the Raman spectra registered for copolymer OTD (Fig. 7.7). At an applied potential of $E_{\text{SCE}} = -0.20$ V the spectrum shows a strong band at 1390 cm^{-1} and medium intensity bands at around 1475 , 1250 and 603 cm^{-1} . Like POPD the

dominating band at 1390 cm^{-1} attains maximum at $E_{\text{SCE}} = -0.10\text{ V}$ and then decreases with a shift to 1374 cm^{-1} . The bands at 1475 and 1250 cm^{-1} exhibit a decrease in intensity and diminished upon oxidation. The intensity of 1475 cm^{-1} band is higher than the corresponding band of copolymer OTC but still lower than that of POPD. The region between $300\text{--}600\text{ cm}^{-1}$ seems to be consisting of several overlapping bands. However, these bands do not appear to be well resolved upon oxidation.

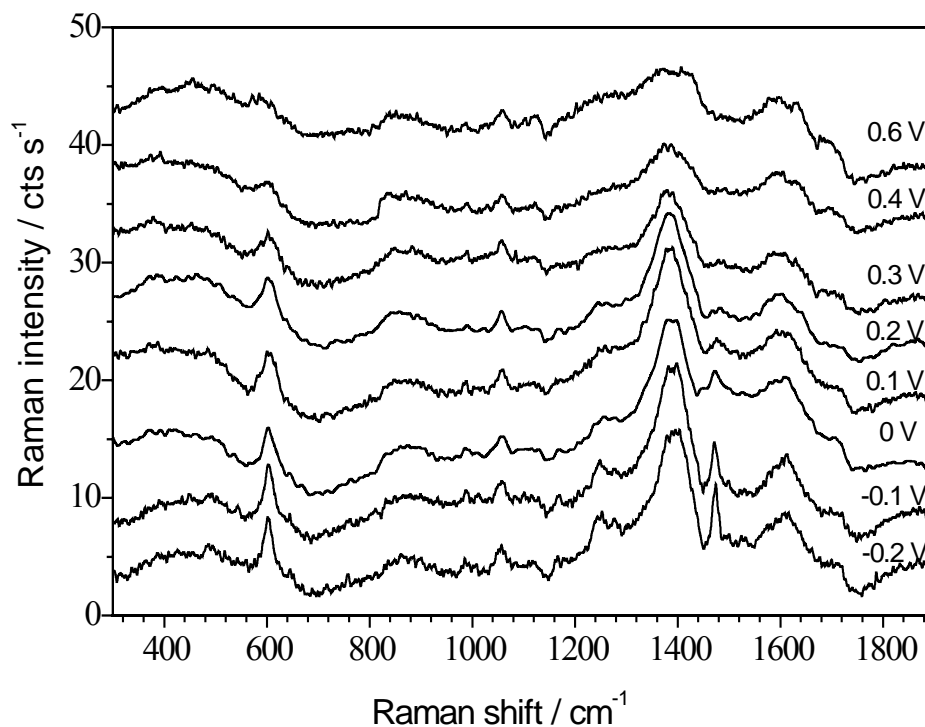


Fig. 7.7 *In situ* Raman spectra of copolymer OTD, obtained at different electrode potentials ranging from $E_{\text{SCE}} = -0.20$ to 0.60 V , in $1.5\text{ M H}_2\text{SO}_4$.

Table 7.5 Major band assignments of Raman spectra of copolymer OTD obtained with $\lambda_{\text{ex}} = 647.1\text{ nm}$

Wavenumbers (cm^{-1}) at electrode potential (V) (vs. SCE)					
-0.20	0.00	0.10	0.20	0.30	Description
603	603	603	606	606	Def(ring)
1253	1248	1247	1247	—	$\nu(\text{C-N})$
1390	1389	1388	1382	1374	—
1475	1473	1471	1470	1470	$\nu(\text{Ring})\text{ P}$
1612	1612	1608	1601	1599	$\nu(\text{C=C})$

Def: deformation mode; P: phenazine type structures; ν : stretching mode.

Thus *in situ* Raman spectroelectrochemical studies POT, POPD and poly(OPD-co-OT) further establish that the electrolysis of a mixed solution of OPD and OT result in a copolymer with structure and properties different than the either homopolymers. Perhaps it results in the block copolymers of POPD and POT with the probability of random or linear polymer chains containing both OPD and OT units. Increasing concentration of OPD in the feed results in an increase of the OPD/POPD segments in the copolymer structure and consequently the copolymer shows more similarities to POPD.

7.4 Raman Spectroelectrochemical Measurements of Poly(*o*-phenylenediamine-co-*m*-toluidine)

Fig. 7.8 depicts the Raman spectra recorded at different potentials for copolymer MTA. At an applied potential of $E_{SCE} = -0.20$ V the copolymer shows one major band at 1395 cm^{-1} , numerous weak intensity bands at 605 , 1168 , and 1467 cm^{-1} and a broad band around 1615 cm^{-1} . All of these bands show variations in the Raman intensity upon changing the potential to higher values. A summary of all the major bands in the Raman spectra of copolymer MTA along with their assignments is presented in Table 7.6.

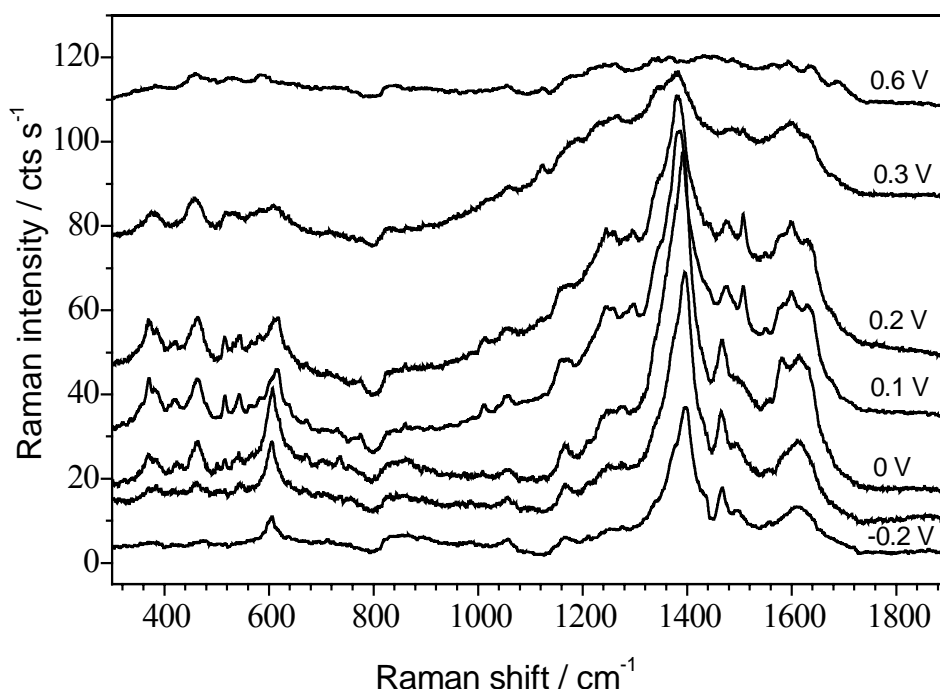


Fig. 7.8 *In situ* Raman spectra of copolymer MTA, obtained at different electrode potentials ranging from $E_{SCE} = -0.20$ to 0.60 V, in $1.5\text{ M H}_2\text{SO}_4$.

Table 7.6 Major band assignments of Raman spectra of copolymer MTA obtained with $\lambda_{\text{ex}} = 647.1\text{nm}$

Wavenumbers (cm^{-1}) at electrode potential (V) (vs. SCE)					
–0.20	0.00	0.10	0.20	0.30	Description
–	–	369	369	376	$\delta(\text{C–H})$
–	–	421	422	–	$\gamma(\text{Ring})$
–	–	463	462	457	$\gamma(\text{C–H})$
–	–	515	515	–	$\delta(\text{Ring})$
–	–	542	542	–	$\delta(\text{Ring})$
605	606	618	617	611	Def(ring)
–	–	1246/1298	1295	–	$\nu(\text{C–N})$ SQ
1168	1168	1168	1166	1166	$\beta(\text{C–H})$
1395	1394	1387	1383	1383	–
1467	1465	1477	1479	–	$\nu(\text{C=N})$ QI
–	–	1507	1507	–	$\nu(\text{C=N}) + \text{Q}$
1615	1613/1581	1632/1602	1629/1602	1600	$\nu(\text{C=C})$ SQ / (C=N) QI

B: benzoid; Def: deformation mode; Q: quinoid type ring; QI: quinoneimine; SQ: semiquinone; β : bending mode; δ : in-plane deformation mode; γ : out-of-plane deformation mode; ν : stretching mode.

The band around 1615 cm^{-1} shows an increase in the intensity with increasing potential up to $E_{\text{SCE}} = 0.00\text{ V}$ and then its intensity decreases with further increase in potential. At an applied potential of $E_{\text{SCE}} = 0.00\text{ V}$ this band splits into two bands centered at 1613 and 1581 cm^{-1} , ascribable to C=C and C=N stretching vibrations of the semiquinoid and quinoneimine type rings, respectively. As the potential passes $E_{\text{SCE}} = 0.20\text{ V}$, the two bands again merge into one to form a broad band around 1600 cm^{-1} . The intensity of the major band at 1395 cm^{-1} increases very sharply with increasing potential and reaches a maximum at $E_{\text{SCE}} = 0.10\text{ V}$. Unexpectedly, this behavior is different from the UV-Vis spectroelectrochemical data of copolymer MTA, according to which the maximum concentration of the charge carriers should occur around $E_{\text{SCE}} = 0.30\text{ V}$. The reason for this difference is not clear. The intensity of the signals at 605 , 1168 and 1467 cm^{-1} also attains maximum at $E_{\text{SCE}} = 0.10\text{ V}$ and then decreases with further increase in potential. These bands are assigned to

ring deformation, C–H bending of quinoid type rings and C=N stretching vibrations of quinonimine type rings, respectively. Various bands of weak to medium intensity appear in the 300-600 cm^{-1} range between the applied potentials of $E_{\text{SCE}} = 0.10$ and 0.30 V.

Fig. 7.9 shows the Raman spectra recorded for copolymer MTB. There is one major band at 1389 cm^{-1} in the spectrum recorded at $E_{\text{SCE}} = -0.20$ V. This band is red shifted in comparison with copolymer MTA. Other bands of weak intensity at 603, 1167, 1251, 1474 cm^{-1} and a broad band around 1609 cm^{-1} can also be observed. The intensity of these bands increases as the potential is gradually swept to anodic direction. After an applied potential of $E_{\text{SCE}} = 0.10$ V the intensity of these signals decrease. Unlike copolymer MTA the broad band around 1609 cm^{-1} does not split but its intensity increases with a maximum at $E_{\text{SCE}} = 0.10$ V. The intensity of the major band at 1389 cm^{-1} is maximum in the potential range of $E_{\text{SCE}} = 0.00$ to 0.20 V. Some weak intensity bands appear in the 300-600 cm^{-1} region upon oxidation. However, the spectra in this region are not well resolved as those of copolymer MTA. The major Raman bands of copolymer MTB are listed in Table 7.7.

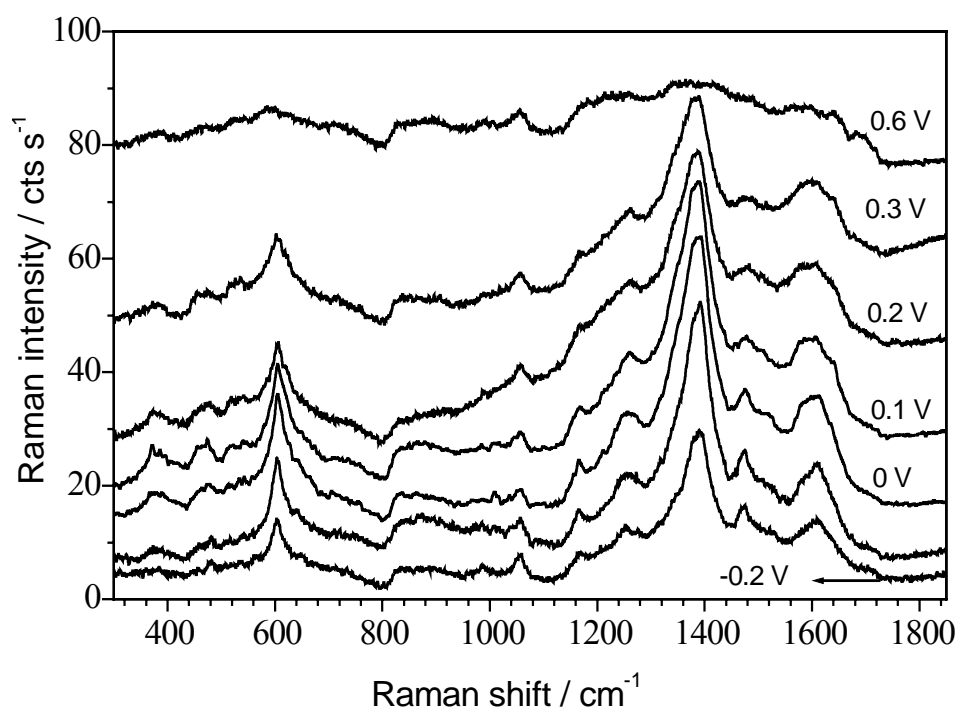


Fig. 7.9 *In situ* Raman spectra of copolymer MTB, obtained at different electrode potentials ranging from $E_{\text{SCE}} = -0.20$ to 0.60 V, in 1.5 M H_2SO_4 .

Table 7.7 Major band assignments of Raman spectra of copolymer MTB obtained with $\lambda_{\text{ex}} = 647.1\text{nm}$

Wavenumbers (cm^{-1}) at electrode potential (V) (vs. SCE)					
−0.20	0.00	0.10	0.20	0.30	Description
–	373	373	373	–	$\delta(\text{C-H})$
479	479	479	463	–	$\gamma(\text{C-H})$
603	604	605	605	601	Def(ring)
1167	1165	1165	1165	1165	$\beta(\text{C-H})$
1251	1256	11256	1256	1256	$\nu(\text{C-N})$ SQ
1389	1393	1391	1390	1390	–
1474	1475	1477	1482	1482	$\nu(\text{C=N})$ QI
1609	1605	1598	1596	1598	$\nu(\text{C=C})$ Q / B

B: benzoid; Def: deformation mode; Q: quinoid type ring; QI: quinoneimine; SQ: semiquinone; β : bending mode; δ : in-plane deformation mode; γ : out-of-plane deformation mode; ν : stretching mode.

Raman spectra registered at different applied potentials for copolymer MTC are shown in Fig. 7.10. The cyclic voltammogram (Fig. 3.12 b) and UV-Vis spectra (Fig. 5.11 c) of copolymer MTC are closely similar to those of POPD (Fig. 3.2 b and 5.7, respectively). However, Raman spectroelectrochemical study reveals differences between the two polymers. At an applied potential of $E_{\text{SCE}} = -0.20$ V, the copolymer shows two bands of very weak intensity at 1383 and 603 cm^{-1} which grow in intensity with further increase in the potential. At $E_{\text{SCE}} = 0.10$ and 0.20 V, the intensity of these bands is considerably high. As the potential passes $E_{\text{SCE}} = 0.20$ V a decrease in the intensity of these bands is observed. New bands can be observed when the potential is successively increased. These bands appear at 1600, 1471, 1258, 1167, 475 and 389 cm^{-1} , respectively, and grow in intensity up to $E_{\text{SCE}} = 0.20$ V. In case of POPD no bands were observed in the region below 605 cm^{-1} (see Fig. 7.4). Unlike POPD the band at 1600 attains maximum intensity at $E_{\text{SCE}} = 0.10$ V and decreases afterwards. After $E_{\text{SCE}} = 0.20$ V all the bands in the spectra show a decrease in the intensity and disappear at 0.60 V. The major Raman bands observed for copolymer MTC are listed in Table 7.8 along with their assignments.

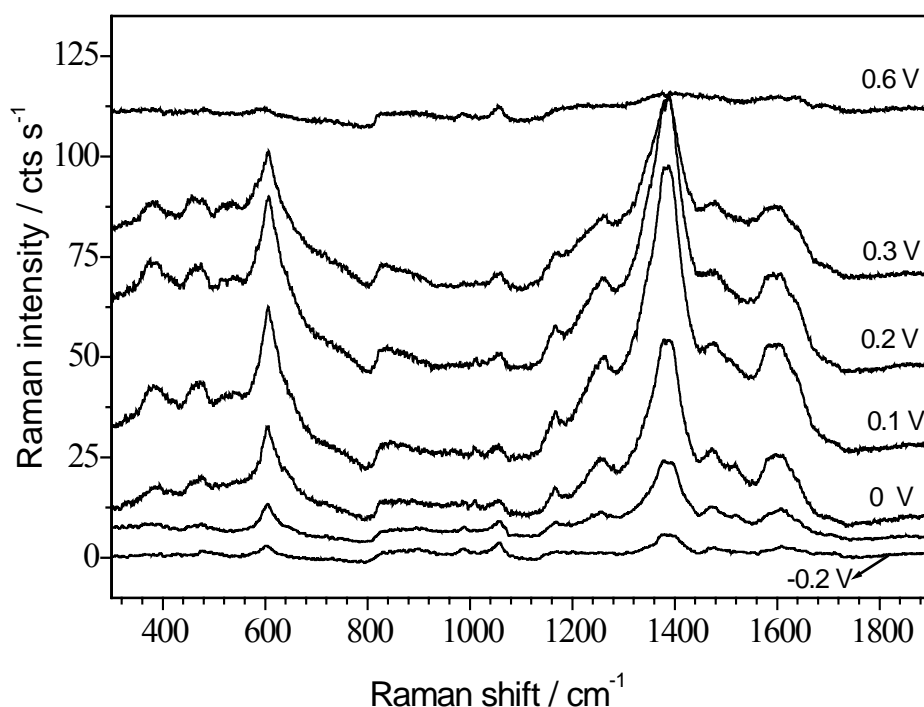


Fig. 7.10 *In situ* Raman spectra of copolymer MTC, obtained at different electrode potentials ranging from $E_{SCE} = -0.20$ to 0.60 V, in 1.5 M H_2SO_4 .

Table 7.8 Major band assignments of Raman spectra of copolymer MTC obtained with $\lambda_{ex} = 647.1$ nm

Wavenumbers (cm^{-1}) at electrode potential (V) (vs. SCE)					
-0.20	0.00	0.10	0.20	0.30	Description
—	389	389	389	—	$\delta(C-H)$
—	475	475	475	—	$\gamma(C-H)$
603	604	605	606	606	Def(ring)
—	1167	1166	1166	—	$\beta(C-H)$
—	1258	1262	1264	—	$\nu(C-N)$
1383	1385	1388	1387	1386	—
1471	1473	1475	1475	—	$(C=N)$ QI
1600	1600	1600	1600	1600	$\nu(C=C)$ Q / B

B: benzoid; Def: deformation mode; P: phenazine type structures; Q: quinoid type ring; QI: quinoneimine; SQ: semiquinone; β : bending mode; δ : in-plane deformation mode; ν : stretching mode.

The differences in the Raman spectra of poly(OPD-co-MT) in comparison with the homopolymers suggest the formation of copolymer from mixed solutions of OPD and MT. Furthermore, Raman spectroelectrochemical studies also suggest that the structure and properties of poly(OPD-co-MT) are different from those of poly(OPD-co-OT) and add support to the results presented in the previous chapters. This is an indicative of the difference in the tendency of OT and MT towards copolymerization with OPD. In comparison with poly(OPD-co-OT), the effect of OPD/POPD units seem to be more pronounced in poly(OPD-co-MT) even at lower OPD feed concentrations.

Summary

The present study describes the results of electrochemical polymerization of OPD, OT and MT and the copolymerization of OPD with OT and MT. Cyclic voltammetry was used for the synthesis of homo-/copolymers. The electrochemical growth characteristics of the copolymers were compared with those of the corresponding homopolymers in order to obtain evidence for copolymer deposition when a mixture of monomers was used. *In situ* conductivities were measured in order to identify differences between the conductivities of the homopolymers and copolymers supporting the assumption of true copolymers instead of merely mixed homopolymers being electropolymerized. The copolymerization process was followed by UV-Vis spectroelectrochemistry. The copolymer films were characterized with UV-Vis and Raman spectroelectrochemistry and FT-IR spectroscopy.

Cyclic voltammetric results showed that copolymers of OPD with OT and MT could be deposited on a gold electrode from mixed solutions containing a constant concentration of OT or MT and various concentrations of OPD. Cyclic voltammetric behavior of the copolymers was changed with a change of OPD concentration in the feed. Growth of the first redox process showed an increasing trend with the increase of OPD concentration in the feed. On the other hand increasing OPD concentration in the feed hindered the growth of 2nd and 3rd redox pairs. Addition of the monomers with an appropriate concentration in the comonomer feed resulted in a copolymer having a broader useful potential range of redox activity as compared to those of the homopolymers. The respective copolymer film showed considerable electrochemical activity relative to homopolymers, in solutions of high pH values. There was a small decrease in the peak currents of the copolymer film with the increase in pH value beyond 4.0, suggesting a slow decay and good electrochemical activity of the copolymer at higher pH value. The copolymer film exhibited good electrochemical stability when subjected to continuous potential scans.

Interesting features were observed when electropolymerization of mixed solutions containing OPD and OT or MT was carried out. The growth features and electrochemical properties of POT and PMT are similar. However, the properties of poly(OPD-co-OT) were found to be different from those of corresponding poly(OPD-co-MT) that could be due to the variation in the monomer units and orientation along the copolymer chains. Copolymerization of OPD seems to be more facilitated if instead of MT, OT is present as one of the comonomers. Relative to OT, a higher concentration of MT was required to get any

evidence of copolymer formation. Moreover, the electrochemical activity of poly(OPD-co-OT), at higher pH values, was better than that of the corresponding poly(OPD-co-MT). *In situ* conductivity measurements further support the assumption of formation of a copolymer as the copolymer show different potential range of conductivity. The resistivity values of the copolymers were between the resistivities of the homopolymers.

In situ UV-Vis spectroelectrochemical results obtained from the electrochemical polymerization of the mixture of OPD and OT or MT suggest the participation of both monomers in the electropolymerization process resulting in formation of a true copolymer. The formation of PPD type of mixed intermediates as a result of cross reaction between OPD and OT or MT cation radicals was deduced from the presence of a band at $\lambda = 497$ nm during the electropolymerization of mixtures of OPD and OT or MT. The significant decrease in the absorbance of this band after switching off potential further supports this assignment. The OPD feed concentration was found to affect the growth features of the band at $\lambda = 497$ nm during the electrolysis and the spectral response of the copolymer films in the background electrolyte solution.

In situ Raman (studied with $\lambda_{\text{ex}} = 647.1$ nm) and UV-Vis spectroelectrochemical characteristics of the copolymers, particularly at lower OPD feed concentration, were found to be considerably different from those of the corresponding homopolymers. Raman spectra of POT showed a band at 1630 cm^{-1} . The unusual dependence of the intensity of this band on applied potential has been correlated with the emeraldine to pernigraniline transition of POT. FT-IR analysis of the copolymers suggests the presence of both OPD and OT or MT units and thus formation of copolymer during the electrolysis of mixed solutions of OPD and OT or MT. Phenazine type cyclic structures increase in the copolymer with increasing OPD concentration in the feed.

The results suggest that electrolysis of mixed solutions of OPD and OT or MT most probably resulted in copolymers having mixtures of copolymer chains with different monomer contents and have a significant number of block segments. The incorporation of OT/POT and MT/PMT units in the copolymer may take place even at the highest OPD feed concentration studied, which resulted in the modification of the overall properties of the respective copolymers. The properties of the copolymers were found to be very sensitive to OPD feed concentration. In fact a copolymer of varying composition of OPD/POP and OT/POT or MT/PMT could be generated just by varying concentration of OPD in the feed.

A good correlation was found between the electrochemical, *in situ* conductivity and spectroelectrochemical characteristics of the polymers studied.

Future Work

A more detailed study of the copolymers, especially those that have shown characteristics markedly different from those of the homopolymers, is required to be carried out with *in situ* FT-IR and EPR spectroscopy or any other appropriate technique in order to understand better the copolymerization and the structure of the copolymers. The copolymers can be tested for possible applications in fabrication of sensors, biofuel cells, rechargeable batteries and corrosion protection.

References

- [1] V.V. Walatka, M.M. Labes and J.H. Perlstein, *Phys. Rev. Lett.* 31 (1973) 1139.
- [2] R.L. Greene, G.B. Street and L.J. Suter, *Phys. Rev. Lett.* 34 (1975) 577.
- [3] C.K. Chiang, C.R. Fincher, Y.W. Park, A.J. Heeger, H. Shirakawa, E.J. Louis, S.C. Gau and A.G. MacDiarmid, *Phys. Rev. Letters* 39 (1977) 1098.
- [4] H. Shirakawa, E.J. Louis, A.G. MacDiarmid, C.K. Chiang and A.J. Heeger, *J. Chem. Soc. Chem. Commun.* (1977) 578.
- [5] A.J. Heeger, *Rev. Mod. Phys.* 73 (2001) 681.
- [6] A.G. MacDiarmid, *Rev. Mod. Phys.* 73 (2001) 701.
- [7] H. Shirakawa, *Rev. Mod. Phys.* 73 (2001) 713.
- [8] J.A. Osaheni and S.A. Jenekhe, *Chem. Mater.* 4 (1992) 1282.
- [9] M.F. Roberts and S.A. Jenekhe, *Chem. Mater.* 6 (1994) 135.
- [10] M. Dotrong, R. Mehta, G.A. Balchin, R.C. Tomlinson, M. Sinsky, C.Y.C. Lee and R.C. Evers, *J. Polym. Sci. Part A: Polym. Chem.* 31 (1993) 723.
- [11] P. Chandrasekhar: in *Conducting Polymers, Fundamentals and Applications, A Practical Approach*, Kulwer Academic Publishers, Boston, 1999, p3-22, p16, p96.
- [12] E.M. Genies, C. Tsintavis and A.A. Sayed, *Mol. Cryst. Liq. Cryst.* 121 (1985) 181.
- [13] H. Kuzmany and N.S. Sariciftci, *Synth. Met.* 18 (1987) 353.
- [14] A.G. MacDiarmid, S.L. Mu, N.L. Somasiri and W. Wu, *Mol. Cryst. Liq. Cryst.* 121 (1985) 187.
- [15] J. Langer, *Mater. Sci.* 10 (1984) 174.
- [16] A. Volkov, G. Tourillon, P.C. Lacaze and J.E. Dubois, *J. Electroanal. Chem.* 115 (1980) 279.
- [17] N.E. Agbor, M.C. Petty and A.P. Monkman, *Sensors and Actuators B: Chem.* 28 (1995) 173.
- [18] S. Shreepathi and R. Holze, *Chem. Mater.* 17 (2005) 4078.
- [19] D. Xie, Y. Jiang, W. Pan, D. Li, Z. Wu and Y. Li, *Sensors and Actuators B: Chem.* 81 (2002) 158.
- [20] E. Punkka, K. Laakso, H. Stubb, K. Levon and W.Y. Zheng, *Thin Solid Films* 243 (1994) 515.
- [21] D. Li, Y. Jiang, Y. Li, X. Yang, L. Lu and X. Wang, *Mater. Sci and Eng. C: Biomimetic and Supramol. Sys.* C11 (2000) 117.

- [22] D. Li, W. Ding, X. Wang, L. Lu and X. Yang, *J. Mater. Sci. Lett.* 20 (2001) 1925.
- [23] B.L. Funt and A.F. Diaz: in *Organic Electrochemistry, an Introduction and a Guide*, Marcel Dekker, New York, 1991, p1337.
- [24] E.M. Genies, G. Bidan and A.F. Diaz, *J. Electroanal. Chem.* 149 (1983) 101.
- [25] R.J. Waltman and J. Bargon, *Tetrahedron* 40 (1984) 3963.
- [26] J.M. Ortega, *Thin Solid Films* 360 (2000) 159.
- [27] G.J. Cruz, J. Morales, M.M.C. Ortega and R. Olayo, *Synth. Met.* 88 (1997) 213.
- [28] Q. Hao, V. Kulikov and V.M. Mirsky, *Sensors and Actuators B: Chem.* 94 (2003) 352.
- [29] R.M. Nyffenegger and R.M. Penner, *J. Phy. Chem.* 100 (1996) 17041.
- [30] J.M.G. Laranjeira, W.M. de Azevedo and M.C.U. de Araujo, *Analyt. Lett.* 30 (1997) 2189.
- [28] J. Lippe and R. Holze, *Synth. Met.* 43 (1991) 2927.
- [32] R. Holze and J. Lippe, *Synth. Met.* 38 (1990) 99.
- [33] R. Holze, *J. Solid State Electrochem.* 8 (2004) 982.
- [34] R. Holze, *Recent Res. Devel. Electrochem.* 6 (2003) 101.
- [35] S.P. Best, R.J.H. Clark, R.C.S. McQueen and S. Joss, *J. Am. Chem. Soc.* 111 (1989) 548.
- [36] M. Thanneermalai, T. Jeyaraman, C. Sivakumar, A. Gopalan, T. Vasudevan and T.C. Wen, *Spectrochim. Acta: Part A* 59 (2003) 1937.
- [37] D. Harvey: in *Modern Analytical Chemistry*, 1st Edition, McGraw-Hill, New York, (2001) pp.397-398.
- [38] M.T. Nguyen and A.F. Diaz, *Macromolecules* 28 (1995) 3411.
- [39] B.L. Rivas and C.O. Sanchez, *J. Appl. Polym. Sci.* 89 (2003) 2641.
- [40] P. Savitha and D.N. Sathyanarayana, *J. Polym. Sci. Part A: Polym. Chem.* 43 (2005) 3040.
- [41] C.H. Yang, T.C. Yang and Y.K. Chih, *J. Electrochem. Soc.* 152 (2005) E273.
- [42] E.M. Genies and M. Lapkowski, *J. Electroanal. Chem.* 236 (1987) 189.
- [43] Y.B. Shim, M.S. Won and S.M. Park, *J. Electrochem. Soc.* 137 (1990) 538.
- [44] A. Zimmermann, U. Kunzelmann and L. Dunsch, *Synth. Met.* 93 (1998) 17.
- [45] J.M. Leger, B. Beden, C. Lamy, P. Ocon and C. Sieiro, *Synth. Met.* 62 (1994) 9.
- [46] A. Malinauskas and R. Holze, *Electrochim. Acta* 43 (1998) 2413.
- [47] A. Malinauskas and R. Holze, *Electrochim. Acta* 44 (1999) 2613.

- [48] A. Malinauskas and R. Holze, *Ber. Bunsenges. Phys. Chem.* 101 (1997) 1859.
- [49] M.S. Wu, T.C. Wen and A. Gopalan, *Mater. Chem. Phys.* 74 (2002) 58.
- [50] T.C. Wen, C. Sivakumar and A. Gopalan, *Electrochim. Acta* 46 (2001) 1071.
- [51] A.A. Shah and R. Holze, *Synth. Met.* 156 (2006) 566.
- [52] P. Santhosh, M. Sankarasubramanian, M. Thanneermalai, A. Gopalan and T. Vasudevan, *Mater. Chem. Phys.* 85 (2004) 316.
- [53] J.E.G. Brame and J. Grasselli: in *Infrared and Raman Spectroscopy*, Marcel Dekker, Inc. New York and Basel, Part A 1976.
- [54] J.R. Ferraro and K. Nakamoto: in *Introductory Raman Spectroscopy*, Academic Press, Inc. SanDiego, 1994.
- [55] D.N. Sathayanarayana: in *Vibrational Spectroscopy: Theory and Applications*, 2nd Addition, New Age International, New Delhi, 2004.
- [56] H.J. Ahonen, J. Lukkari and J. Kankare, *Macromolecules* 33 (2000) 6787.
- [57] D.L. Wise, G.E. Wnek, D.J. Trantolo, T.M. Cooper and J.D. Gresser: in *Electrical and Optical Polymer Systems*, Marcel Dekker, New York, 1997, p23, p167.
- [58] T.J. Skotheim: in *Hand Book of Conducting Polymers*, Marcel Dekker, New York, (1986).
- [59] S. Kakuda, T. Momma, T. Osaka, G.B. Appetecchi and B. Scrosati, *J. Electrochem. Soc.* 142 (1995) L1.
- [60] T. Momma, S. Kakuda, H. Yarimizu and T. Osaka, *J. Electrochem. Soc.* 142 (1995) 1766.
- [61] T. Osaka, T. Nakajima, K. Shiota and T. Momma, *J. Electrochem. Soc.* 138 (1991) 2853.
- [62] W.K. Lu, R.L. Elsenbaumer and B. Wessling, *Synth. Met.* 71 (1995) 2163.
- [63] J.M. Pernaut and J.R. Reynolds, *J. Phys. Chem. B* 104 (2000) 4080.
- [64] J.M. Yeh, C.L. Chen, Y.C. Chen, C.Y. Ma, K.R. Lee, Y. Wei and S. Li, *Polymer* 43 (2002) 2729.
- [65] T. Nagaoka, K. Kakuno, M. Fujimoto, H. Nakao, J. Yano and K. Ogura, *J. Electroanal. Chem.* 368 (1994) 315.
- [66] T. Kobayashi, H. Yoneyama and H. Tamura, *J. Electroanal. Chem. Interfac. Electrochem.* 161 (1984) 419.
- [67] A.F. Diaz, J.F. Robinson and H.B. Mark, *Adv. Polym. Sci.* 84 (1988) 113.

- [68] H. He, J. Zhu, N.J. Tao, L.A. Nagahara, I. Amlani and R. Tsui, *J. Am. Chem. Soc.* 123 (2001) 7730.
- [69] G. Inzelt, M. Pineri, J.W. Schultze and M.A. Vorotyntsev, *Electrochim. Acta* 45 (2000) 2403.
- [70] H. Shinohara, T. Chiba and T. Aizawa, *Sensors and Actuators* 13 (1988) 79.
- [71] I.A. Vinokurov, *Sensors and Actuators: B* 10 (1992) 31.
- [72] F. Selampinar, L. Toppare, U. Akbulut, T. Yalcin and S. Suzer, *Synth. Met.* 68 (1995) 109.
- [73] H.J. Ahonen, J.Kankare, J. Lukkari and P. Pasanen, *Synth. Met.* 84 (1997) 215.
- [74] J.Y. Shimano and A.G. MacDiarmid, *Synth. Met.* 123 (2001) 251.
- [75] H. Shirakawa, *Synth. Met.* 125 (2001) 3.
- [76] D.N. Dibarnot and F.P. Eppaillard, *Analyt. Chim. Acta* 475 (2003) 1.
- [77] Y. Cao, P. Smith and A.J. Heeger, *Synth. Met.* 48 (1992) 91.
- [78] Y. Wei, R. Hariharan and S.A. Patel, *Macromolecules* 23 (1990) 758.
- [79] S.W. Salaneck, W.S. Huang, I. Lundstrorn and A.G. MacDiarmid, *Synth. Met.* 13 (1986) 291.
- [80] J.C. LaCrix and A.F. Diaz, *J. Electrochem. Soc.* 135 (1998) 1457.
- [81] P.S. Rao, S. Subrahmanya and D.N. Sythyanarayana, *Synth. Met.* 128 (2002) 311.
- [82] P.S. Rao, D.N. Sythyanarayana and S. Palaniappan, *Macromolecules* 35 (2002) 4988.
- [83] S. Takeda, *Thin Solid Films* 343 (1999) 313.
- [84] C. Liao and M. Gu, *Thin Solid Films* 408 (2002) 37.
- [85] W.W. Focke, G.E. Wnek and Y. Wei, *J. Phys. Chem.* 91 (1987) 5813.
- [86] A.J. Epstein, J.M. Ginder, F. Zuo, R.W. Bigelow, H.S. Woo, D.B. Tanner, A.F. Richter, W.S. Huang and A.G. MacDiarmid, *Synth. Met.* 18 (1987) 303.
- [87] A. Watanabe, K. Mori, Y. Iwasaki, Y. Nakamura and S. Niizuma, *Macromolecules* 20 (1987) 1793.
- [88] J.C. Chiang and A.G. MacDiarmid, *Synth. Met.* 13 (1986) 193.
- [89] J.M. Ginder, A.F. Richter, A.G. MacDiarmid and A.J. Epstein, *J. Solid State Commun.* 63 (1987) 97.
- [90] T. Jeevananda, Siddaramaiah, S. Seetharamu, S. Saravanan and L. D' Souza, *Synth. Met.* 140 (2004) 247.
- [91] M. Sato, S. Tanaka and K. Kaeriyama, *J. Chem. Soc. Chem. Commun.* (1986) 873.

- [92] K.Y. Jen, R. Oboddi and R. Elsenbaumer, Polym. Mater. Sci. Eng. 53 (1985) 79.
- [93] D.R. Gagnon, J.D. Capistran, F.E. Karasz and R.W. Lenz, Polym. Bull. 12 (1984) 293.
- [94] E. Ruckenstein and S. Yang, Synth. Met. 53 (1993) 283.
- [95] S. Yang and E. Ruckenstein, Synth. Met. 59 (1993) 1.
- [96] Y. Lee, D. Shin, J. Cho, Y.H. Park, Y. Son and D.H. Baik, J. Appl. Polym. Sci. 69 (1998) 2641.
- [97] T. Jeevananda, S. Palaniappan and Siddaramaiah, J. Appl. Polym. Sci. 74 (1999) 3507.
- [98] D.C. Liao, K.H. Hsieh, Y.C. Chern and K.S. Ho, Synth. Met. 87 (1997) 61.
- [99] T. Jeevananda, M. Begum and Siddaramaiah, Eur. Polym. J. 37 (2001) 1213.
- [100] T. Jeevananda and Siddaramaiah, Eur. Polym. J. 39 (2003) 569.
- [101] J. Yue and A.J. Epstein, J. Am. Chem. Soc. 112 (1990) 2800.
- [102] S.A. Chen and G.W. Hwang, J. Am. Chem. Soc. 116 (1994) 7939.
- [103] Y. Cao, P. Smith and A.J. Heeger, Synth. Met. 48 (1992) 91.
- [104] H.S.O. Chan, S.C. Ng, W.S. Sim, K.L. Tan and B.T.G. Tan, Macromolecules 25 (1992) 6029.
- [105] S. Cattarin, L. Doubova, G. Mengoli and G. Zotti, Electrochim. Acta 33 (1988) 1077.
- [106] Y. Wei, W.W. Focke, G.E. Wnek, A. Ray and A.G. MacDiarmid, J. Phys. Chem. 93 (1989) 495.
- [107] M. Probst and R. Holze, Macromol. Chem. Phys. 198 (1997) 1499.
- [108] M. Probst and R. Holze, Ber. Bunsenges. Phys. Chem. 100 (1996) 1286.
- [109] M. Probst, Ph.D. Thesis Chemnitz University of Technology, 1996.
- [110] K. Chiba, T. Ohsaka, J. Ohnuki and N. Oyama, J. Electroanal. Chem. 219 (1987) 117.
- [111] T. Hahiwara, T. Demura and K. Iwata, Synth. Met. 18 (1987) 317.
- [112] E.T. Samulski, Polymer 26 (1985) 177.
- [113] J.C. Lacroix, P. Garcia, J.P. Audiere, R. Clement and O. Kahn, Synth. Met. 44 (1991) 117.
- [114] P. Snauwaert, R. Lazzaroni, J. Riga and J.J. Verbist, Synth. Met. 18 (1987) 335.
- [115] C. Barbero, J. Zerbino, L. Sereno and D. Posadas, Electrochim. Acta 32 (1987) 693.
- [116] S. Sankarapavinasam, Synth. Met. 58 (1993) 173.

- [117] H.J. Salavagione, J. Arias, P. Garces, E. Morallon, C. Barbero and J.L. Vazquez, J. Electroanal. Chem. 565 (2004) 375.
- [118] J. Schwarz, W. Oelssner, H. Kaden, F. Schumer and H. Hennig, Electrochim. Acta. 48 (2003) 2479.
- [119] R.I. Tucceri, J. Electroanal. Chem 562 (2004) 173.
- [120] H.S.O. Chan, P.K.H. Ho, S.C. Ng, B.T.G. Tan and K.L. Tan, J. Am. Chem. Soc. 117 (1995) 8517.
- [121] N. Oyama and T. Ohsaka, Synth. Met. 18 (1987) 375.
- [122] K. Sasaki, M. Kaya, J. Yano, A. Kitani and A. Kunai, J. Electroanal. Chem. 215 (1986) 401.
- [123] U. Hayat, P.N. Bartlett, G.H. Dodd and J. Barker, J. Electroanal. Chem. 18 (1987) 371.
- [124] U. Hayat, P.N. Bartlett and G.H. Dodd, Polym. Commun. 27 (1986) 362.
- [125] A. Watanabe, K. Mori, A. Iwabuchi, Y. Iwasaki and Y. Nakamura, Macromolecules 22 (1989) 3521.
- [126] T. Ohsaka, T. Okajima and N. Oyama, J. Electroanal. Chem. 200 (1985) 159.
- [127] T. Ohsaka, T. Okajima and N. Oyama, J. Electroanal. Chem. 215 (1987) 191.
- [128] S.K. Manohar, A.G. MacDiarmid, K.R. Cromack, J.M. Ginder and A.J. Epstein, Synth. Met. 29 (1989) 349.
- [129] M. Leclerc, J. Guay and L.H. Dao, Macromolecules 22 (1989) 649.
- [130] A. Thyssen, A. Hockfeld, R. Kessel, A. Meyer and J.W. Shultze, Synth. Met. 29 (1989) 357.
- [131] M.V. Kulkarni, A.K. Viswanath and U.P. Mulik, Mater. Chem. Phys. 89 (2005) 1.
- [132] R.J. Mortimer, J. Mater. Chem. 5 (1995) 969.
- [133] M. Leclerc, J. Guay and L.H. Dao, J. Electroanal. Chem. 251 (1988) 21.
- [134] A.G. Green and A.E. Woodhead, J. Chem. Soc. Trans. 97 (1910) 2388.
- [135] U. König and J.W. Schultze, J. Electroanal. Chem. 242 (1988) 243.
- [136] R.L. Clark and S.C. Yang, Synth. Met. 29 (1989) 337.
- [137] F. Cataldo, Eur. Polym. J. 32 (1996) 43.
- [138] X.G. Li, M.R. Huang, W. Duan and Y.L. Yang, Chem. Rev. 102 (2002) 2925.
- [139] A.H. Premasiri and W.B. Euler, Macromol. Chem. Phys. 196 (1995) 3655.
- [140] H.S.O. Chan, S.C. Ng, T.S. A. Hor, J. Sun, K.L. Tan and B.T.G. Tan, Eur. Polym. J. 27 (1991) 1303.

- [141] J. Yano, *J. Polym. Sci. Part A: Polym. Chem.* 33 (1995) 2435.
- [142] C. Barbero, J.J. Silber and L. Sereno, *J. Electroanal. Chem.* 263 (1989) 333.
- [143] I. Losito, F. Palmisano and P.G. Zambonin, *Anal. Chem.* 75 (2003) 4988.
- [144] X. Lin and H. Zhang, *Electrochim. Acta* 41 (1996) 2019.
- [145] L.L. Wu, J. Luo and Z.H. Lin, *J. Electroanal. Chem.* 417 (1996) 53.
- [146] A. Malinauskas, M. Bron and R. Holze, *Synth. Met.* 92 (1998) 127.
- [147] L.L. Wu, J. Luo and Z.H. Lin, *J. Electroanal. Chem.* 440 (1997) 173.
- [148] H.P. Dai, Q.H. Wu, S.G. Sun and K.K. Shiu, *J. Electroanal. Chem.* 456 (1998) 47.
- [149] K. Martinusz, G. Inzlet and G. Horanyi, *J. Electroanal. Chem.* 404 (1996) 143.
- [150] K. Ogura, M. Kokura, J. Yano and H. Shiigi, *Electrochim. Acta*, 40 (1995) 2707.
- [151] K. Ogura, M. Kokura and M. Nakayama, *J. Electrochem. Soc.* 142 (1995) L152.
- [152] J. Yano, A. Shimoyama and K. Ogura, *J. Electrochem. Soc.* 139 (1992) L52.
- [153] Q. Deng and S. Dong, *J. Electroanal. Chem.* 337 (1994) 191.
- [154] S.R. Sivakkumar and R. Saraswathi, *J. Appl. Electrochem.* 34 (2004) 1147.
- [155] L.F.D'Elia, R.L. Ortiz, O.P. Marquez, J. Marquez and Y. Martinez, *J. Electrochem. Soc.* 148 (2001) C297.
- [156] J.A. Conklin, S.C. Huang, S.M. Huang, T.L. Wen and R.B. Kaner, *Macromolecules* 28 (1995) 6522.
- [157] S.S. Pandey, S. Annapoorni and B.D. Malhotra, *Macromolecules* 26 (1993) 3190.
- [158] X.G. Li, L.X. Wang, Y. Jin, Z.L. Zhu and Y.L. Yang, *J. Appl. Polym. Sci.* 82 (2001) 510.
- [159] R. Anbarasan, J. Jayaseharan and A. Gopalan, *J. Appl. Polym. Sci.* 85 (2002) 2317.
- [160] Y. Sahin, S. Percin, M. Sahin and G. Ozkan, *J. Appl. Polym. Sci.* 91 (2004) 2302.
- [161] R. Mazeikiene and A. Malinauskas, *Synth. Met.* 92 (1998) 259.
- [162] A.L. Sharma, V. Saxena, S. Annapoorni and B.D. Malhotra, *J. Appl. Polym. Sci.* 81 (2001) 1460.
- [163] H. Tang, A. Kitani, S. Maitani, H. Munemura and M. Shiotani, *Electrochim. Acta* 40 (1995) 849.
- [164] L.M. Huang, T.C. Wen and A. Gopalan, *Mater. Lett.* 57 (2003) 1765.
- [165] S. Mu, *Synth. Met.* 143 (2004) 259.
- [166] N.P. Ozcicek, K. Pekmez, R. Holze and A. Yildiz, *J. Appl. Polym. Sci.* 89 (2003) 862.
- [167] A.A. Karyakin, A.K. Strakhova and A.K. Yatsimirsky, *J. Electroanal. Chem.* 371

- (1994) 259.
- [168] A.A. Karyakin, I.A. Maltsev and L.V. Lukachova, *J. Electroanal. Chem.* 402 (1996) 217.
- [169] J.Y. Lee and C.Q. Cui, *J. Electroanal. Chem.* 403 (1996) 109.
- [170] P.A. Kilmartin and G.A. Wright, *Synth. Met.* 88 (1997) 153.
- [171] P. Savitha and D.N. Sathyanarayana, *Polym. Int.* 53 (2004) 106.
- [172] P. Savitha and D.N. Sathyanarayana, *Synth. Met.* 145 (2004) 113.
- [173] D.D. Borole, U.R. Kapadi, P.P. Mahulikar and D.G. Hundiware, *Polym. Adv. Technol.* 15 (2004) 306.
- [174] D.D. Borole, U.R. Kapadi, P.P. Mahulikar and D.G. Hundiware, *J. Appl. Poly. Sci.* 90 (2003) 2634.
- [175] D.E. Stilwell and S.M. Park, *J. Electrochem. Soc.* 135 (1988) 2254.
- [176] B.J. Johnson and S.M. Park, *J. Electrochem. Soc.* 143 (1996) 1277.
- [177] A.G. MacDiarmid, J.C. Chiang, A.F. Richter and A.J. Epstein, *Synth. Met.* 18 (1987) 285.
- [178] D. Wei, T. Lindfors, C. Kvarnström, L. Kronberg, R. Sjöholm and A. Ivaska, *J. Electroanal. Chem.* 575 (2005) 19.
- [179] M. Ujvari, G. Lang and G. Inzelt, *Electrochem. Commun.* 2 (2000) 497.
- [180] M.D. Levi and E.Y. Pisarevskaya, *Electrochim. Acta* 37 (1992) 635.
- [181] W.C. Chen, T.C. Wen and A. Gopalan, *J. Electrochem. Soc.* 148 (2001) E427.
- [182] M.K. Ram, M. Salerno, M. Adami, P. Faraci and C. Nicolini, *Langmuir* 15 (1999) 1252.
- [183] C.H. Yang and T.C. Wen, *J. Appl. Electrochem.* 24 (1994) 166 and references therein.
- [184] L.A.M. Ruotolo, A.A. Liao and J.C. Gubulin, *J. Appl. Electrochem.* 34 (2004) 1259.
- [185] J.W. Schultze and H. Karabulut, *Electrochim. Acta* 50 (2005) 1739.
- [186] R. Mazeikiene and A. Malinauskas, *Synth. Met.* 128 (2002) 121.
- [187] R. Mazeikiene and A. Malinauskas, *Synth. Met.* 123 (2001) 349.
- [188] R. Mazeikiene and A. Malinauskas, *Mater. Chem. Phys.* 83 (2004) 184.
- [189] S.Ye, S. Besner, L.H. Dao and A.K. Vijh, *J. Electroanal. Chem.* 381(1995) 71.
- [190] M.A. Goyette and M. Leclerc, *J. Electroanal. Chem.* 382 (1995) 17.
- [191] A.A. Shah and R. Holze, *J. Solid State Electrochem.* 11 (2006) 38.

- [192] G. D'Aprano, M. Leclerc and G. Zotti, *Macromolecules* 25 (1992) 2145.
- [193] E.Y. Pisarevskaya, E.V. Ovsyannikova and N.M. Alptova, *Russian J. Electrochem.* 40 (2004) 969.
- [194] T. Komura, T. Yamaguti and K. Takahashi, *Electrochim. Acta* 41 (1996) 2865.
- [195] M.T. Nguyen and A.F. Diaz, *Macromolecules* 28 (1995) 3411.
- [196] J.W. Chevalier, J.Y. Bergeron and L.H. Dao, *Macromolecules* 25 (1992) 3325.
- [197] for an overview see: R. Holze in: *Advanced Functional Molecules and Polymers*, in: H.S. Nalwa (Ed.) Vol. 2, Gordon & Breach, Amsterdam, (2001), p. 171.
- [198] T.C. Wen, C. Sivakumar and A. Gopalan, *Spectrochim. Acta Part A*: 58 (2002) 167.
- [199] H.S. Kolla, S.P. Surwade, X. Zhang, A.G. MacDiarmid and S.K. Manohar, *J. Am. Chem. Soc.* 127 (2005) 16770 and references therein.
- [200] T.C. Wen, L.M. Huang and A. Gopalan, *Electrochim. Acta* 46 (2001) 2463.
- [201] M.A. del Valle, F.R. Diaz, M.E. Bodini, G. Alfonso, G.M. Soto and E.D. Borrego, *Polym. Int.* 54 (2005) 526.
- [202] J.S. Cho, S. Sato, S. Takeoka and E. Tsuchida, *Macromolecules* 34 (2001) 2751.
- [203] A. Malinauskas and R. Holze, *Synth. Met.* 97 (1998) 31.
- [204] V. Brandl and R. Holze, *Ber. Bunsenges. Phys. Chem.* 101 (1997) 251.
- [205] M. Leclerc, J. Guay and L.H. Dao, *J. Electrochem. Soc.* 251 (1988) 21.
- [206] L.M. Huang, T.C. Wen and A. Gopalan, *Synth. Met.* 130 (2002) 155.
- [207] J.E. de Albuquerque, L.H.C. Mattoso, R.M. Faria, J.G. Masters and A.G. MacDiarmid, *Synth. Met.* 146 (2004) 1.
- [208] A.J. Dominis, G.M. Spinks, L.A.P. Kane-Maguir and G.G. Wallace, *Synth. Met.* 129 (2002) 165.
- [209] K. Chiba, T. Ohsaka, Y. Ohnuki and N. Oyama, *J. Electroanal. Chem.* 219 (1987) 117 and references therein.
- [210] E.M. Genies, A. Boyle, M. Lapkowski and C. Tsintavis, *Synth. Met.* 36 (1990) 139.
- [211] N.S. Sariciftci, H. Kuzmany, H. Neugebauer and A. Neckel, *J. Chem. Phys.* 92 (1990) 4530.
- [212] Z. Ping, *J. Chem. Soc. Faraday Trans.* 92 (1996) 3063.
- [213] N.S. Sariciftci, M. Bartonek, H. Kuzmany, H. Neugebauer and A. Neckel, *Synth. Met.* 29 (1989) E193.

- [214] T. Ohsaka, Y. Ohnuki, N. Oyama, G. Katagiri and K. Kamisako, *J. Electroanal. Chem.* 161 (1984) 399.
- [215] M. Ohira, T. Sakai, M. Takeuchi, Y. Kobayashi and M. Tsuji, *Synth. Met.* 18 (1987) 347.
- [216] J. Tang, X. Jing, B. Wang and F. Wang, *Synth. Met.* 24 (1988) 231.
- [217] S.A. Chen and H.T. Lee, *Synth. Met.* 47 (1992) 233.
- [218] W.R. Salaneck, B. Liedberg, O. Inganas, R. Erlandsson, I. Lundstrom, A.G. MacDiarmid, M. Halpern and N.L.D. Somasiri, *Mol. Cryst. Liq. Cryst.* 121 (1985) 191.
- [219] X.G. Li, W. Duan, M.R. Huang and Y.L. Yang, *J. Polym. Sci. Part A: Polym. Chem.* 39 (2001) 3980.
- [220] X.G. Li, M.R. Huang and Y. Yang, *Polymer* 42 (2001) 4099.
- [221] Z. Ping, H. Neugebauer and A. Neckel, *Electrochim. Acta* 41 (1996) 767.
- [222] N. Chandrakanthi and M.A. Careem, *Polym. Bull.* 45 (2000) 113.
- [223] D. Shan and S. Mu, *Synth. Met.* 126 (2002) 225.
- [224] T.C. Wen, L.M. Huang and A. Gopalan, *Synth. Met.* 123 (2001) 451.
- [225] S. Shreepathi and R. Holze, *Macromol. Chem. Phys.* (accepted).
- [226] M.S. Wu, T.C. Wen and A. Gopalan, *Mater. Chem. Phys.* 74 (2002) 58.
- [227] T. Jeevananda, Siddaramaiah, S. Seetharamu, S. Saravanan and L. D'Souza, *Synth. Met.* 140 (2004) 247.
- [228] R. Murugesan and E. Subramanian, *Mater. Chem. Phys.* 80 (2003) 731.
- [229] K.A. Thomas and W.B. Euler, *J. Electroanal. Chem.* 501 (2001) 235.
- [230] M.R. Huang, X.G. Li and Y. Yang, *Polym. Degrad. Stab.* 71 (2001) 31.
- [231] T.J. Durnick and S.C. Wait, *J. Mol. Spectrosc.* 42 (1972) 211.
- [232] W.H. Li, X.Y. Li and N.T. Yu, *Chem. Phys. Lett.* 327 (2000) 153.
- [233] M.R. Huang, X.G. Li and W. Duan, *Polym. Int.* 54 (2005) 70.
- [234] A. Buzarovska, I. Arsova and L. Arsov, *J. Serb. Chem. Soc.* 66 (2001) 27.
- [235] S. Quillard, K. Berrada, G. Louam, S. Lefrant, M. Lapkowski and A. Pron, *New J. Chem.* 19 (1995) 365.
- [236] M.I. Boyer, S. Quillard, G. Louarn, G. Froyer and S. Lefrant, *J. Phys. Chem. B* 104 (2000) 8952.
- [237] R. Mazeikiene, G. Niaura and A. Malinauskas, *Electrochem. Commun.* 7 (2005) 1021 and references there in.

- [238] R. Mazeikiene, G. Niaura and A. Malinauskas, *Electrochim. Acta*, 51 (2006) 1917.
- [239] D. Wei, T. Lindfors, C. Kvarnstrom, L. Kronberg, R. Sjoholm and A. Ivaska, *J. Electroanal. Chem.* 575 (2005) 19.
- [240] A.A. Shah and R. Holze, *Electrochim. Acta* 52 (2006) 1374.
- [241] K. Berrada, S. Quillard, G. Louam and S. Lefrant, *Synth. Met.* 69 (1995) 201.
- [242] R. Mazeikiene, G. Niaura and A. Malinauskas, *J. Electroanal. Chem.* 580 (2005) 87.
- [243] E.P. Cintra and S.I. Cordoba de Torresi, *J. Electroanal. Chem.* 518 (2002) 33.
- [244] J.E. Pereira da Silva, D.L. A. de Faria, S. I. Cordoba de Torresi and M. L. A. Temperini, *Macromolecules* 33 (2000) 3077.
- [245] H. Jiang, X. Sun, M. Huang, Y. Wang, D. Li and S. Dong, *Langmuir* 22 (2006) 3358.
- [246] K. Martinusz, E. Czirok and G. Inzelt, *J. Electroanal. Chem.* 379 (1994) 437.
- [247] A.A. Shah and R. Holze, *J. Electroanal. Chem.* 597 (2006) 95.
- [248] M.I. Boyer, S. Quillard, M. Cochet, G. Louarn and S. Lefrant, *Electrochim. Acta* 44 (1999) 1981.

Selbständigkeitserklärung

Hiermit erkläre ich an Eides statt, die vorliegende Arbeit selbständig und ohne unerlaubte Hilfsmittel durchgeführt zu haben.

Chemnitz, den 21.05.2007

(Salma Bilal)

Curriculum Vitae

Personal Information

Name: Salma Bilal
Date of Birth: September 7th, 1979
Place of Birth: Nowshera, Pakistan
Nationality: Pakistani
Address: Tehsil & District Bannu,
Village & Post Office Ghoriwala
N.W.F.P. Pakistan

Education

1997-1999: **B.Sc.** (Chemistry, Botany and Zoology)
Government Girls College Nowshera
1999-2001: **M.Sc.** (Physical Chemistry) (Gold Medallist)
Department of Chemistry, University of Peshawar
2001-2002: **B.Ed.**
Institute of Education, University of Peshawar
2004-Till date: **Ph.D.** student, Institute of Chemistry, Chemnitz University of
Technology, Germany

Publications

- 1) Electrochemical copolymerization of *o*-toluidine and *o*-phenylenediamine
Salma Bilal and Rudolf Holze, *Journal Electroanalytical Chemistry* 592 (2006) 1.
- 2) Electrochemical copolymerization of *m*-toluidine and *o*-phenylenediamine
Salma Bilal and Rudolf Holze, *Electrochimica Acta* 52 (2006) 1247.
- 3) *In situ* UV-Vis spectroelectrochemistry of poly(*o*-phenylenediamine-co-*m*-toluidine)
Salma Bilal and Rudolf Holze, *Electrochimica Acta* 52 (2007) 5346.
- 4) A Spectroelectrochemical study of the copolymerization of *o*-phenylenediamine and *o*-toluidine
Salma Bilal and Rudolf Holze, *Journal of Electrochemical Society* (submitted).
- 5) Electrochemical synthesis and characterization of novel conducting poly(*o*-phenylenediamine-co-*o*-toluidine)
Salma Bilal and Rudolf Holze, *Elektrochemische Grundlagenforschung und deren Anwendung in der Elektroanalytik (Proceedings of ELACH7)*, U. Guth und W. Vonau (Hrsg.), KSI, Waldeim 2006, S. 45.
- 6) Concentration and temperature dependence of surface parameters of some aqueous salt solutions, Khurshid Ali, Anwar-ul-Haq, **Salma Bilal**, Shazia Siddiqi, *Colloid and Surfaces A: Physicochemical and Engineering Aspects* 272 (2006) 105.
- 7) Thermodynamic parameters of surface formation of some aqueous salt solutions, Khurshid Ali, Anwar-ul-Haq, **Salma Bilal**, Shazia Siddiqi, *Colloid and Surfaces A: Physicochemical and Engineering Aspects* (accepted).
- 8) New natural urease inhibitors from *Ranunculus repens*
Wahib Noor Khan, Muhammad Arif Lodhi, Irshad Ali, Azhar-ul-Haq, **Salma Bilal**, Rukhsana Gul, Muhammad Iqbal Choudhary, *Journal of Enzyme Inhibition & Medicinal Chemistry* 21 (2006) 17.

Conference Contributions

- 1) Contribution to Elektrochemische Grundlagenforschung und deren Anwendung in der Elektroanalytik (ELACH7) from September 17–20, 2006 in Waldeim Germany with the seminar entitled “Electrochemical Synthesis and Characterization of Novel Conducting Poly(*o*-phenylenediamine-co-*o*-toluidine)”.
- 2) Contribution to GDCH-JCF Frühjahrssymposium from March 22–27, 2007 in Chemnitz Germany with the poster entitled “ Electrochemical Synthesis and Spectroelectrochemical Characterization of Novel Conducting Poly(*o*-phenylenediamine-co-*o*-toluidine)”.